DEVELOPMENT, CHARACTERIZATION AND OPTIMIZATION OF THE PHYSICAL, MECHANICAL AND CORROSION BEHAVIOR OF Fe-SiC-ZrO_2 COMPOSITES

Mulisa Olani Fita

A Thesis Submitted to Department of Mechanical Engineering

School of Mechanical, Chemical and Materials Engineering

Presented in Partial Fulfillment of the Requirement for the Degree of Master’s in Manufacturing Engineering

Office of Graduate Studies

Adama Science and Technology University

October-2022

Adama, Ethiopia

DEVELOPMENT, CHARACTERIZATION AND OPTIMIZATION OF THE PHYSICAL, MECHANICAL AND CORROSION BEHAVIOR OF Fe-SiC-ZrO_2 COMPOSITES

By Mulisa Olani Fita

Advisor: Dr. Devendra Kumar Sinha

A Thesis Submitted to Department of Mechanical Engineering

School of Mechanical, Chemical and Materials Engineering

Presented in Partial Fulfillment of the Requirement for the Degree of Master's in Manufacturing Engineering

Office of Graduate Studies

Adama Science and Technology University

October-2022

Adama, Ethiopia

CANDIDATE'S DECLARATION

Declaration I hereby declare that this Master Thesis entitled "**Development, characterization and optimization of the physical, mechanical and corrosion behavior of Fe-SiC-ZrO_2 composites"** is my original work. That is, it has not been submitted for the award of any academic degree, diploma or certificate in any other university. All sources of materials that are used for this thesis have been duly acknowledged through citation.

Mulisa Olani Fita	______________	__________
Name	Signature	Date

RECOMMENDATION OF ADVISOR

I the advisor(s) of this thesis, hereby certify that I have read the revised version of the thesis entitled "**Development, characterization and optimization of the physical, mechanical and corrosion behavior of Fe-SiC-ZrO_2 composites**" prepared under my guidance by **Mulisa Olani Fita** submitted in partial fulfillment of the requirements for the degree of Mater's of Science in Manufacturing Engineering. Therefore, I recommend the submission of revised version of the thesis to the department following the applicable procedures.

Dr. Devendra kumar Sinha	________________	____________
Main Advisor	Signature	Date
________________________	________________	____________
Co-advisor	Signature	Date

APPROVAL OF ADVISOR

I the advisors of the thesis entitled “**Development, characterization and optimization of the physical, mechanical and corrosion behavior of Fe-SiC-ZrO_2 composites**” and developed by **Mulisa Olani Fita** hereby certify that the recommendation and suggestions made by the board of examiners are appropriately incorporated into the final version of the thesis.

Dr. Devendra kumar Sinha	________________	____________
Main Advisor	Signature	Date
_________________________	________________	____________
Co-advisor	Signature	Date

APPROVAL BY BOARD OF EXAMINERS

We, the undersigned, members of the Board of Examiners of the thesis **Mulisa Olani Fita** have read and evaluated the thesis entitled "**Development, characterization and optimization of the physical, mechanical and corrosion behavior of Fe-SiC-ZrO_2 composites**" and examined the candidate during open defense. This is, therefore, to certify that the thesis is accepted for partial fulfillment of the requirement of the degree of Master of Science Manufacturing Engineering.

. ______________________________ ________________ ________________

Chairperson Signature Date

______________________________ ________________ ________________

Internal Examiner Signature Date

______________________________ ________________ ________________

External Examiner Signature Date

Final approval and acceptance of the thesis is contingent upon submission of its final copy to the Office of Postgraduate Studies (OPGS) through the Department Graduate Council (DGC) and School Graduate Committee (SGC).

______________________________ ________________ ________________

Department Head Signature Date

______________________________ ________________ ________________

School Dean Signature Date

______________________________ ________________ ________________

Office of Postgraduate Studies, Dean Signature Date

ACKNOWLEDGEMENT

My profoundest thanks go to my advisor, **Dr. Devendra kumar Sinha**. His respectful professional character along with his sincere commitment and patience to help the students to be better versions of themselves in their research and future careers, make **Dr. Devendra kumar Sinha** an exceptional advisor to work with and I am grateful for the chance of being in his research team. I am taking this opportunity to express my gratitude to **Dr. Getnet Asrat Mengesha** for his time and constructive idea during my work.

Table of Contents

List of Tables

List of Figures

Nomenclature

COF	Coefficient of friction
DOE	Design of Experiments
GRA	Grey Relational Analysis
GRC	Grey Relational Code
MPa	Mega Pascal
MMCs	Metal Matrix Composites
NaCl	Sodium Chloride
OM	Optical Microscopy
PM	Powder Metallurgy
PMC	Polymer Matrix Composites
RPM	Revolution Per Minute
SEM	Scanning Electron Microscope
SCE	Standard Calomel Electrode
S/N	Signal to Noise ratio
SiC	Silicon Carbide
TiB_2	Titanium Bromide
TiC	Titanium Carbide
UTM	Universal Tasting Machine
VH	Vickers Hardness
Wt.%	Weight percentage
µm	Micrometer
XRD	X-ray diffraction
ZrO_2	Zirconium dioxide

ABSTRACT

The iron is one of the most versatile engineering materials having all-round applications in construction, automobile, aerospace, ship, building industries etc. However, Fe has lower corrosion resistance, low strength to weight ratio, and high density. The aim involved in designing metal matrix hybrid composite materials is to combine the desirable attributes of metals and Ceramics. Present work is focused on the study of behavior of Fe/SiC-ZrO_2 composites produced by the powder metallurgy. Experiments have been designed using L9 Taguchi orthogonal array to acquire the data. Grey relational analysis approach is used for optimization of process parameters in order to obtain the best values of mechanical properties like density, hardness and compressive strength. An analysis of variance is employed to investigate the influence of three controlling parameters, viz., SiC-ZrO_2 composition, compaction pressure, & sintering on sintered density, hardness and corrosion rate of the composites. The optimal combination of the three controlling parameters has been obtained for minimum sintered density, maximum hardness and minimum corrosion rate. in 3%NaCl solution at room temperature where studied. Furthermore, the investigation of deformation behavior through bulk deformation i.e., extrusion process has been done on the mechanical, electrochemical and microstructural properties of the sintered sample. The lower density has been recorded for Fe-10%SiC-5%ZrO_2 specimen. When the wt% addition of SiC and ZrO_2 increases, the hardness and compression strength of the composites were increased. The highest hardness (485.4HV) and compression strength (310MPa) for the composite was obtained with Fe -10% SiC-10% ZrO_2 specimen. The higher corrosion resistance of the composites was obtained for Fe-10%SiC-10% ZrO_2 due to the addition of corrosion resistance reinforcement and well compacted of the sample. The density and hardness of the sample after deformation was found to be 5.021 g/cm^3 and 544.6HV respectively, which have shown remarkable improvement in material properties. Fairly distributed of reinforcement particle, good microstructure and minimum porosity is shown for extrudate specimen. The results also indicate that the extruded hybrid composite specimens are exhibiting marginally lower order corrosion rate compared to sintered specimen of the similar specimen from 24.47 to 12.124 (mpy). This research work is expected to help all industries and researchers working in this area of focus.

Key words*: hybrid metal matrix composites, iron matrix, corrosion resistance, microstructure*

CHAPTER ONE

INTRODUCTION

1.1. Background of the Study

Materials, which have significantly different physical or chemical properties combine, together to form composite materials. Metal matrix composite, materials have wide area of application in daily life. Sometimes the monolithic materials cannot fulfill the demands in accordance with the modern industrial requirement and the combine properties of material is, needed, *Karl Ulrich Kainer, (2006).* The metal matrix composite material have variety of properties and can improve the limitation of the monolithic materials. Various domains of engineering application contain ferrous-based metal matrix composites material because of its wide application area, *P. Jha et al. (2021).* Iron material are fit for many constructions, shipbuilding, aerospace and automobile application.

The reinforcement material in metal matrix can have many different objectives to add on the matrix material. Some of these are, used to reduce the density of the material and the others are to improve the other mechanical properties such like compression strength, corrosion resistance and wear resistance properties. Composite materials are categorized as metal matrix composite (MMC), ceramic matrix composite (CMC) and polymer matrix composite (PMC), depending on the nature (properties) of the matrix and reinforcement material. Depending on the fabrication process to be, used and the phase needed to produce the reinforcement phase can be either particulate form or fiber form. Compared with monolithic materials the microstructure and the interfaces of metal matrix composite materials cannot be consider in isolation, they are mutually related.

Chemical interactions and reactions between the matrix and the reinforcement component determine the interface adhesion, modify the characteristics of the composite components and affect the mechanical characteristics significantly. The formation of the interface between the matrix and the reinforcing phase has a substantial influence on the production and characteristics of the metallic composite materials. The adhesion between both phases usually determined by the interaction between them. During the production of the molten matrix e.g. by infiltration, wettability becomes significant. The actual infiltration process for the production of metallic composite materials consists of several indexing steps: the formation of a contact between the melt and the reinforcement at the surface of a fiber or particle preform, the infiltration with the melt flow through the preform and the solidification procedure. At the beginning of the infiltration a minimum pressure must usually developed, so that infiltration can follow. Usually a pressure-free spontaneous infiltration is not the rule, and is only possible with thin preforms with reactive systems and with long process times, *Herbert Danninger et al. (2017).*

The reduced life time of Fe based materials due to corrosive attack causes high costs in many applications. One ways to reduce the corrosion rate of the materials is to raise the composition of chromium in the iron matrix to at least 12% *Oladayo et al. (2017).* However, many applications require resistance to corrosion and wear at the same time. Such demands can be, met by a martensitic matrix, which contains embedded carbides that exhibit sufficient wear resistance if they are harder than the acting abrasive particles and of similar size, *Karlsohn et al. (2008).* Classification of composite material with different metal matrix.

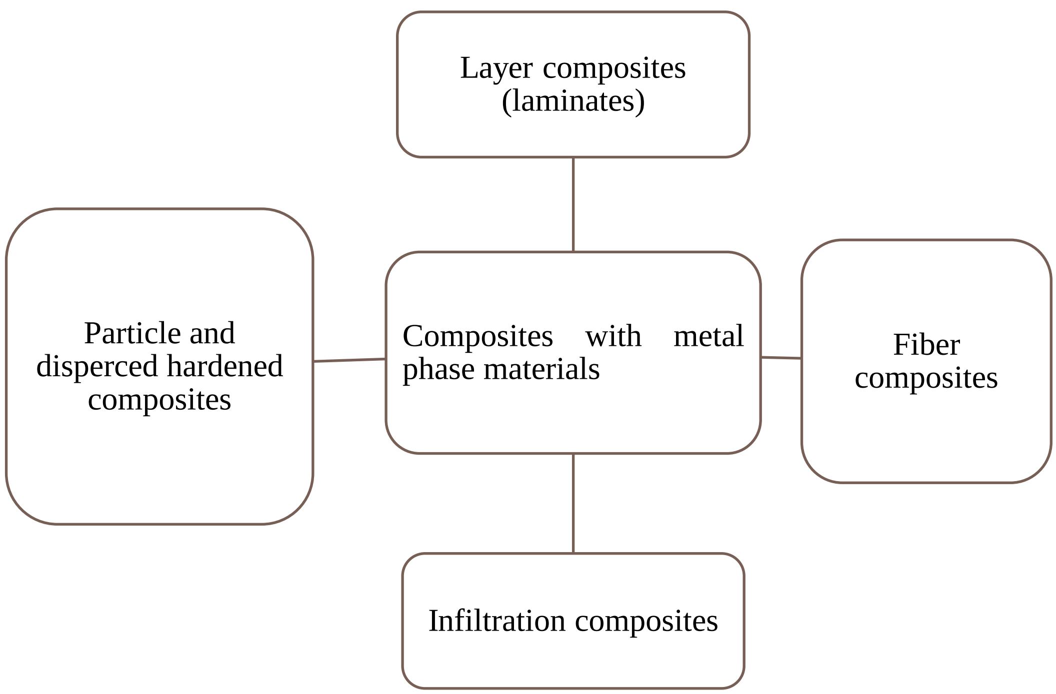

Figure 1.1 Classification of composite materials with different size of metal matrix *Karl Ulrich Kainer, (2006).*

1.2. Particle reinforcements

Depending on the size and shape of the reinforcement material, metal matrix composites can be, classified as whiskers, monofilament and particles. The shape and size of the reinforcement affect the properties of the produce material and different fabrication method is, needed. Powder form of reinforcements can be termed as particulates. For an example whiskers MMC can be produced by using stir casting and particles are usually used powder metallurgy to fabricate the product. Usually ceramic materials are used as reinforcement material because of their advantages such like low density, mechanical compatibility (a thermal expansion coefficient which is low but adapted to the matrix), chemical compatibility, thermal stability, high Young's modulus, high compression and good process ability and economic efficiency, *Karl Ulrich Kainer (2006), Ajith James Cyriac (2005).*

Adding the good corrosion resistance ceramic particles to iron metal matrix is one of the significant study of many researcher to improve the corrosion properties of the ferrous material. Ceramic material such as Al_2O_3, ZrO_2, nitrides (TiN) and carbides (TiC, WC, SiC) are usually preferred to reinforce the iron matrix. The potential commercial applications makes SiC to be considered by many as most important carbide. *W.M. Tang et al. (2003)* reported high temperature structural applications materials usually need SiC as the reinforcement material and alone because of its critical mechanical properties like excellent heat resistance. In the structural materials build from SiC material the interface between SiC and basic metal is critical. Several studies mainly concern Al-SiC systems but more recently, Iron based matrices have significantly attracted considerable attention of researchers due to their easily available because of its cheaper than that of Aluminum and good mechanical properties with higher strength compared to Aluminum *J.J. Williams, et al (2010), R Daniel de Souza Gomes1 and Claudia Giovedi (2019).*

The effect of the addition of ZrO_2 reinforcement to iron on the density and hardness of Fe-ZrO_2 by adding the ZrO_2 5%, 10%, 20% and 30% through powder metallurgy is experimented by *Jha et al. (2014)*. Engineering properties, such as mechanical strength, fracture toughness, corrosion resistance, and creep are, known to depend on the microstructure.

Generally better values of structural and mechanical properties is, carried out by many researchers for iron based metal matrix. However, based on the existing literature, Fe-SiC-ZrO_2 metal matrix composites has not been previously, developed.

Figure 1.2. The corrosion effect on fasteners *W.M. Tang et al. (2003)*

The effect of the concentration of the combine of SiC and ZrO_2 on the mechanical behavior of Fe-based composites, a detailed analysis of the impact of the concentration of SiC and ZrO_2 on the structural, morphological, and mechanical properties of Fe-SiC-ZrO_2 composites is, also reported in the present study. This will be the first report that describes the characterization of Fe-SiC-ZrO_2 composites developed through the powder metallurgy process. Moreover, to rectify the lack of reports the effect of extrusion process on the deformation behavior of developed materials.

1.3. Statement of the Problem

Iron metal matrix composites (FeMMCs) are attractive for a wide variety of aerospace, transportation, structural, automobile and defense applications. However, Fe has lower corrosion resistance, low strength to weight ratio, and high density. To overcome this problem, silicon carbide (SiC) and zirconium dioxide (ZrO_2) are, added as a reinforcement particle to improve the mechanical and electrochemical behavior of Fe metal matrix composites. The iron is one of the most versatile engineering material having all-round applications in construction, automobile, aerospace, ship, building industries etc. However, as far as the strength to weight ratio is concerned, still iron metal lack the property due to which the effectiveness of the material has been found to be less. Therefore, it is very necessary to reduce the weight of the iron metal matrix composites and increase its strength through dispersion strengthening mechanism.

Usually iron alloy are fabricated through casting process which need secondary manufacturing process such like machining that increase the manufacturing cost and it affect the overall costs of cast parts. To overcome this problem, PM technique is the most economical method for fabricating the near net shape for particulate hybrid reinforced composite. The aim of this research is to enhance the strength to weight ration and reduce the corrosion resistance of iron metal matrix composites reinforced through SiC and ZrO_2 thereby making it suitable to various industrial applications such as in construction industry, ship building and automobile etc.

1.4. Objectives of the Study

1.3.1 General Objective

Development, characterization and optimization of Physical, mechanical and corrosion behavior of Fe-SiC-ZrO_2 composites including the analysis of deformation behavior through extrusion process.

1.3.2. Specific Objectives

The specific objectives are as follows:

- Development of Fe based hybrid metal matrix composites with reinforcement of SiC and ZrO_2 with varying weight percentage.
- Analysis of microstructure, phase, gran size and particle distribution of reinforcements over matrix.
- Study physical, mechanical and corrosion behavior of Fe-SiC-ZrO_2 composite.
- Evaluate the microstructural, corrosion behavior and mechanical properties of hot extruded material.
- Multi objective optimization of the experimental results using grey relation analysis & identification of most significant control factor by ANOVA analysis

1.5. Significance of the study

This research work has both academicals and practical importance. From practical aspect, this study helps in determining the suitability of light weight high strength of iron composite materials especially for automobile and construction applications. In the academic aspect, it add more knowledge to the pre-existing researches on Fe based hybrid metal matrix and their specific application on aerospace, construction and automotive. The significance of research is as follows:

- The corrosion properties of the iron alloy material will be, improved and the work can reduce the extra of iron materials.
- It will contribute to improve the limitations of the construction material thereby improving the life of construction elements. The research goal is to produce a low-cost product which have good mechanical and electrochemical properties as high-cost materials such as stainless steel and tungsten alloy material
- This research will be as initial input for other researcher. The appealing properties of Fe-SiC-ZrO_2 composite will make them attractive for various industrial applications.
- The GDP of the nation is, expected to be, improved. Since Our country, Ethiopia has enough resource of iron ore, so preparing the method of improving iron properties and fabricated, it locally is critical issue in terms of economic benefit.

1.6. Scope of the Study

The scope of this research work is focus on the development of Fe-SiC-ZrO_2 composite material. Improvement of the mechanical and electrochemical (corrosion) properties of the material is expected from this research. Moreover, the testing and characterization of the developed samples has been, aimed for checking its suitability for construction industry and automobile. The current research have been, enlarged its scope to the study of deformation behavior and process parameter optimization of developed material through Powder metallurgy.

1.7. Thesis organization

Chapter 1 Introduction	In the earlier sections of this chapter, the basic introduction, statement of problem, objective of the work and limitation of the work is, adumbrated. The detailed contribution of the dissertation is structured, with total number.
Chapter 2: Literature Survey	The systematic exhaustive detail literature review focused on the work already available was briefly, presented. The review is typically divided into four primary sections: the first pertains to the previous knowledge on the effect of different reinforcement material on iron based MMC the second is, the effect of hot extrusion on the mechanical and electrochemical behavior of the iron based metal matrix reviewed. Methodology for process parameter optimization through Taguchi based grey relation analysis is, also mentioned. The application of the iron based hybrid metal matrix is, reviewed.
Chapter 3: Materials and Methodology	Experimental procedure for the work are, presented in this chapter. Testing and characterization process of produced sample briefly presented. The effect of extrusion through the die was, analyzed by comparing the properties before and after extrusion.
Chapter 4: Results and Discussions	In this chapter, results and discussion of several tests for both sample before and after extrusion are combined.
Chapter 5: Conclusions	The conclusions of this work is done depending on the results. The future recommendation and suggestion are mentioned in this chapter. Over all concluding remarks along with the future scope of the research were outlined in this section.

CHAPTER TWO

LITERATURE REVIEW

2.1. Introduction

This research work focuses on the preparation of the Fe-SiC-ZrO_2 hybrid metal matrix composite by powder metallurgy process. The scope of this thesis also includes work on multi objective optimization of processing parameters through a study the effects of different processing conditions and parameters on density, hardness and corrosion properties. Microstructure, phase morphologies and mechanical properties like compression test also studied. The secondary operation so called extrusion is also performed to study the effect of extrusion process on the mechanical (hardness, compression), microstructure and electrochemical (corrosion resistance) performance of the material.

This chapter provides a review of the published literature on introduction to composite materials and its fabrication processes, the effect of different reinforcement particles on mechanical properties and electrochemical properties of the matrix material. The microstructures characterization and optimization of process parameters of metal matrix composites through powder metallurgy have been, reviewed to place the research problem in perspective. The review also include for the principles of extrusion and its parameters include the factor affecting the extrusion process. Literature also extended for the concept of optimization process. From the summery of this literature review, the gap areas are, identified, then, discussed for further investigations and studies.

2.1. Classification of Metal Matrix Composites

Depending on the size of the reinforcement material, metal matrix composite classified into three main categories.

- Particle reinforced MMCs
- Short fiber or whisker reinforced MMCs
- Continuous fiber or sheet reinforced MMCs

Among those types of the metal matrix composite particle, reinforced MMCs have become popular and very important for many, reason. Inexpensive of the process is one of the reason for the importance of discontinuous reinforced MMCs. Compared to fiber, reinforced composites they have also relatively isotropic, *Karl Ulrich Kainer (2006).*

The particulates reinforced metal matrix composites (PMMCs) is one of the new structural materials, and a rapid development can be seen in recent years because of excellent properties and wide application prospects in the near future. For several years, research on fabrication methods and material property estimations for particulates reinforced metal matrix composites has been one of the focuses in composite fields. Various materials have been combined with each other and give intended properties and are different from their base materials. Such composite materials make this concept true and reinforcement in a matrix of this material contributes enhancement properties. But, neither matrix nor particulate alone but only MMCs can able to fulfil the requirement. In general, PIMCs are manufactured either by solid state (P/M processing) or liquid state (stir casting, infiltration and in-situ) processes. PIMCs are less expensive compared to CFIMCs. Mechanical properties of PIMCs are inferior compared to whisker/short fibre/continuous fibre reinforced IMCs but far superior compared to unreinforced iron alloys. These composites are isotropic in nature and can be subjected to a variety of secondary forming operations including extrusion, rolling and forging, *Dharmendra Kumar Singh (2014).*

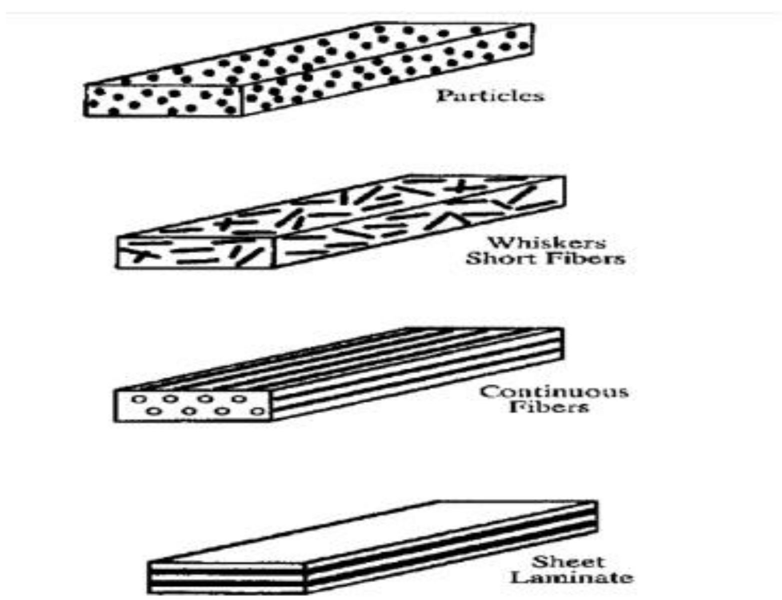

Figure 2 1. Types of reinforcement depending on size and orientation.

The Short fibre or whisker-reinforced metal matrix composites (SFMMCs) contain reinforcements with an aspect ratio of greater than five, but are not continuous. Whisker reinforced composites are produced by either by PM processing or by infiltration route. Mechanical properties of whisker-reinforced composites are superior compared to particle or short fibre reinforced composites. The strengthening provided by the short fibers is less than long fibers. This is because a segment at each end of the fiber is not fully stressed. The matrix transfers the applied stresses to the fibers through shear stresses occurring at the interface. Here the finite length at each end of the fiber reaches a maximum.

The Continuous fibre-reinforced metal matrix composites (CFMMCs) having reinforcements are in the form of continuous fibres (of alumina, SiCp or carbon) with a small diameter. The fibres can either be parallel or pre woven, braided prior to the production of the composite as shown in Figure 2.1 IMCs having fibre volume fraction up to 40% are produced by squeeze infiltration technique. The strength and failure mode of aligned continuous fiber matrix composites depend on the angle (θ) between the applied stress (σ) and the fiber direction. The maximum strength output is obtained when θ = 0 degrees, it is called longitudinal strength. The applied stress is shared between the fibers and matrix. The stress is transferred to the fiber by the shear stress at the fiber/matrix interface *Ajith James Cyriac (2011).*

2.1.1. The effect of different reinforcement material on properties of iron based MMCS

Jha et al. (2013) show that the reaction between Fe and ZrO_2 takes place during the sintering process, leading to the formation of nano size Zr_6Fe_3O. Therefore, the researcher conclude that increase the ZrO_2 content have positive effect on the reactive phase formation. Nano size dispersion of the Zr_6Fe_3O phase and dense phase microstructure is, reported from the SEM and XRD results. Varies phase formed of Zr_6Fe_3O during the variety of temperature and time was affect the density and the hardness from the experimental study. Study for two types of sintering methods, solid state sintering and reactive sintering. for solid state process show no change in the fraction of ceramics reinforcement in the composites and due to the densification process the metallic characteristics is increased. The hardness of the specimen is increase due to the presence of ceramic phase during reactive sintering process. The decreasing of the hardness with increasing the sintering time was also, reported during the solid state sintering. Reactive sintering is leading to increase when the sintering temperature is increase and the formation of ceramic Zr_6Fe_3O nanoparticles is takes place.

Poornaprakash et al. (2011) carried out the densities of the pellets by the water immersion method. The experimental study show that as the amount of SiC is increase the crystallite size gradually increases. Researcher was used Debye–Scherer equation to determine the average grain size of composites. Both dry and wet milling mechanical alloying processes used simultaneously to fabricate Fe-SiC composites with the various composition of SiC (15%, 20% and 30%). Improved mechanical properties like Poisson's ratio and elastic moduli are, reported with increasing the content of SiC. Decreasing density is, reported during the increase the content of SiC, which resulted due to sub grain strengthening. Carried out the effect of particle size of iron and size of reinforce particle on properties of materials. The systematical study is determined using current direct heating dynamic hot press sintering.

Oladayo et al. (2017) presents the effect of the zirconia on the corrosion properties of ductile iron. White silica sand, bentonite, water, cylindrical pattern, scraps engine block, zirconia powder of 50nm particle size and Ferrosilicon are, used as a materials, for the research work and sand casting techniques is, used to produce the samples. Variations of 0.2 vol%, 0.5vol%, and 1vol% and 2vol% zirconia reinforcement were added on the iron matrix to improve the corrosion properties. The potentio-dynamic polarization for the ductile iron and its alloy were, investigated in 3% NaCl and the highest corrosion resistance is, reported for 2% of zirconia. Hence, the results indicated that the addition of calculated amount of ZrO_2 into the ductile iron could result in good corrosion resistance of the composite compared to pure ductile iron.

Wang, M et al. (2021) carried out the effect of SiC and SiC + Ti_3AlC_2 on iron matrix and optimization process of the fabrication parameters. The average particle sizes of the SiC and Ti_3AlC_2 powders were ~10 µm and ~5 µm, respectively. Each mixture of powders was, mixed for 5h in a planetary high-energy ball mill and compacted under 40MPa through cold-pressing machine. From the reported results, most of the iron powders were approximate ellipsoid and the reinforcements were uniformly distributed. No obvious particle agglomerating or iron powder breakage was, observed. Irregular-shaped islands could be, seen in the samples with Ti_3AlC_2 and uniform distribution of the SiC particles over the matrix is, observed through XRD analysis of the samples. The researcher carried out that the relative density decreased with an increasing particle content in the samples that were, reinforced only by SiC from 95 to 93%.

Yufang Yanga and Kangju Li (2012) investigation is done on iron matrix with SiC as reinforcement material and inveterate the optimum particle size. Better mechanical properties reported with the big particle size of the iron powder and the reason believed the large size particle of iron powder contribute better effect on dispersion of reinforcing particle. The hardness is increase with the increase particle size of the material. The hardness and tensile strength properties of the composite materials increase at 50.6µm of particle size of the matrix and 15µm particle size of reinforce materials.

Saxena et al. (2019) developed the sample of Fe-Si based metal matrix reinforced with Al_2O_3 to study the phase, microstructure, and wear properties. Using 2 wt% and 5 wt% of Si and rest Fe powder mix and fabricated by powder metallurgy and sintered process at different temperature schedules. Phase formation, microstructure, and mechanical behavior of prepared composites affected by the amount of Si in matrix phase, ceramic reinforcement (Al_2O_3) contents. Fe–Si phase formation, and better mechanical behavior reported during the increasing of sintering temperature and time and the maximum phase formation is, achieved at 1200°C for 3h. As a result, of solid state the diffusion between the present elements were reported. Using the SEM the grain size, their distribution, and densification behavior in the specimens is, shown. The uniform distribution of phases in the wt. % 5 of SiC with 95 wt. % of Fe is observed in the micrograph. The presence of the pores through the specimen and the grain size is, observed starting from 260nm during the process. The bond between iron and silicon is better when 2% is, added and the brittle behavior is observed when more Si is added which is due to the insufficient bonding. The strongly bonded structure reduces the wear rate of the specimen. Wear rate of specimen is calculated using 0.5, 1.0, 1.5, and 2Kg on the, basis of total volume loss occurred during the experiment and the specimen with 5wt. % of Si and 95wt. %Fe which sintered at 1000°C, show less wear loss at low load condition. The hardness of the specimen is, reduced with the increasing the Al_2O_3 content from 5% to 10% due to the insufficient bonding between ceramic and matrix material.

Fradaric John.C (2017) the galvanic coupling of aluminum with a noble reinforcement was proposed, by many researchers, as the main corrosion enhancement mechanism in Al – 12Si – ZrC, when exposed to chloride containing solutions. The particulate MMC was, produced by powder metallurgy followed by hot extrusion. Average corrosion weight loss for composite after 28 days exposure demonstrated higher corrosion rates with increased Al size and volume fractions. The number of pit initiation sites appears to increase with the volume fraction of the reinforcement. SEM micrographs for Al – 12Si – ZrC immersed in aerated 0.1N HCl, 0.1N H_2SO4 and held at a potential of 150 mV more positive relative to the open circuit potential. Reported, larger pits in the Al–12Si–ZrC in material.

2.2. Metal Matrix Composites Fabrication Techniques

Several techniques have been, proposed to produce the metal matrix composites, namely, stir casting, powder metallurgy, two-phase processes, deposition techniques and in situ processes, *M. Rosso (2006).* Among them, powder metallurgy is unique fabrication techniques as it has the ability to produce high quality, complex parts to close tolerances in an economical manner.

2.2.1. Stir casting process

In this fabrication technique, the reinforcements are, introduced into a molten metal, then liquid composite is, cast into various shapes by conventional casting techniques or can be cast into ingots for secondary processing and finally the system ends up by solidification of matrix phase. To achieve the better mechanical properties of composite, a good wettability between the dispersed phase and the molten metal is required. In some cases, in order to improve the wettability between the dispersed reinforcement and matrix phases, wetting agents such like MoS_2 can be, added into the liquid. One of the advantages of this fabrication is its manufacturing ability for large number of MMCs, *Babak Jahani (2016).* The reinforcement material are preheated in order to avoid thermal mis-match and improve its mixing ability with the matrix material. Thermal mis-match create during the stir casting has significant effect. The quality of the composite sample can achieve with proper wetting between the reinforcement particles and matrix alloy *Honnaiah. C et al. (2016).*

2.2.2. Powder metallurgy

Powder metallurgy is a flexible manufacturing process capable of delivering a wide range of new materials, microstructure and properties. It is applicable for versatile industrial material and automobile parts. Powder metallurgy is the manufacturing process which done by blending powdered materials, compacting into desired shape, and then sintering the compacted material in adjusting temperature to bond the material. Powder metallurgy include cold pressing and sintering or hot pressing to produce primarily sample. The most process for the techniques of powder metallurgy is mixing the powder of metal matrix and reinforcement material by using the ball milling to control the distribution of the reinforce particle. The main step for powder metallurgy techniques is Powder production; Compaction, Sintering, & Secondary operation such like machining, extrusion and other finishing process. Now days, Powder metallurgy is become very effective techniques for the production of composite materials *Saxena et al. (2019).* Powder metallurgy is critical techniques to produce components with good mechanical and tribological properties such as strength, hardness, impact resistance and wear resistance. The major factors to be, controlled in fabrication are size of powder, milling time and method, pressing pressure of dies, sintering temperature and time and cooling type. The hardness of the product depends on the sintering temperature, weight, sintering time, powder size, *A. Loganathan. (2010).* The advantages and disadvantages of powder metallurgy techniques as shown on Figure 2.2.

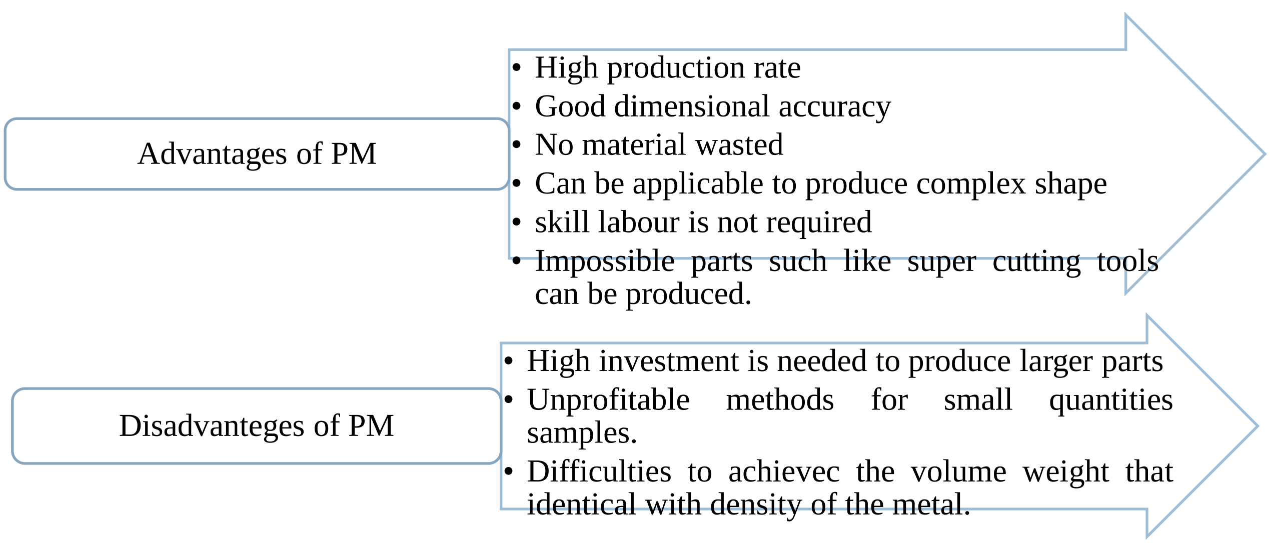

Figure 2.2 Advantages and disadvantages of powder metallurgy methods.

2.2.2.1. Effect of process parameters of powder metallurgy

A. Powder blending/Mixing

Mixing the powder of the same chemical composition of the same or different sizes by mechanically or manually is called blending process. Blending of ceramic particles with matrix is a key step of powder metallurgy and it facilitates the uniformity in the shapes of powder particles to control homogeneity of the final distribution of the reinforcement particles. Proper blending of matrix and reinforcement powders can reduce the agglomeration of the powder particles and porosity in green compacts after compaction. Different methods can used to blending the powder. Ball milling is the versatile method used for blending of metal powders into desired size. The size of particles have its own effect on the sintering process and small particles sinter faster than coarse particle size, *Debasis Chiara (2021).*

During the mixing process, the rotational speed of mixer has an important role and optimal mixing of powder occurs at 75% of critical speed. Bending also used to reduce the friction between die wall and powder during compaction. The ball milling process is significant to achieve the homogeneous distribution of the reinforcement into metal matrix, *Vemula Vijaya Vani and Sanjay Kumar Chak (2020).* Blending time is vary from few minute to several day depending on the material to be mix and the results desired, *Katerina Skotnicova et al. (2015).*

Powder blending is done, because of its significant effect on the properties of the composite material. Significant strain hardening occurs, which is dependent on the particle diameter and content. Generally, higher hardening contributions are made by smaller particle diameters than by coarser particles. For smaller particle diameters the work hardening and the grain size influence contributes the most to the increase in the yield strength, *Karl Ulrich Kainer (2006).*

B. Compaction techniques

Under high pressure, powders are compacted by various methods such as die compaction, cold isostatic compaction, cold forging and warm compaction, where the application of pressure packs the powders and reduces porosity. Several methods of powder compaction shown as Figure 2.3 below. During die compaction, pressure applied to the powder with punches that move in the vertical direction and green density increases with increasing compaction pressure. The general die compaction process illustrated in Figure 2.3. For die compaction, a lubricant such as graphite should be applied between the die wall and the powder. This is because the friction between the powder and die wall during die compaction leads to an inhomogeneous density distribution, which causes residual stresses in the green body. This may cause unwanted defects, such as pores and cracks in PM parts during subsequent high temperature consolidation, *Honnaiah. C et al. (2016).*

The addition lubricant materials such like MoS_2, Mg, paraffin waxes are necessary to provide the desired compaction properties. These lubricants used to reduce the friction between die and powder to be compact during the fabrication process. Wettability is one factor of the powder metallurgy and it affect the properties of the production. Several methods of powder compaction are, grouped into two types.

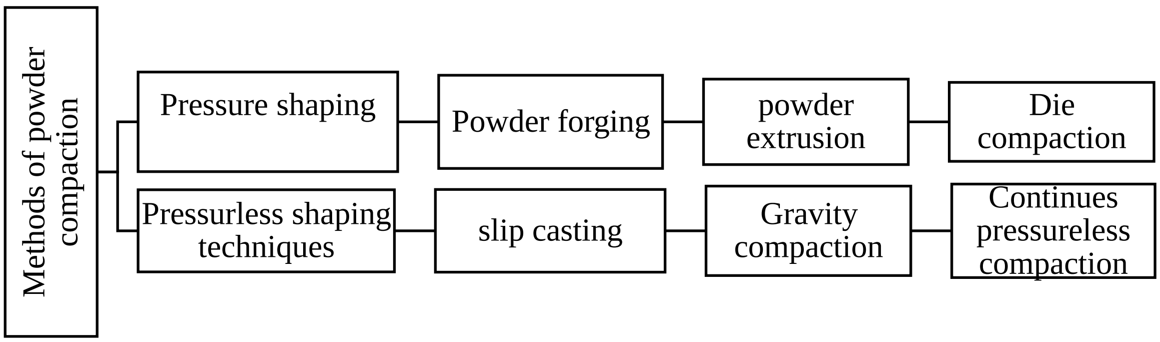

Figure 2.3 Classification of composite materials with different size of metal matrix

The addition of Lubricant into the powder is, used to decrease the friction between the die and the powder during the compaction process. As the compaction pressure is increased, ejection of green

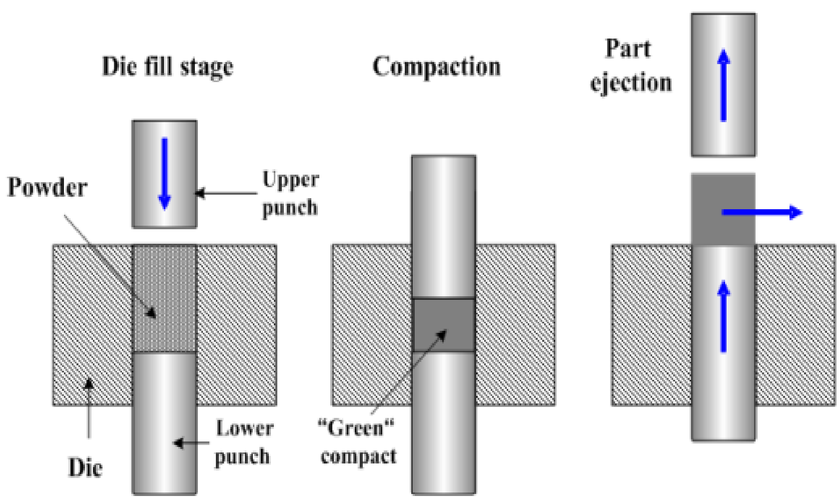

Figure 2.4 Powder compaction process redraw from Huiyang Lu, (2016)

Powder mass from the die becomes more difficult. Lubricants used to minimize die wear, and ease ejection after the green compact is form. Usually the 0.5 to 1.5 wt. % of soft material such like Ca, Zn, Li and Mg are added to the material to be pressed as lubricants.

C. Sintering process

Sintering is the process which, compacted composite material chemically bond themselves into a coherent body under the influence of an elevated temperature. After cold compaction is done, the pressed ‘’green compact’’ is then usually taken for sintering. During sintering, the green compact is usually heated in a protection atmosphere such as argon, hydrogen or nitrogen. The individual powder's particles (which were either loose or physically bonded together) are bonded to produce a solid structural part with the desired properties. Several changes take place during sintering process like shrinkage, formation of solid solution and development of the final microstructure. In many cases, sintering results in reduction/elimination of porosity and leads to densification. Sintering is the culmination of powder processing operations, which determines the final product, *Edyta Wyszkowska (2015)*. During this process, the green compact is consolidated forming its final shape and microstructure. Sintering process is influenced by several factors:

- Temperature
- Time
- Atmosphere
- Pressure (during green compact production)
- Pressure during sintering
- Particles dimensions and shapes
- Phase changes
- Formation of liquid phase

The sintering temperature done below the melting point of the matrix material and usually it carried out at 60 to 75% of the melting point of the components. The sintered parts usually promote the densification or shrinkage of the parts, however, by controlling the different parameters sintering can take place without any shrinkage; no net dimensional change is quite possible. Sintering is a complex process and it can have different stages, driving forces and material transport mechanisms for any given metal and set of sintering conditions, *G.S. Upadhyaya (2002)*, *Katerina Skotnicova et al. (2015)*. These parameters used to control the complexity of the sintering process.

Figure 2.5 Stage of sintering process Katerina Skotnicova et al. (2015).

The sintering temperature significantly affect the structure of composites materials, highly bonded structure is, obtained due to higher diffusion rates. By applying sintering process after the compaction of powder at controlled atmosphere physical and mechanical properties of the materials can improved, *Adnan Khan et al. (2020).* Densification also occur during the sintering process. The innovative ultra-fast sintering technique called electro sinter-forging (ESF) was, evaluated in the densification of Fe-Cr-C steel by *Gobber, F.S et al. (2021).* This innovative process is used to reduce sintering time and as promoter for metal matrix composites because of its fast process. There are two types of sintering process depending on the presence phase namely liquid Phase and activated sintering methods. Liquid phase methods of sintering technology is widely made in the field of sintered steels, cemented carbides, heavy alloys, bronzes and silicon nitride systems. The rate and magnitude of any change occurring during sintering is increase with increasing the sintering temperature. The effect of the sintering time is small in comparison to the sintering temperature.

Porosity occur during sintering is difficult to avoid completely because of the loss of driving force due to increasing time at any temperature. The desired properties should be, achieved by controlling both sintering temperature and time, *G.S. Upadhyaya (2002).* The significant advantages of electro-sinter-forging (ESF) led to the emerging of novel applications and forming and sintering process can done using one machine to achieve near net shape in a very rapid process. Comparison to conventional sintering the ESF has low wear of tooling and generally higher precision of parts produced. The process is relatively simple and the have technical and manufacturing advantages to combine with the possibility of creating innovative materials such as metal composites and diamond composites with high performances, properties, and extremely high densities *Gobber, F.S et al. (2021).*

Sintering mechanism have two types of transport mechanisms namely; surface transport and bulk transport. A neck is, formed, when sintering takes place between two particles. Bulk transport generally occurs at high temperature and surface transport occurs at low temperature. No shrinkage or densification takes place in surface transport mechanism, since mass originates and terminates at the surface. Shrinkage or densification is takes place in bulk transport mechanisms. The mass originates at the particle interior and deposits at the neck. Bulk transport mechanism includes volume diffusion, grain boundary diffusion, plastic flow and viscous flow, *Debasis Chiara (2021).*

2.3.Effect of parameter of PM on the properties of metal matrix composites

P. jha et al. (2021) produce the sample Iron with (10, 20 and 30) wt.% of ZrO_2 by powder metallurgy method. Developed the mathematical models to predict the density and hardness of Fe-ZrO_2 metal matrix composites. The experiments were, performed on the plan of response surface methodology (RSM)-based Box–Behnken design. From the experimental analysis weight percentage of ZrO_2 affects, the hardness of the material was reported. The significance of the process parameters on the density and hardiness was, analyzed with ANOVA. The interaction term (sintering temperature, sintering time, and weight percentage of reinforcement material have P-value greater than 0.05. The density of the sample was, affected by the sintering time, weight of ZrO_2 and its interaction. Optimization analysis was, applied for hardness and density. Sintering temperature (900–1100°C), weight percentages (10–30) of ZrO_2, and sintering time (1–3 h) are the main parameters these considered for the investigations. Minitab software is used to develop the mathematical models and is more establish the relationship and to understand the effect of process parameters (sintering temperature, wt.% of ZrO_2 and sintering time) on the responses (density and hardness) is more establish relationship and create more understanding with the developed mathematical model.

Amarjit Singh et al. (2021) Study the compaction and the densification behavior of iron powder and coal fly ash (CFA) mixtures during powder metallurgy (P/M) processing. Ball milling process is used to mix the iron particle with the different amount of CFA in the presence of toluene.

Flowability and compressibility characteristics of the starting materials were, estimated using the Hausner ratio and Carr's index and Archimedes principle is, used to estimate the sintered densities of the compacts after it cool down. Increasing the amount of CFA results for significant improvements in the flowability and compressibility behaviors of iron. The fundamental consideration for the successful fabrication is higher green density and the study show the CFA has the significant effect on the fabrication performance. The enhancement of compacting pressure affect the green density of the sample.

Kumar and A.K. Das (2020) investigated the influence of ceramic (SiC) on the wear behavior and hardness of 10%, 20%, and 30% SiC by weight of steel material. The specimen prepare from AISI 304 stainless steel plates of dimension 100 mm × 50 mm × 8 mm, were cut and ground with 220 grade emery paper. The Fe powder with the size: 40–50 μm; and pure SiC powder were prepared with different weight percentage of reinforcement material. Wear test were carried out using pin-on-disc type tribometer at 20 N normal load, fixed sliding speed of 250 rpm and radius of sliding path 15 mm. Wear test show that when the content of SiC reinforcement increase in the matrix the wear mechanism transform from severe plastic deformation to brittle fracture. Coating of 304 steel with the SiC reinforced Fe-based composite is successfully developed and there is no major defect in the interface zone. The composition amount of the wt. % of SiC in coating is directly influencing the hardness of coating, therefore, maximum micro hardness was measured as 663 HV0.1 of 30%-SiC reinforcement. TIG surface modification technique is used to coating process and the process is successfully, performed.

Zhongsheng Liu et al (2010) The overall best properties of the Fe based SiC reinforced composites is investigated with 5wt% of SiC sintered at 950°C ,96% in relative density, 4121 MPa in hardness and 646 MPa in bending strength. The three-point flexural strength test was, carried out. Comparative study results between the Fe/SiC (Cu) and Fe/SiC under 950°C. Fe/SiC composites are that SiC particles are not mixed with the iron to sinter directly and the strength of Fe/SiC(Cu) is greater than that of Fe/SiC composites. When the SiC content increases, the flexural strength and hardness are significantly higher than that of pure iron. The sintering shrinkage and densification in the matrix are, affected by the SiC particles. Densification of the specimen is became difficult with the increasing the contents of SiC particle. A proper amount of Cu can improve the property of the Fe/SiC composites.

J. Pelleg (2009) Mixtures of Fe and 5% SiC chopped fibers were prepared by vibration to increase the density. Varies mechanical tests include ultimate tensile strength (UTS), yield stress (YS) and Vickers hardness (VHN) are determined. The Fe matrix is complete sintered at 1173 K without void formation at grain junctions. No significant reaction has taken place between the SiC particle and the matrix during the sintering at 1173k temperature. When the temperature is, rise from 1173 to 1373 K complete disintegration of the SiC particles has occurred and the matrix structure was composed of pearlite and ferrite. Ball milling is preferential into grain boundaries of the matrix at the beginning stage of the fabrication to enhance the strengthening by increasing the distribution of reinforcement through the matrix. The effect of the grain size and estimate strength to be, expected from composite is study by using Hall–Petch relation.

Gupta et al. (2015) Investigated corrosion characteristics of Iron (Fe)–Alumina (Al_2O_3) metal matrix nanocomposites (MMNCs) which synthesized by powder metallurgy (P/M) technique. The iron alumina metal matrix is, produced using different weight percentage of Alumina and Green specimens prepared by compacting under a load of 7 tons. The specimen also sintered in an argon atmosphere in the temperature range 900 - 1100°C for 1 - 3 hours. The formation of nano size iron aluminate can affect Wettability, Hydrophobicity, and Roughness of the surface. It decrease the wettability and roughness of the composite and increase the hydrophobicity of the specimen. These properties are significantly affect the corrosion resistance of the specimen. Carried out from the study the corrosion characteristics of the nanocomposites were much better than that of pure iron specimen this is due to the formation of nano iron aluminate phase during the increasing of sintering temperature. The formation of reaction between iron matrix and alumina particles due to optimum amount of nano iron aluminate phase for this temperature and time of sintering is at 900°C and for 2 hours respectively. This optimum amount and specific sintering temperature and time are, used to improve the corrosion resistance of the nanocomposites specimen.

Oladayo et al. (2017) carried out, the effect of zirconia dispersion on mechanical and corrosion properties of iron based metal matrix composites. Ductile Iron composite sample was produced by sand casting process with varied percentage composition of zirconia and mechanical test like hardness and tensile are conducted for different sample which develop with different percentage composition of zirconia ceramic particles. With regard to electrochemical, the effect of the zirconia on the corrosion property of the composite in 3M NaCl solution at room temperature was reported. The polarization curves was, measured at a scan rate of 0.2mV/s. With the variations of 0.2vol%, 0.5vol%, 1vol% and 2vol% zirconia reinforcement, the corrosion potential of the samples alloyed with 2% ZrO_2 moved to a less negative potential (from 0.66229V to 0.59948V) and the reason is reported is due to the addition of zirconia, which have a good corrosion resistance properties. Resistance of the composite against corrosion is increase with the increasing the zirconia reinforcement. Researcher also reported the hardness of the iron based composite also increase with the increasing of the zirconia reinforcement.

2.4. Secondary operation

In most of the cases the primary product manufactured by powder metallurgy route need the secondary treatment in order to improve the mechanical properties of the component. The process also helps in the distribution of reinforcement particles, removal of internal pores, and improved uniformity in density across the product as well as removal of oxide layers by the internal particle shearing effect. The secondary operation can give the final product a better surface finish and dimensional tolerances. For the specific cases, where there are ceramic reinforcements, secondary processes like extrusion, rolling, forging help to improve the metal-ceramic bond strength and consequently the properties of the product improves, *Sambit Kumar Mohapatra (2016).* This process leads in turn to enhancement of ductility, then both hardness and wear resistances get increase and enhance.

2.5. Extrusion process

The process of confining the metal in a closed cavity and then allowing it to flow from opening to achieve the desired shape is, called Extrusion process. The equipment consists of a cylinder or container into which the heated metal billet is loaded. On one end of the container, the die with the necessary opening is fixed. From the other end, a plunger or a ram compress the metal billet against the container wall and the die plate, thus forcing it to flow through the die opening, acquiring the shape of the opening. The extruded metal, then, carried by the metal handling system as it comes out of the die. Secondary process like extrusion is, performed to enhanced properties like higher strength, stiffness and weight savings in comparison to other materials. Particle reinforced MMCs are attractive due to their cost-effectiveness, isotropic properties, and their ability to be processed using similar technology used for monolithic material, *Honnaiah. C et al. (2016).* The process also helps in the uniform distribution of reinforcement particles, removal of internal pores, and improved uniformity in density across the product as well as removal of oxide layers by the internal particle shearing effect. Better surface finish and dimensional tolerance can achieve during the secondary operation, *C. Venkatesh1, and R. Venkatesan (2014).* In this research, hot extrusion done in order to check the deformation behavioral of the sample and to analysis, the effect of extrusion on the corrosive properties of iron based composites.

2.5.1. The effect of extrusion process on MMCs materials

Metal Extrusion is a metal forming manufacturing process in which a cylindrical billet inside a closed cavity is, forced to flow through a die of a desired cross section. These fixed cross sectional profile extruded parts are called "Extrudates" and pushed out using either a mechanical or hydraulic press. The extrusion technique was developed in 1797 by Joseph Bramah was first used to extrude lead pipes by Thomas Burr. Extrusion process can should be, applied for the improvement of densification and hence mechanical properties for powder metallurgical process can be, achieved with size reduction. The process performed with hot extrusion or cold extrusion depending on the goal, *Honnaiah. C et al. (2016).* Thus, the compacted product can be, implemented in structural application. Both the wear resistance and corrosion resistance has been improved with the extrusion process for composite material. In this process, the cross sectional area of the specimen is reduced as per the design of the die. Many researcher are done on the area and few of paper are, reported with iron base material.

Kuhnke et al. (2020) determined varies factors which affect the extrusion force in the quasi-steady state. This experiment show that Temperature of the billet materials as well as friction between copper and die cone are the main factors. The increase in profile exit temperature suggests an increase in billet temperature and therefore the reduction in flow stress for both billet materials. The DEFORM 2D used in order to investigate the material flow in indirect extrusion of CCA rods. The aluminum core is, exposed to compressive stresses while high tensile stresses prevail in the copper sleeve due to different flow velocities. During the variation of temperature and lubrication condition fluctuation of tensile stress is, reported and it is stable during constant temperature. By the means of FE-analysis and validated by comparison with longitudinal cross sections of the extruded rod material flow during sleeve fracture was visualized. With continuation of the composite extrusion possibly lost contact of copper and thermocouple is regained, the strain rate recovers and the temperature increases again. Stepwise shape of the temperature curve is, formed due to sequence repeats sleeve fracture.

Sambit Kumar Mohapatra (2016) The FEM analysis results through DEFORM 3D is agree with the experimental values. Both round and square profile die used to extrude and Al-6063 is used as extrude material. The techniques can take as a better predictor before the experiment to control the different parameter by using optimal value. The less influence of ram velocity on strain rate is, reported during cold extrusion process. Cosine dies need less load the linear converging for the extrusion operation. At optimum die length, the maximum load required for extrusion by cosine die is 2-3% less than that of linear converging die. The flow behavior of metal inside the container, conical and inner punch cone is, significantly influenced by punch shape. Significant improvement on the grain refinement and bond strength of composite material during the analysis of extrusion is, reported. Design of the die also have significant effect on the wear condition create during the extrusion process.

Abdul Nazeer and Mir Safiulla, (2020) determined the effect of secondary processing (Cold Extrusion) on mechanical and wear properties of Al6063 reinforced with SiC, Al_2O_3 and CeO_2 particles. Stir casting used to produce the composite sample by varying reinforcement from 0% to 8% in steps of 2%. Extrusion process with an extrusion ratio of 1.93 with a total strain of 1.45 applied after casting the composite. Observed that an improvement in ultimate tensile strength of cold extruded composites is appreciably high, when compared with their cast counter parts. Among all composite studied Al6063+CeO_2 for 8wt% has lowest wear rate. As the content of reinforcement increased, the mechanical properties have increased. Cold extruded composites possess the lowest wear rates. Impact strength also improved after extrusion process is, done. Matrix alloy exhibits the least reduction in the impact strength values after cold extrusion (4.6%). Increase of the yield strength with the increasing of SiC particle were reported. Improvement difference for all sample is the same both during the extruded process and due to the addition of reinforcement particle.

Metal extrusion process can be sub divided and grouped into the following categories depending on the medium used to apply force, direction of extrusion flow, working temperature, etc.

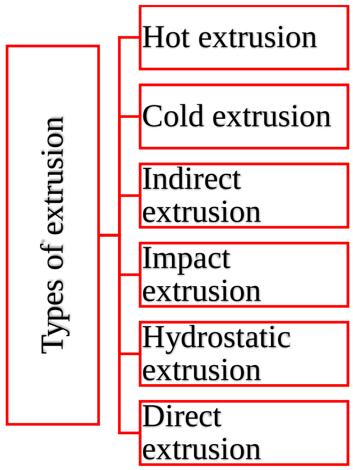

Figure 2. 6 The types of extrusion process

2.5.2. Cold and hot extrusion

Some important advantages of cold extrusion are increased strength due to strain hardening, close tolerances, improved surface finish, absence of oxide layers, high production rates because of no need of the addition of time to preheating the billet. The starting billet in direct extrusion is usually round in shape, but the final shape is, determined by the shape of the die opening. Obviously, the largest dimension of the die opening must be smaller than the diameter of the billet. The direct extrusion can be, used for both hot and cold extrusion process and simple tooling compared to other extrusion process. No need modification for the billet during the direct extrusion. Good surface finish parts could produce with cold extrusion. High strength due to strain hardening, improved accuracy, high rate of production are also the quality of cold extrusion process. The challenge in cold extrusion process is the tool subjected to the higher stresses due to apply the higher pressure. Proper lubrication is necessary for preventing seizure of tool and work piece. Phosphate coated billets are lubricated with soap.

Hot extrusion can be, applied for higher extrusion ratios. Inhomogeneous deformation can occur due to die wall chilling of the billet. Metal may get, oxidized. The oxide layer can increase friction as well as the material flow. Glass is, used as lubricant for hot extrusion.

Molybdenum disulfide or graphite are the solid lubricants used in hot extrusion. Canned extrusion using thin walled cans made of copper or tin is usually, used for extruding highly reactive metals and metal powder *Hassanein Ibraheem Khalaf (2016).*

The advantages of extrusion process

- Low cost due to reduced raw material wastage and high production rate.
- Material can be, deformed without tear as it only exerts compressive and shear forces in the stock part, so it can be, recommended for composite material.
- Parts that formed have excellent surface finish, which minimizes post-processing machining.
- Metal extrusion tends to produce a favorable elongated grain structure in the direction of the material.
- The process could achieved for the minimum wall thickness of ~1mm (aluminium) to ~3mm (steel) during the process.
- The grain structure and strength properties are enhanced in cold and warm extrusion.

2.5.3. Factor affecting the extrusion process

Extrusion is an extremely flexible manufacturing process, as a single press can be used to extrude various materials and a large number of profiles by simply changing the die and the associated tooling with it. Extrusion Process is highly influenced by the process parameters required for determining the quality of process and extrude. Factors that affect the quality of extrusion are die design, extrusion ratio, billet temperature, lubrication, and extrusion speed. The extrusion process involves calculation of certain parameters. The cross-sectional area of the specimen is reduced as per the design of the die.

2.5.3.1. Design of die

The punches and dies used in cold extrusion are, subjected to severe working conditions and are made of wear-resistant tool steels, e.g., high-alloy chromium steels, *P.Tiernan et al. (2005).* The critical parameters for the die design are die angle and orifice shape. Low angle of the die leading to increased friction at the die–billet interface because of its large surface area of the die is create. On the other hand, a large die angle causes more turbulence in the metal flow during reduction, increasing the ram force required. Larger ram force create the more friction during the process, *Hassanein Ibraheem Khalaf (2016).*

Die materials used for hot extrusion include tool, alloy steels and carbides. Important properties of these die materials include high wear resistance, high hot hardness, and high thermal conductivity to remove heat from the process. Die materials for cold extrusion include tool steels and cemented carbides. Wear resistance and ability to retain shape under high stress are desirable properties. Carbides are, used when high production rates, long die life, and good dimensional control are required, *P.Tiernan et al. (2005).*

2.5.3.2.Temperature and ram velocity

Sambit Kumar Mohapatra (2016) Present that controlling the temperature is the key factor in extrusion, which decides product quality and life of the die. During extrusion, the temperature at die exit is high which decides the microstructure and surface property of the product and improves the die abrasion that causes the error in shape and dimensional tolerances of the extrudate. The flow of the metal improve with the higher extrusion temperature but the temperature has its negative effect the other properties of the material. The less influence of ram velocity on strain rate is, reported during cold extrusion process. Due to extrusion process, the grain refinement improves which in turns improve the mechanical properties of composite. Higher temperature generated due larger friction which recrystallization and grain refinement takes place.

2.6. Multi-objective optimization

Optimization techniques are, designed to determine the 'best' operating variables of a system that can create the highest achievable levels of performance for the system under the existing constraints. There different methods of optimization, which can be used, for different applications based on process design considerations. These methods can be, divided into two main groups, a) deterministic methods and b) probabilistic methods. In deterministic methods, the outcome could be exactly predictable, but in probabilistic methods, only few estimations could be possible on the outcome. Single performance characteristics can be, easily optimized by Taguchi method. However, it is a challenging task for analyzing and solving multi performance characteristics. GRA is one of the techniques used for optimization of control factors having multi-performance, *Dharmendra Kumar Singh (2014).*

Anand et al. (2021) were carried out research on optimization of process parameters in powder metallurgy of AA6061 alloy+ wt.% SiC using grey relation approach. This paper describe the selection of powder metallurgy parameter reinforcement percentage, compaction pressure, sintering time fabrication process of metal matrix composites material to optimize the performance parameters like density, hardness and wear using grey relational approach. The experimental work in this research is, carried out to know effect of process parameters on the hardness and corrosion rate. Grey Relational grade is, used to find the optimal parameter.

A common problem is to optimize the values of several responses simultaneously. This occurs quite frequently, because many products have to meet several different goodness criteria. The problem in such applications is that the individual optima can be contradictory, i.e. the optimal values for one of the responses may be far from the optimal values for some other response. Several different techniques, such as finding the so-called Pareto optimal result, exist.

2.7. Fe-SiC-ZrO_2 hybrid Composites

Recently many scientists and engineers motivated to study new composite materials because of its wide application and improved properties. Metal matrix have been studied and improved time to time. In recent years, many studies were, reported on using of conventional ceramics as reinforcing phase in composites with metal matrix of aluminum, copper, iron, cobalt and their alloys, *Sachin (2015).* The most commonly used ceramic particles include oxides (e.g., Al_2O_3 and ZrO_2), nitrides (e.g., TiN and Si_3N_4), and carbides (e.g., SiC, TiC, Cr_3C_2, VC, WC and B_4C) *Daud, S. N. A., et al. (2019).* Among the reinforcing materials for MMCs, in recent year's hybrid metal matrix have received special attention by engineering world. Among these common ceramic reinforcements, SiC and ZrO_2 are being vastly used for reinforcing steel matrix, due to their high thermal stability at higher temperature, good wear resistance, good corrosion resistance, high hardness, low density and their relative stability with steel matrix *P. Jha et al. (2021), Daud, S. N. A., et al. (2019).*

These types of composites are promising candidates for many applications in the ground transportation, thermal management, aerospace, recreational and infrastructure industries. SiC and ZrO_2 can be, considered as a main candidate for reinforcing the MMC composites with applications where hardness, high melting point, chemical inertness, radiation stability or light, weight are expected.

2.8. Possible Applications of Metal Matrix Composites

Many of light alloy composite materials have, in automotive engineering, a high application potential in the engine area (oscillating construction units: valve train, piston rod, piston and piston pin; covers: cylinder head, crankshaft main bearing; engine block: part-strengthened cylinder blocks). In the aviation industry the high specific strength, the high Young's modulus, the small thermal expansion coefficient, the temperature resistance and the high conductivity of the strengthened light alloys are of interest compared with polymer materials, e.g. for reinforcements, axle tubes, rotors, housing covers and structures for electronic devices, *Karl Ulrich Kainer (2006).* In ceramic/iron, (ferroalloy) matrix composites are more suitable for wear resistant materials at high temperatures than aluminum matrix with lower melting point and lower strength. Among various ceramic reinforcing phases, silicon carbide ceramics are, often used in the industrial production of steel matrix composites due to its low price and better thermal matching performance with steel materials. The zirconia ceramics is, usually used to improve the corrosion properties of the iron matrix at high temperature, *Oladayo et al. (2017).* Depending on these properties of iron based metal matrix have wide application area in automobile, military equipment, industry and construction materials, *H.M. Zakaria (2014).* For the Construction materials like bolt and nut, rivets, and other fasteners, the improvement of wear and corrosion resistance is critical. Fastener material can be important when choosing a fastener due to differences between materials in strength, brittleness, corrosion resistance, galvanic corrosion properties and, of course, cost.

2.9.Research Gap

Even though several research has been done on development and mechanical characterization of Fe-based reinforced composite and few research on electrochemical properties, of SiC and ZrO_2 reinforced Fe based hybrid composite was not yet done. More over deformation analysis with extrusion process for Fe- SiC-ZrO_2 hybrid composite was not widely investigated before. In addition to this design of experiment for optimizing the physical, mechanical and electrochemical property of the composite with finding best parameters combination was done mainly for single response optimization but for multi response optimization it was rarely done.

CHAPTER THREE

MATERIALS AND METHODS

3.1. Introduction

This chapter consists the materials used for the fabrication of iron based hybrid metal matrix composite, fabrication approach and methods for samples preparation, experimental procedure and set ups for testing activities. The instruments and equipment's used and methodology of data analysis are organized in the current chapter. The place where the experiment and characterization is conduct also mention with some specific parameter. The steps for optimization process, formulas and ASTM standard for different experiments and tests also mention under the chapter.

3.2. Materials

3.1.2. Matrix and reinforcement materials

Commercially available Iron powder with 99.8 wt.% purity (prepared by Jhd, Shantou, China) was considered as the matrix for composite preparation. Table 3.1 presents its chemical composition of iron matrix material, which used in current research work. The iron particles had an average size of less than 200µm. Powder metallurgy technique was, adopted to develop Fe-SiC-ZrO_2 composites. Detail properties of Fe particles are, shown in table below Table 3.2.

Table 3.1 Chemical composition of matrix powders

Alloying elements, wt.%				
S	N	Cu	SiO_2	Fe
0.06	0.005	0.005	0.1	Balance

Table 3.2. Physical and mechanical properties of the Fe material.

Properties	Properties the matrix material (Fe)
Density	7.874g/cm^3
Melting point	1538°C
Modulus of elasticity	200 GPa
Hardness	HRB 79
Compression strength	220-2520MPa

3.1.3. **Silicon carbide (SiC) reinforcement particles**.

Silicon carbide is non-oxide ceramic material made up of silicon and carbon atoms. SiC ceramic rarely found in natural as mineral, but it has been, produced in powder form. Usually Silicon carbides powder had the average size of ~350 nm *Grzegorz Królczyk et al. (2020).* Detail properties of SiC particles are, shown in table below Table 3.3 and Figure 3.1(b) show the powder of silicon carbide particles. The basic reasons for choosing the SiC reinforcement are its low cost and easy commercial availability, high corrosion resistance as well as higher hardness. By adding the SiC reinforcement on the iron matrix, corrosion properties and mechanical properties such like hardness and compression strength can be improved.

Table 3.3 Detail properties of SiC particles

Properties the reinforcement material	Properties the reinforcement material
Name of material	SiC
Density	3.217g/cm
Melting point	2730°C
Modulus of elasticity	410 GPa
Hardness	2800 (HV)
Compressive Strength	3900MPa

3.1.4. Zirconium dioxide reinforcement particles

Adding zirconium reinforcement on iron matrix can improve the corrosion resistance of the iron based material, *Oladayo et al. (2017).* The physical and mechanical properties of the zirconia are shown in the Table 3.4 below. The powder of zirconia to be, used is shown on Figure 3.1(c). The basic reasons for choosing the ZrO_2 reinforcement are its high corrosion resistance as well as higher hardness at high temperature.

Table 3.4 Physical and mechanical properties of zirconium dioxide

Properties the reinforcement material	Properties the reinforcement material
Name of material	ZrO_2
Density	5.68g/cm^3
Melting point	2,715 °C
Modulus of elasticity	94.5 GPa
Hardness	1220(HV)
Compressive strength	3000Mpa

Figure 3.1 Powder of (a) iron, (b) silicon carbide, (c) zirconium dioxide

3.1.5. Die material for powder metallurgy and extrusion process

Compaction and extrusion die materials were procured for designing, fabricating and heat-treating them to required hardness and toughness. High carbon (C) and high chromium (Cr) cold work steel, generally known as D3 die steel was, used for fabrication of die extrusion. The studies shows that the higher hardness and wear resistance of die steel make it suitable for tooling applications such as extrusion, powder metallurgy tooling, draw dies, and blanking and forming tools, *Avadesh K Sharma (2020) Sambit Kumar Mohapatra (2016).*

3.2. Methods

Over all steps for sample fabrication and characterization is described in diagram for below in Figure.3.4. The Powder metallurgy process steps including: mixing, forming (compaction), and sintering as well as the other fabrication process and testing steps are listed. Figure 3.4 presents a general flow chart for current research work. Initially, raw materials obtained from commercial then alloy powders are mixed together with different additives (e.g. MoS_2). Before going to thesis work the preliminary work were done. The different characterization and optimization is done for physical, mechanical and corrosion behavior of Fe-SiC-ZrO_2 composites.

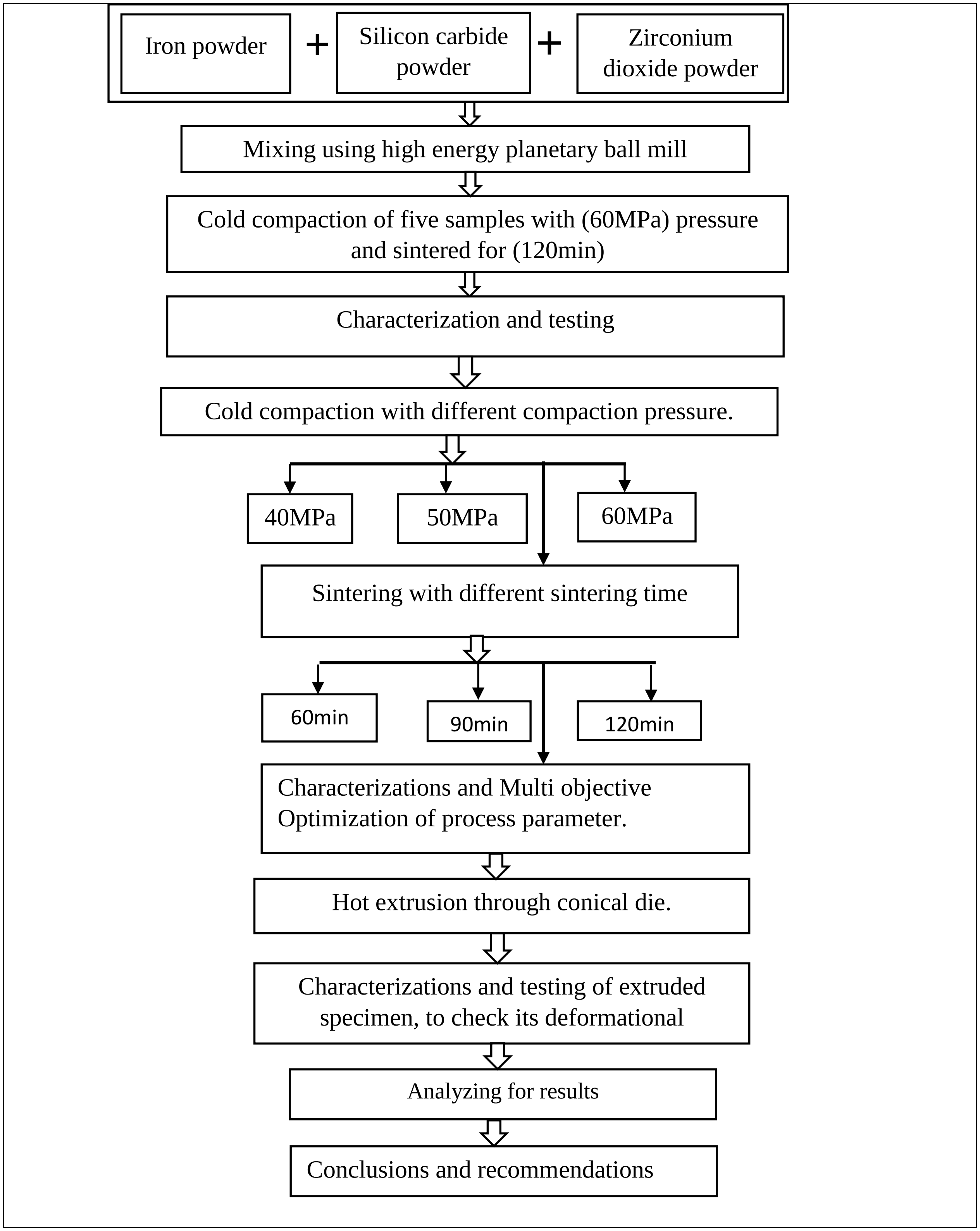

Figure 3.2. Methods for the current research work.

3.2.1. Fabrication of samples through powder metallurgy

The samples fabricated and tested to check whether it can produce through powder metallurgy and not. Several studies have shown that molybdenum disulfide enhances sinter ability and the densification process during sintering of steel composites. Densification leads to improved mechanical properties that is a factor to consider when determining why molybdenum disulfides provides its lubricating properties when prepared with powder metallurgy. As shown on Table 3.5 the five sample fabricated as first round, to check the manufacturability and the basic properties of the hybrid composite materials.

Table 3.5 the hybrid composite fabricated by powder metallurgy

Sample number(designation)	**Sample**
S1	$Fe+5\%SiC+10\%ZrO_2+4\%MoS_2$
S2	$Fe+10\%SiC +5\%ZOr_2+4\%MoS_2$
S3	$Fe+7.5\%SiC +7.5\%ZOr_2+4\%MoS_2$
S4	$Fe+10\%SiC +10\%ZOr_2$
S5	Pure iron

3.3. Sample Fabrication method

3.3.1. Blending of Powder

Reinforcement particles SiC and ZrO_2 powder at different volume levels were mixed with Iron powder for 3hr using high energy (planetary) ball /mill machine (which available at material department, ASTU, according to ASM V.7.). Proper blending of matrix and ceramic powders reduces the agglomeration of the powder particles. Over mixing leads to reduction in flow characteristic of the mix, leading to poor homogeneity in particle distribution *V.V. Vani and S.K. Chak (2020).* The weight ratio of zirconia ball to powder was maintained 10: 1. At a speed of 200rpm for all composition, the mixture was, allowed for blending and homogenously mixing. In general, lubricant was added and homogeny blended to reduce friction between the powder mass and the surface of the die and obtain a good compaction.

Figure 3.3. High energy planetary ball mixer used to mix the powders.

3.3.2. Powder compaction

After mixing powder for desired blending time, the 12-13-gram Fe-SiC-ZrO_2 powder was poured in to die cavity. The powder was compacted by applying load with 40, 50 and 60MPa different pressure at uniform rate for each composition of sample through the application of hydraulic pressing machine for 30min holding time. The basic purpose of compaction is to obtain a green compact with sufficient strength to withstand further handling operations. These compaction pressures are used for cold pressing iron-based metal matrix *Babak Jahani (2016).* Therefore, a green compacted sample having 20mm diameter and various height depending on the applied pressure and compressibility of the matrix and composite. The effect of pressure on the density and hardness of cold-pressed samples was investigated to find the optimum applied pressure for cold pressing. Typically, tool of the hydraulic pressing machine in the vertical orientation with the punch tool forming the bottom of the cavity, as shown in Figure 3.4 below.

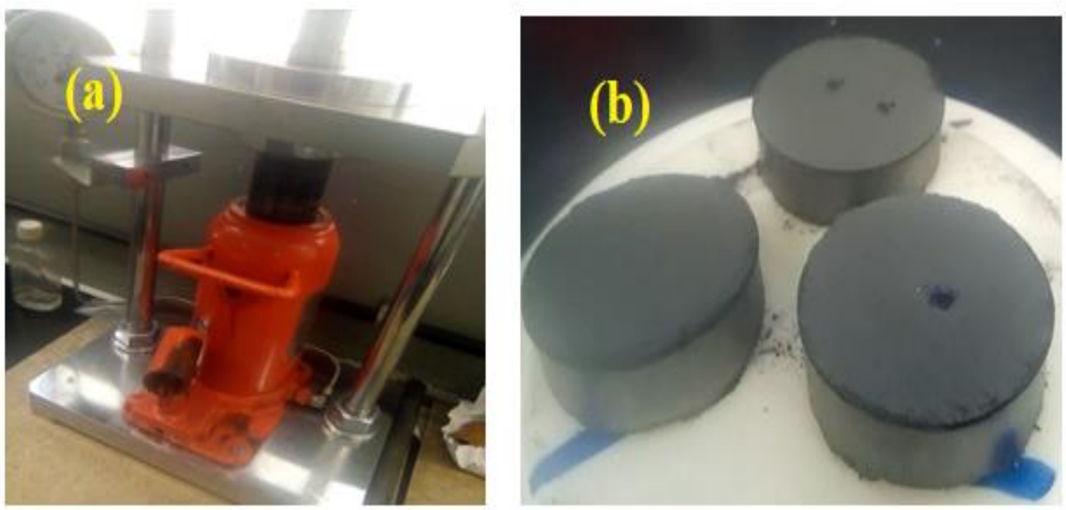

Figure 3.4 a) Powder compaction process through hydraulic pressing machine and b) green compacted samples (S1, S2, S3).

3.3.3. Sintering process

Cold pressed samples were subjected to sintering in air controlled furnace at sintering of temperature of 1000℃ at 10 different dwell times for sintering time of 60,90,120min. It is the process of consolidating either loose aggregate of powder or a green compact of the desired composition under controlled conditions of temperature about 70 to 90% of absolute melting point and soaking time *Dharmendra Kumar Singh (2014)*. After the targeted dwell period, the temperature of the sample was, allowed for furnace cooling.

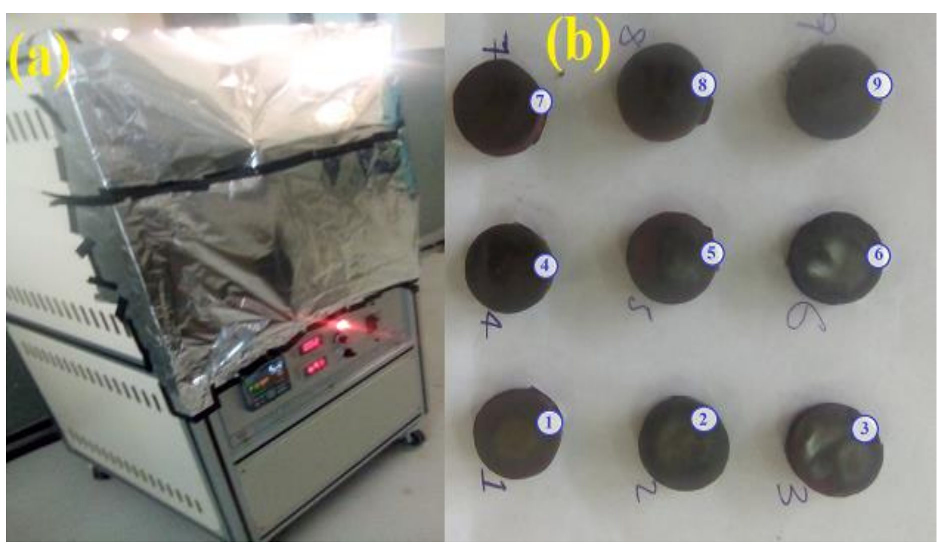

Figure 3.5.Sintering furnace experimental set up (a) and sintered samples (b)

3.3.4. Design and Fabrication of die parts

The die used for the process is a mathematically contoured cosine die developed for round to cylindrical shape extrusion. A 2D and 3D model of the die set with the above-mentioned design parameters was prepared using SOLIDWORKS modeling software as shown in Figure 3.6 below. A D3 die steel stock of 95 mm diameter and 50 mm diameter was, procured from MIDI (Addis Abeba, Ethiopia) and cut into the required size for die chamber punch and guide plate with power hacksaw. The pre- machining of die chamber, punch was, done by facing, turning, drilling and boring operation on lathe machine. Heat treatment of die cylinder and punch set was, done in muffle furnace after the pre-machining in three steps as stress reliving, hardening and tempering. Stress relieving was, done at 650 °C for one hour and cooled slowly. For hardening, the die parts were, directly placed in a furnace preheated to 1000 °C, soaked for 25-30 minutes, and then quenched in still air to harden it. The parts were, placed in the furnace for tempering and the temperature of furnace is increased, to desired tempering temperature (900°C) and cooled slowly in furnace. Finally, the surface finishing operation of die parts was, done using cylindrical grinder.

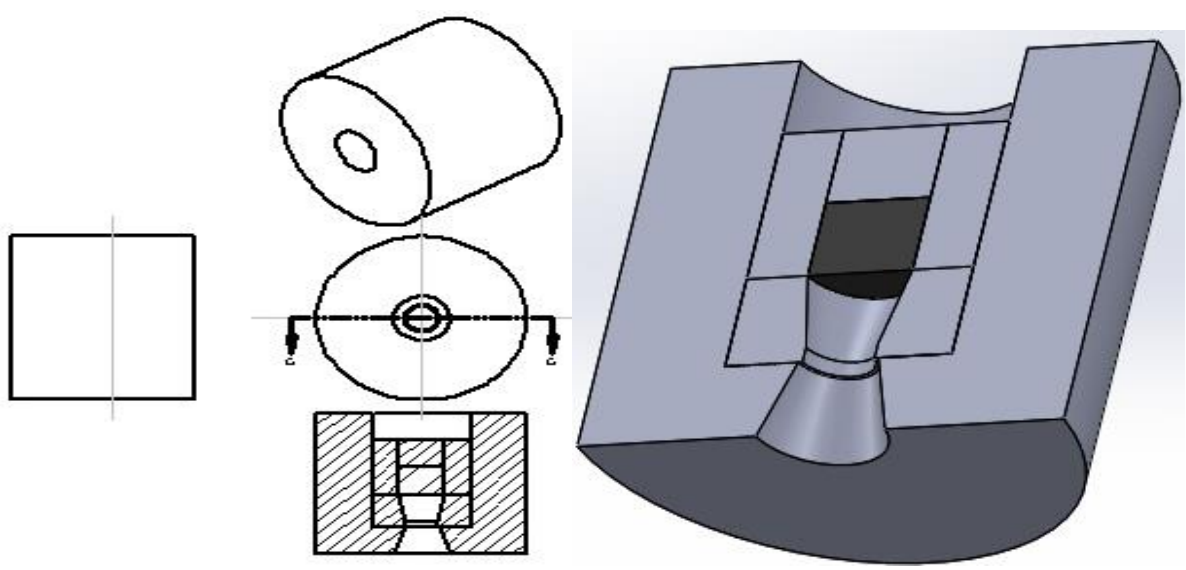

Figure 3.6 Schematic drawing with (a) 2D and (b) 3D model of assembly extrusion die

3.3.5. Hot extrusion process

Before proceeding towards the hot extrusion process, the sintered billets of Fe with different percentage composition of SiC and ZrO_2 composites were soaked at 800 ◦C to 900 °C, for 10min to homogenous the sample temperature throughout the volume. The solid lubricant graphite powder is mixed with semi solid lubricant grease and applied the mixture to the inner surface of the die in order to decrease the friction during extrusion process. Graphite is often used as a solid lubricant for its cheapness and availability combined with an often-low friction coefficient. A necessary condition for graphite to be lubricating is that the environment is humid (e.g. air), which reduces the material's shear strength to satisfying levels. The 25mm length specimen prepared by cold compaction followed by sintering was, subjected to hot extrusion as a secondary processing. Hot extrusion then took place at an operating temperature of 800◦C-900◦C with a ram rate of 3 mm/min and extrusion ratio of 7:2 (Extrusion Ratio = area of billet/area of shape) using a 1500KN hydraulic press as shown on Figure 3:12 below. Normally, acceptable extrusion ratios for hard alloys, are limited to 35:1 and for soft alloys, it is 100:1. The normal extrusion ratio range for hard alloys is from 10:1 to 35:1, and for soft alloys is 10:1 to 100:1. These limits should not be considered absolute since the actual shape of the extrusion can affect results *Sambit Kumar Mohapatra (2016).* The higher the extrusion ratio, the harder the part is to extrude which is the result of the increased resistance to metal flow. Hard alloys require maximum pressure for extrusion and are even more difficult because of their poor surface characteristics, which demand the lowest possible billet temperature. Since the Fe-SiC-ZrO_2 composite is hard material because of SiC and ZrO_2 the current work used 7:2 extrusion ratio. In the present work, the composite samples are, hot extruded from 12mm diameter to 9mm diameter.

Figure 3.7 Hot extrusion set up during operation

3.4. Specimen preparation and testing process

After successfully fabricate the composite sample and sintered, the composite was then prepared for a different characterization and testing process such like microstructural, mechanical test, physical, characterization, and corrosion test. In order to achieve the desired shape for the process the developed sample were going to the below process. For physical, mechanical, and corrosion tests, the specimen is prepared to the required shape and size according to desired shape and size by machining on a lathe. Chemical etchant was also used to prepare a specimen for microstructural characterization of the composite. Required shape and size for different process as per ASTM standard machining on lathe and cutting using abrasive cutter was, done.

- Grinding, Polishing and Etching of specimens

The desired size of the sample has been, subjected to Grinding and polishing to remove the cut marks; levels and free from excessive deformation. After cutting the specimen to desired dimension, ground the surface of the sample with sandpaper of grit sizes of 120, 400, 800, 1200, and 2000 grits. After grinding, to removes the artifacts of little stock and make the surface mirror polishing was, performed by adding diamond suspension. When doing this, moderate Pressure is, needed at the start of each step and then gradually reduce the Pressure to keep the specimen from plastic deformations. A two-wheel system, motor control, 50 to 500 rpm, RB 204 Metpo-II Model polishing machine was, used. After the specimen is grinded gradually, it subjected to etching using Keller's chemical etchant was done. Etching is the process of making microstructural features through selective chemical attack to present the grains and grain boundaries clearly.

3.4.1. Microstructure characterization

All Iron metal matrix samples fabricated by optimized P/M process were cross-sectioned, mounted using epoxy (Thermoset acrylic) as shown in Figure 3.9; all samples were grinded and polished prior to microstructural observation. The microstructures of samples were observed by scanning electron microscopy (SEM) and optical microscope (OM). Microstructural characterization of sintered specimen is quite essential for the determination of microstructural features. The influence of processing parameters on the microstructure of PM parts has been, extensively investigated *Jha et al. (2013) N. Chawla, X. Deng (2004).* Improved microstructure of PM parts is a function of homogenous distribution of the reinforcing/alloying phase over the matrix. Sample preparation for examination was, done by grinding through 600, 800, 1200 and 2000 grit papers followed by polishing with alumina paste. The cross section of sintered samples were, etched with Keller's reagent to obtain a better contrast. The etched samples were, dried and the microstructure was, observed by using Optical Microscope (OM) at different magnifications. In the present investigation, 5x and10x magnifications were, used to calculate grain size and distribution of reinforcement particles in the iron matrix. In order to further explore the reactions between the reinforcing particles and the iron matrix, an EDS analysis was carried out in the (SiC-ZrO_2)/Fe composites. Average grain size of optical microscopy image is done using ImageJ software. Image analysis was performed to determine (a) presence, location, size and distribution of porosities, (b) morphology and distribution of reinforcing particles, (c) bonding and interface of matrix and reinforcement. Crystallite size also determine using XRD data. The relationship between the crystal grain size and the full width at half maximum (FWHM) of diffraction peak was deduced by Scherrer for the first time, known as the Scherrer equation as shown in equation (3.1). The result obtained from the Scherrer equation is actually the grain height perpendicular to the crystal plane. By using the Scherrer equation, we can quantitatively calculate the relationship between the FWHM of diffraction peak and the crystal grain size. The Scherrer equation shown as

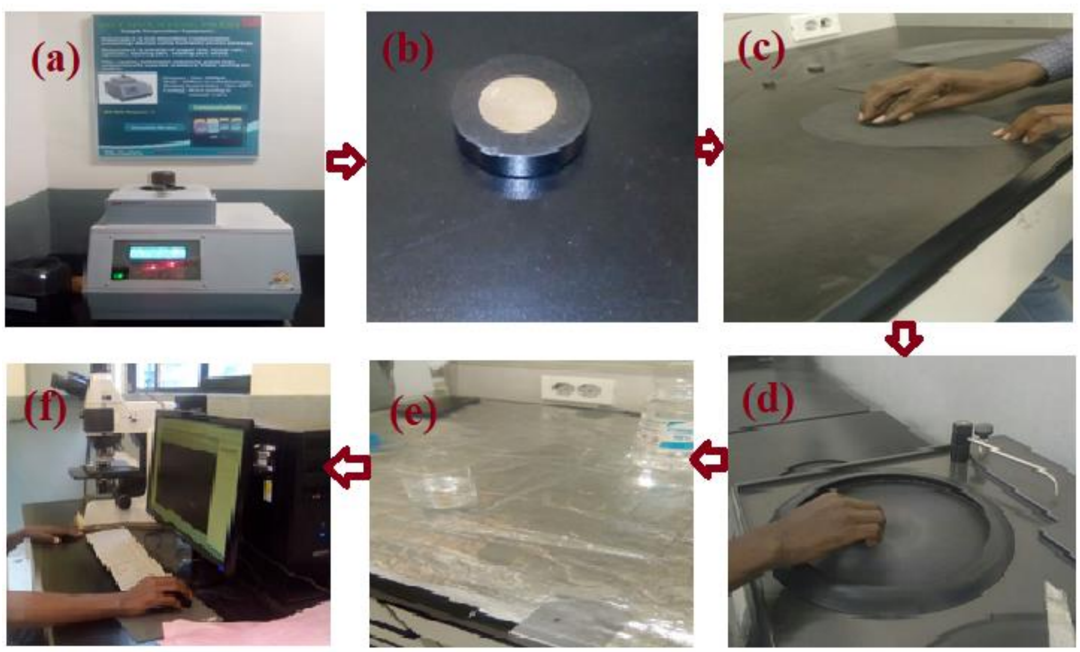

Figure 3.8 Specimen preparation process set up for optical microscopy (a) mounting (b) mounted sample (c) (d) polishing (e) etching (f) OM observation

$$D = \frac{K\lambda}{\beta \cos\theta} \tag{3.1}$$

Where

D crystallite size

λ XRD radiation of wavelength (nm)

K is Shape factor can be 0.62 - 2.08.

β Measuring full width at half maximum of peaks in radian located at any 2θ in the pattern

Phase analysis of sintered samples was, performed via X-ray diffraction (XRD, at ASTU) observations with Cu Kα radiation at 40 kV and 40 mA. Phase identification and quantitative phase analyses were, performed via Rietveld analyses using the X'pert High score software.

3.4.2. Density measurements

The density of the sample was, examined after sintering. Densities of the solid sintered as well as extruded specimen were, measured by following Archimedes' principle. In this principle, the mass of the specimen is to be, measured in air and in a selected fluid. The relation for calculating the density is, presented as follows:

$$\rho_{Sample} = \frac{W_A * \rho_{fluid}}{W_A - W_{fluid}} \tag{3.2}$$

Where W_A is the weight of the sample at atmospheric air, W_{fluid} is the weight of the considered sample in a fluid and ρ_{fluid} is the density of the considered fluid. Processed composites were, measured five times each to get an accurate density. Density of the specimens was determined from the mass and dimensions. The fluid considered for the measurement was distilled water because its density is 1 gm/cc3 (ρw = density of distilled water at 25°C = 997.044 kg/m^3) at normal temperature and pressure condition *Sambit Kumar Mohapatra (2016)*.

As shown in Figure 3.8, the densities of the specimens were, measured by Archimedes' principle using water immersion method at room temperature according to ASTM B962-15 using the Equation (3.3).

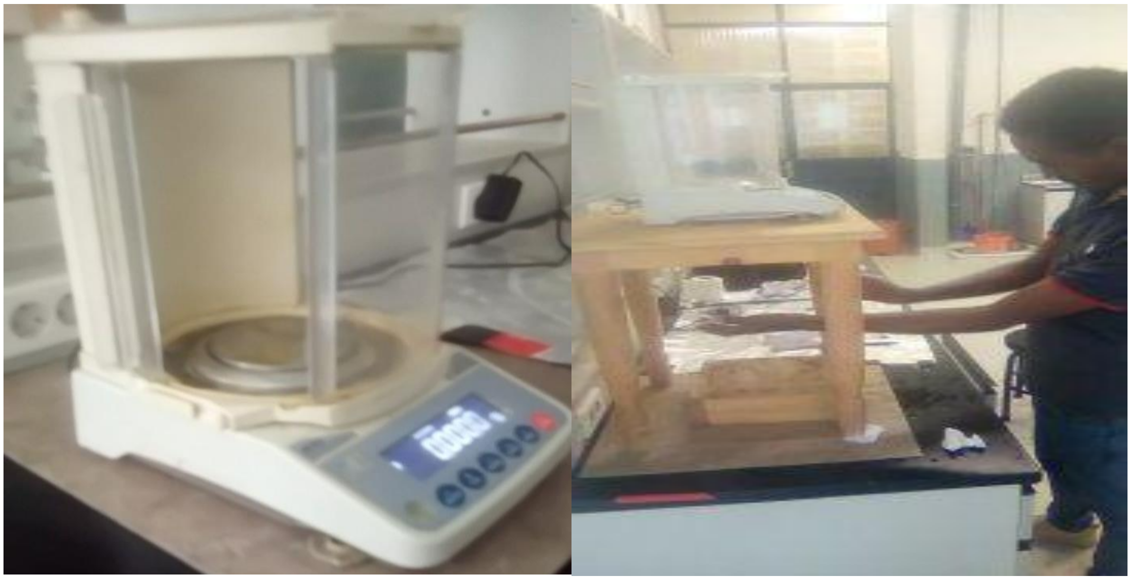

Figure 3.9. Density measurement by Archimedes method.

The percentage improvement in densification by hot extrusion is calculated, by the relation illustrated as follows:

$$Percentage\ improvement\ in\ densification = \frac{extruded\ density - sintered\ density}{sintered\ density} \qquad (3.3)$$

3.4.3. Hardness Test

The hardness test was carried out using micro Vickers hardness tester (Model: HVS-50 PC), test was carried out at a load of 10kg and a dwell period of 7 seconds was maintained to avoid spring back effects, as per ASTM standard E92-17 . The sample surface was, given a fine finish by polishing it through series of emery papers of increasing grit 800 up to 2000 before going to hardness test. Vickers hardness of the sintered MMCs was then determined by dividing the applied load to the impressed area. The load was, applied through a diamond pyramid having the face angle of 136° between the opposite faces at the vertex. Hardness test in porous materials associated with a big variations in test results, to minimize uncertainties arising from this variation, at least three tests at random locations were, done on each sample to minimize the effect of the inhomogeneity of the microstructure and to make sure that all phases and features were, covered by indenter. The results were, reported as the average value along with Standard Deviations (STDV).

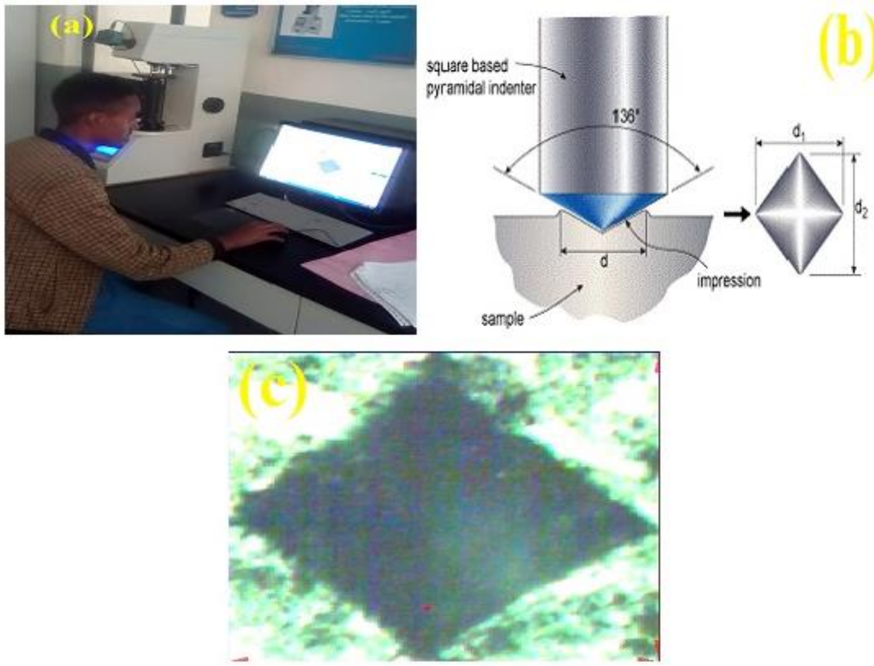

Figure 3.10. Schematic view of (a) hardness test observation (b) angle of pyramid indenter and (c) actual indentation shape during micro hardness test.

$$HV=P= \frac{\text{constant X test force}}{\text{surface area of indentation}} = \frac{0.102x2F(\sin\frac{136^2}{2})}{d^2} \qquad (3.4)$$

Where F is loading force, α indenter with angle (136°), d is leaving an indentation with a mean diagonal, on the material specimen.

3.4.4. Compression Test

Compressive strength of a material is, defined as the ability of the material to withstand compressive loading without failure. Compression test is done by compressing a standard specimen using a UTM, analyzed as per the ASTM standards such as ASTM E9 with length of 25mm and 12.7mm diameter. The effect of the reinforcement composition, compaction pressure and sintering time on the compression test is, done. ASTM E9 testing covers the apparatus, specimens, and procedure for axial-load compression testing of metallic materials at room temperature. The data obtained from a compression test may include the yield strength, the yield point, Young’s modulus, the stress-strain curve, and the compressive strength. Actual Young's modulus can be expressed as:

$$E = \frac{stress}{strain} = \frac{\sigma}{\varepsilon} \tag{3.5}$$

where

- E is the Young's modulus (modulus of elasticity)
- σ Stress
- ε strain

Figure 3.11. Universal testing machine setup used for compression test

An objective in the development of light metal composite materials is to increase the modulus of elasticity (Young’s modulus). Which potential arises here, can be estimated by the mixture rule, whereby the well-known border cases apply only to certain geometrical alignments of the components in the composite material. The universally used models are the following linear and inverse mixture rules: Although the rule of mixtures (ROM) can be applied to determine the Young's modulus of composites *Karl Ulrich Kainer (2006),* mostly in continuous fibers reinforced composites, many studies, *Delavari et al. (2011)* suggested the ROM is invalid in the estimation of Young's modulus for particle-reinforced composites. In this case, the Tsai-Halpin equation, *M. Wang et al. (2014)* can be utilized to predict the Young's modulus for such composites.

$$E_c = \frac{E_m\left(1+2S\eta V_p\right)}{1-\eta V_P} \tag{3.6}$$

In the Eq. (3.6), the parameter η is given by the following equation

$$E_c = \frac{(\frac{E_P}{E_m} - 1)}{(\frac{E_P}{E_m} + 2S)} \tag{3.6a}$$

Where E_m and E_p are the Young's modulus of the matrix material and reinforcement particles, respectively. Vp is the reinforcements particle volume content in the composite; S is the particle aspect ratio.

3.4.5. Corrosion test

Corrosion tests were carried out by immersing the specimens in a bath of 3% NaCl for 2hours. The specimens for the tests were, cut to size 12mm diameter and 8mm length. Composite specimens were polished with emery polishing paper 800 no. and then with 12 µm diamond paste on a double disc polishing machine to remove any sort of stray marks from the surface of the specimen and to make it mirror polished. The electrochemical measurements were performed in a three electrode, cell using an electrochemical analyzer (SP−300 EC-LAB, BioLogic Science Instruments, ASTU, Material science laboratory). Iron based composite specimens with an exposed area of $1cm^2$ were, used as working electrodes, graphite electrode was, used as an auxiliary (counter) electrode, and standard calomel electrode (SCE) or mercury was used as reference electrode. Tafel curves were obtained by changing the electrode potential automatically from -250 to + 250 mV versus corrosion potential (E_{corr}) at a scan rate of $1mVs^{-1}$. Experiments were, done to observe the effect of reinforcement content on the corrosion behavior of fabricated composite through powder metallurgy.

The fabrication and processing of MMCs sometimes lead to the formation of an interphase between the matrix and the reinforcements, which can also influence corrosion, H.M. Zakaria (2014). Three samples were, tested for each material. Electrochemical parameters such as corrosion potential (E_{corr}), corrosion current density (I_{corr}), corrosion rate (Cr) and corrosion protection efficiency (µp) obtained from Tafel polarization curves. Values of corrosion potential

(E_{corr}), corrosion current density (I_{corr}), were evaluated from anodic and cathodic regions of Tafel plots. The linear segments of anodic and cathodic curves were, extrapolated to obtain corrosion potential and corrosion current densities (I_{corr}). Protective efficiency was, calculated from the measured I_{corr} values using the following relationship:

$$\mu_p(\%) = \left(\frac{I^{o}_{corr} - I^{i}_{corr}}{I_{corr}}\right) * 100 \qquad (3.7)$$

Where I°_{corr} and I^{i}_{corr} are values of corrosion current density for pure iron and for specimens with $SiC\text{-}ZrO_2$ as reinforcement respectively.

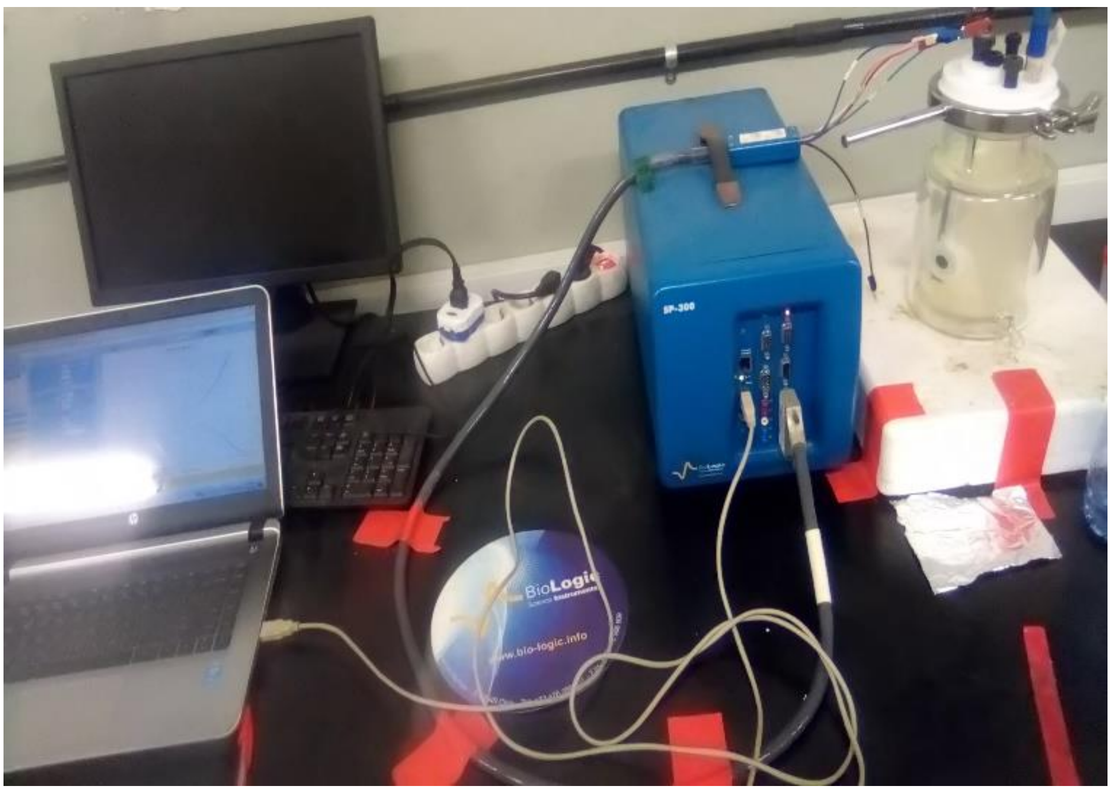

Figure 3.12 Corrosion test operation setup with potentiator

The corrosion rate was calculated using the conversion formula

$$Corrosion\ rate\ in\ (mpy) = \frac{C.EwI_{corr}}{d} \qquad (3.8)$$

Where C is the conversion constant (0.129), E_w is the equivalent weight of the specimen (g), d is the density of the specimen (g/cm^3).

3.5. Testing and Characterization of extruded specimen

Density, hardness, corrosion tests, Optical microscopy and Scanning electron microscopy have also been, performed for the extruded specimen. Improvement of densification and hence mechanical properties for powder metallurgical process can be, achieved with size reduction which is widely, performed with hot extrusion process. The ductility enhances using the metalwork technology like the hot extrusion process. The same procedure is take to characterization of extruded billet. Once the optimum sample is, known the extrusion process is conduct for the better sample and then the characterization is, done for it.

3.6. Taguchi based Grey relational analysis method

The integrated Grey based Taguchi method combines both the algorithms of Taguchi method and grey relational analysis to determine the optimum value of process parameters with multiple performance characteristics. Taguchi method is, employed for optimization but Taguchi method is single response optimization technique so it is used with gray relational methodology. Gray rational analysis convert the multi response into single response and this single response is then optimize using Taguchi method. The outcomes revels that there is significant improvement in the operation after applying optimal parameter setting. The optimum powder metallurgy process parameter factors with multiple performance characteristics were determined by using orthogonal array with the grey relational analysis *M. Wang et al. (2014).* Since the powder metallurgy experimentation is costly and time consuming, it is essential to perform the effective experiments with few runs to find out the most significant factors. The performance characteristic is analysis of the S/N ratio, that is, the lower-the-better, the higher-the-better, and the nominal the-better. The S/N ratio for each level of process parameters is computed based on the S/N analysis. Regardless of the category of the performance characteristic, the larger S/N ratio corresponds to the better performance characteristic.

Smaller-the-better

This is expressed as

Signal to noise ratio for the smaller the better

$$\eta = -10\ log(\sum_{i=1}^{n} \frac{Y_i^2}{n}) \tag{3.9}$$

Where

$\sum_{i=1}^{n} \frac{Y_i^2}{n}$ = means of sum of square observed data's

Larger-the-better

This is expressed as:

$$\eta = -10\ log_{10}(\sum_{i=1}^{n} \frac{1}{Y_i^2} / n) \tag{3.10}$$

$\sum_{i=1}^{n} \frac{1}{Y_i^2} / n$ Mean of sum of squares of reciprocal of measured data's

3.6.1. Grey relational analysis

This theory was, proposed by Professor Deng Jhu-Long in 1982, and until now has been applied successfully in various fields. To analyse the input parameters, the experimental design was done using the Taguchi orthogonal array method to minimize the number of experiments *P.P. Ikubanni, M. Oki, A.A. Adeleke et al. (2021)*. Based on the Taguchi design, L9 orthogonal array was, selected. There are three main steps involved in GRA for analysis. In the Grey relational analysis, the quality characteristics are first normalized, ranging from zero to one. This process is, known as Grey Relational Generation. Then the Grey Relational Coefficient based on normalized experimental data is, calculated to represent the correlation between the desired and the actual experimental data. Then overall Grey Relational Grade (GRG) is determined by averaging the Grey relational coefficient corresponding to selected responses. The overall performance characteristic of the multiple response process depends on the calculated GRG. This Grey relational approach converts a multiple response process optimization problem into a single response optimization problem. The optimal parametric combination and then evaluated, which would result in the highest Grey relational grade. The optimal factor setting for maximizing the overall Grey relational grade can be performed using the Taguchi method.

Step 1. Normalization

In this step, measured features of quality characteristics i.e. density, hardness and corrosion rate are first normalized ranging from zero to one. This process is, known as Grey relational generation. Three approaches are, used for normalization. If the target value of original sequence is infinite, then it has a characteristic of “the-larger-the better.” The original sequence can be normalized using equation (3.11)

$$X_i^*(k) = \frac{X_i^0(k) - \min X_i^0(k)}{\max X_i^0(k) - \min X_i^0(k)} \tag{3.11}$$

When the smaller-the-better characteristic of the original sequence is considered, then the original sequence should be normalized using equation (3.12)

$$X_i^*(k) = \frac{\max X_i^0(k) - X_i^0(K)}{\max X_i^0(k) - \min X_i^0(K)} \tag{3.12}$$

Where $X_i^0(k)$ is the value after the grey relational generation (data preprocessing), max $X_i^0(k)$ is the largest value of $X_i^0(k)$, min $X_i^0(k)$ is the smallest value of $X_i^0(k)$, and X^0 is the desired value.

Step 2. Calculation of Grey relational coefficient

In this step, the Grey relational coefficient is, calculated to express the relationship between the ideal and the actual experimental results. The grey relational coefficient can be found using equation (3.13)

$$\xi_i(k) = \frac{\Delta \min + \varsigma . \Delta \max}{\Delta_{oi}(k) + \varsigma . \Delta \max} \tag{3.13}$$

Where $\xi(\in 0,1) =$ distinguished coefficient, $\xi = 5$ is generally used. $\xi_i(k)$ is grey relational coefficient, $\Delta \min$ is the smallest value of $\Delta_{0i}(k)$, $\Delta \max$ is the largest value of $\Delta_{0i}(k)$, $\Delta_{0i}(k)$ is the deviation sequence of the reference sequence $X_O^*(k)$ and the comparability sequence $X_i^*(k)$ namely

$$\Delta_{oi}(k) = \left| x_o(k) - x_i(k) \right| \tag{3.14}$$

$$\Delta_{\max} = \max_{\forall j \varepsilon i} \max_{\forall k} \left| x_o^*(k) - x_j^*(k) \right| \tag{3.14a}$$

$$\Delta_{\min} = \min_{\forall j \varepsilon i} \min_{\forall k} \left| x_o^*(k) - x_j^*(k) \right| \tag{3.14b}$$

Step 3. Grey relational grades

After the grey relational coefficients are, found, we can determine the mean value of the grey relational coefficients as the grey relational grades:

$$\gamma_i = \frac{1}{n} \sum_{k=1}^{n} \xi_i(k) \tag{3.15}$$

Where γ_i is, the grey relational grade for the ith experiment and n is the number of performance characteristics.

Step 4. Analysis of variance (ANOVA)

Analysis of variance (ANOVA) is a common statistical process applied mostly to experimental results to determine the percentage effect of each factor. The ANOVA table given for an analysis helps to determine which factors need to be controlled. Since the quality of any product is, measured with a single criterion, or the combination of multiple criteria, regardless of the quality of the measurement, the performed measurement will belong to one of the following three characteristics. Based on the number of factors and levels, an experimental plan of Taguchi L9 orthogonal array has been, selected under different combination, which is, shown in Table 3.6. Every column of orthogonal array denotes a factor and its levels; every row denotes the level of different factors in each experiment.

Table 3.6.Factors and their levels used in L9 orthogonal array

Input Parameters (factors)		Levels		
		1	2	3
Wt.% of reinforcement	A	15	20	30
Compaction pressure	B	40	50	60
Sintering time	C	60	90	120

The process parameters of each P/M route were, designed based on desired properties of the final products and some fabrication considerations such as cost effectiveness. As P/M processes optimized, three powder metallurgy process parameters such as the weight percentage of SiC and ZrO_2 reinforcement(15,20,30)wt% with different compaction pressure (40, 50 and 60) MPa, sintering time (60, 90 and 120)minute were selected, based on the size of the sample to be fabricated. Therefore the effect of these parameters on the mechanical properties of the develop samples were analyzed through multi objective optimization using Minitab 21 software to runs the GRA.

Table 3.7 . L9 (3^4) Orthogonal Taguchi experimental design for preparation of Fe-SiC-ZrO2 metal matrix composite Samples

Samples No.	Reinforcements (SiC and ZrO_2) (wt%)	Compaction pressure(MPa)	Sintering time(min)	Fe matrix
S1	15	40	60	Balance
S2	15	50	90	
S3	15	60	120	
S4	20	40	90	
S5	20	50	120	
S6	20	60	60	
S7	30	40	120	
S8	30	50	60	
S9	30	60	90	

Step 5. Response Table for Grey relational Grade

Calculate the Grey Relational Grade for Response Table for each process parameters at their different levels and select the maximum value for grey relation grade for each process parameters from all the levels.

Step 6. Selection of Optimal levels of Process Parameters

By choosing the maximum value of grey relational grade from response table for each process parameters at their different level, we can find the optimal levels of process parameters.

Step 7. Conformation Test

After the optimal level of parameters is, identified, a confirmation test is, carried out to predict and verify the improvement of the quality characteristic using the optimal level of design parameters. The predicted values of GRG at the optimal levels are, calculated by using the relation.

$$\gamma = \gamma_m + \sum_{i=1}^{q} (\bar{\gamma}_i - \gamma_m) \qquad (3.16)$$

where γ_m is the total mean grey relational grade, $\bar{\gamma}_i$ is the mean grey relational grade at the optimum level, and 'q' is the number of main parameters that significantly affect the density, hardness and corrosion rate. Conduct the conformation experiment and verify the optimal process parameter setting by selecting the optimal combination of process parameters. The characteristics that higher value represents desired response, such as hardness of the composites, "higher the best/larger the best (LB)", LB and the characteristic that lower value represents desired response, such as corrosion rate and density (for light weight material) "lower the best/smaller the best (SB)" are used. Therefore, LB for the hardness and SB for the density and corrosion rate has been, selected for obtaining optimal performance characteristics *Dharmendra Kumar Singh (2014)*.

CHAPTER FOUR
RESULTS AND DISCUSSIONS

4.1. Introduction

In this chapter, the experimental work results of all tests have been, discussed in detail. Preliminary work done before the thesis in order to fix the different parameter. Analysis of density and hardness is done for preliminary work. Many analyses of different tests are, performed in the study such like density, hardness, corrosion rate, compression, XRD, Optical microscopy and SEM analysis of hybrid composite made from iron matrix with SiC and ZrO_2, reinforced metal matrix. Sample prepare as per as L9 orthogonal array to perform optimization process is also presented here to study the effect of process parameters. Taguchi experimental design with signal-to-noise (S/N) ratio and analysis of variance was used performed and for analysis of hybrid composite. Taguchi based Grey relation analysis method is, conducted to multi objective optimization, process. The results for extrusion process also mention in this chapter and finally the summary of result is done at the end of the chapter.

4.2. Analysis of preliminary samples behaviors.

The Table 4.1 below shows the composition and sample designation of five samples, which developed with, fixed compaction pressure and sintered time and temperature. The aim of fabricate those five samples is to insure the manufacturability of the Fe-SiC-ZrO_2 composite through powder metallurgy and the effect of reinforcement composition on the properties of iron matrix.

Table 4 1. Sample designation.

Sample (code)	**Samples**
S1	Fe+5%SiC+10%ZrO_2+4%MoS_2
S2	Fe+10%SiC +5%ZrO_2+4%MoS_2
S3	Fe+7.5%SiC +7.5%ZrO_2+4%MoS_2
S4	Fe+10%SiC +10%ZrO_2
S5	Pure iron

4.2.1. Sintered density

Density of the specimen produced by cold compaction then sintering is known as sintered density. The densities of the sintered compacts were determined using the Archimedes principle. Figure 4.1 shows the plot of pure iron and density versus percentage of SiC-ZrO_2 for five specimens. Since the density of both SiC and ZrO_2 is less than Fe, the addition of SiC and ZrO_2 leads to decrease in density of the material. The densities of iron matrix, SiC and ZrO_2 reinforcement are 7.87, 3.217 and 5.68 g/cm^3, respectively. Reinforcements concentration of about 10%SiC and 5%ZrO_2 leading to decrease in density after that for 7.5% SiC and 7.5%ZrO_2 leading to increase in density despite the increase in SiC and ZrO_2 parallel content in the composites. From the Figure 4.1 the influence of ZrO_2 on density of composite than that of SiC reinforcement is observed. This may be due to the higher density of ZrO_2 than SiC ceramic. Specimen four (S4) shows a high value of density (4.823 g/cm^3) next to pure iron (7.847g/cm^3). The sintered density for the specimens S1, S2, S3, S4 and S5 was found to be 4.367g/cm^3, 3.794g/cm^3, 4.573g/cm^3 4.823g/cm^3 and 7.847 g/cm^3, respectively.

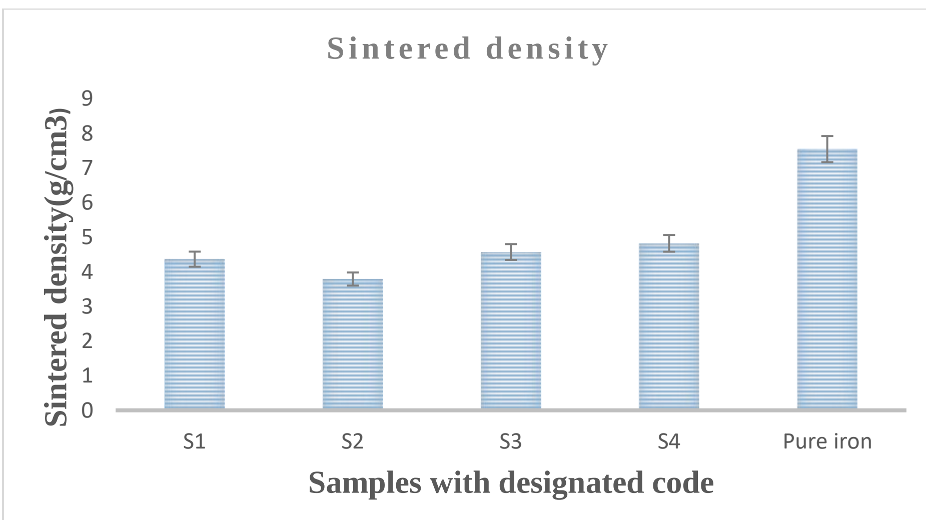

Figure 4.1 Sintered density of developed specimen with different reinforcement composition.

The lower density during the mixed and sintered of iron matrix with weightless ceramics reinforcement is due to the porosity formed because of the unreacted particles. Sintering process may decrease that porosity at some extent.

4.2.2. Hardness test

Figure 4.2 shows the Vickers hardness value of the sintered specimens Fe-SiC-ZrO_2 hybrid composites with different reinforcement contents. The hardness results of five specimens are 394.8, 435.4, 460.7, 477 and 327.4 respectively. It can be seen that with the increasing of the (SiC-ZrO_2) content, the micro-hardness also increases, which is attributed to the increase of hard SiC-ZrO_2 ceramic particulates. Sample four (S4) has the highest hardness value, which can reach 477 HV higher than that of pure iron, which has 327.4 HV. Due to the presence of hard ceramics namely SiC and ZrO_2 the hardness value for specimen is varied, with the variation of reinforcement concentration.

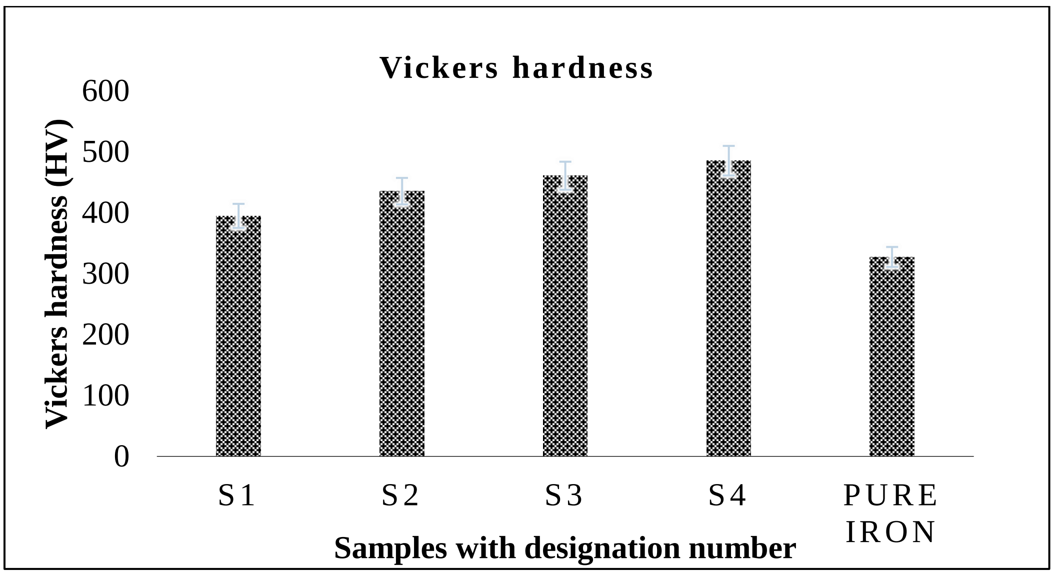

Figure 4.2 Vickers hardness for iron and reinforced composite with varies reinforcement composition.

4.3. Microstructure of sintered specimens

Observation of the microstructure is the basic investigation during material characterization process. From observed patterns of the microstructures, it is possible to reason on the actual properties of analyzed specimens. Among many investigated Fe-SiC-ZrO_2 sample, three most representative samples have been, chosen and described in more detail in current research. The phase and microstructure of the composites was observed by means of XRD (at ASTU) and scanning electron microscopy (SEM, Haramaya University) respectively.

4.3.1. X-ray diffraction Analysis (XRD)

Figure 4.3 shows the X-ray diffraction (XRD) pattern of Fe-7.5SiC-7.5ZrO_2, Fe-10SiC-10ZrO_2 and Fe-15SiC-15ZrO_2 specimens. Diffraction peaks present in the specimen were matched with the XRD-JCPDS files of different compounds. The results confirm the presence of Fe (high-intensity peaks) and reinforcements (SiC and ZrO_2) in the nanocomposites matrix, as represented by different symbols, *Mingtao Wang et al. (2021)*. The intensity of the reinforcement peaks is minimal as compared to the matrix due to their small weight percentage and may be below the detectable limit of the XRD technique *Aneta Szewczyk-Nykiel (2017).* However, with a further increase in the concentration of the reinforcement, an increment in the peak intensities can be noticed, enabling its appearance in the XRD spectra. From XRD results, it is clear that the phenomenon of partial reaction between Fe and ZrO_2 takes place during the sintering process, leading to the formation of Zr_6Fe_3O. Similar reactive sintering has been reported by *Jha et al. (2013), Fehmi Nair and Mustafa Hamamcı (2020)*. This new phase was confirmed by the SEM results. Since the addition of SiC and ZrO_2 is small, therefore, major peaks of Fe are, observed in all the patterns and only a few minor peaks of SiC and ZrO_2 can be, seen. Formation of a new phase, along with these, a few minor peaks of Fe_2O_3 and SiO_2 are, also observed, which may be due to trap of oxygen during sintering. Saxena et al. (2019) reported related results. Figure 4.3 shows the presence of Fe, SiC, ZrO_2, Fe_2O_3, Zr_6Fe_3O and SiO_2 phases.

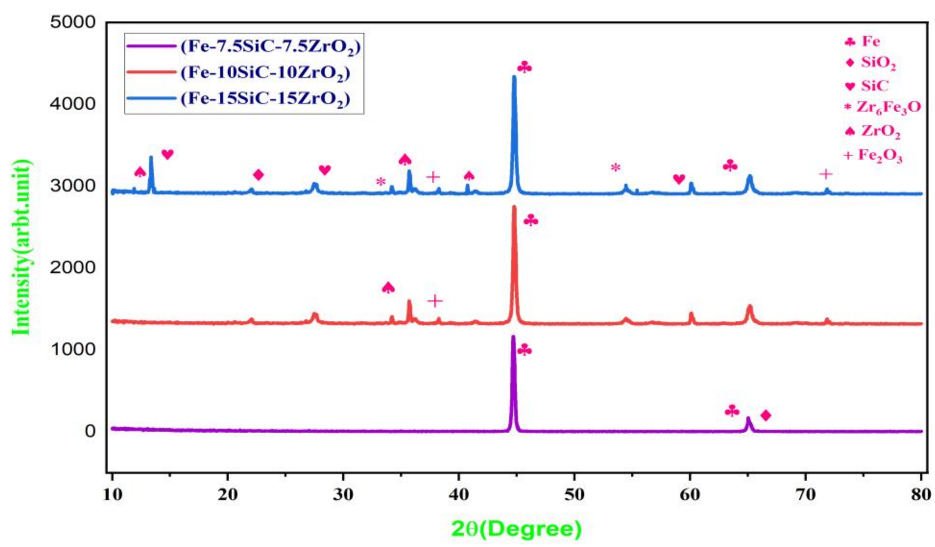

Figure 4.3 XRD pattern of Fe-7.5SiC-7.5ZrO_2, Fe-10SiC-10ZrO_2 and Fe-15SiC-15ZrO_2

It was further observed that the number of peaks of Fe_2O_3, SiO_2, and Zr_6Fe_3O were more in the specimen with Fe-15SiC-15ZrO_2 due to higher concentration of SiC and ZrO_2. From the X'pert high score software analysis of crystallographic, the crystal structures of Fe and Fe_2O_3 are hexagonal and rhombohedral, respectively.

Crystallite size determined using the XRD data. In order to determine the maximum applicable range of the Scherrer equation for Fe-SiC-ZrO_2, take K as 0.94 (recommended between (0.68-2.08), λ as 1.54056 (Å) which is the X-ray diffraction wavelength and θ as different since the average value is used, diffraction peak angle obtain from the XRD data plotted using origin also varied as shown on Table 4.2.

Table 4 2. Crystallite size determination using XRD data

Parameters		Calculations value			
K	**λ (Å)**	Peak position 2θ(°)	FWHM	D(μm)	Average crystallite size (μm)
0.94	1.54056	44.7942	0.2862	31.35	32.62
		44.72334	0.2866	31.31	
		44.718	0.25478	35.2	

From the literature, the grain size is equal or greater than crystallite size. The average crystallite size value (**32.63 μm)** which obtain from XRD data is agree with the average grain size which calculate using line intercepted method. Analysis results from XRD data of crystallite and OM measurements of grain size show a good correlation with each other.

4.3.2. Optical microscopy

The distribution of the reinforcing particles in the iron matrix was observed using optical microscopy (OM), as shown in Figure 4.4. The grain size was calculated from Optical microscope image through image software. Depending on OM image the grain size was calculated from **24.85μm to 164.1μm** using line intercept method. The average grain size is calculated from five trial value from different location of specimen image is **71.53μm.**

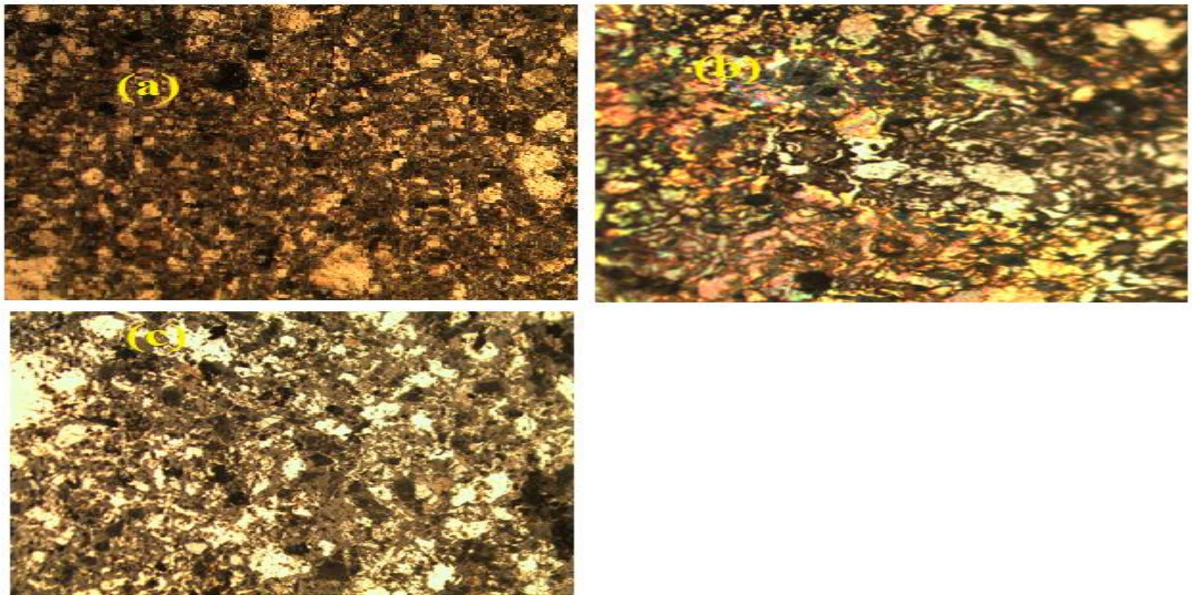

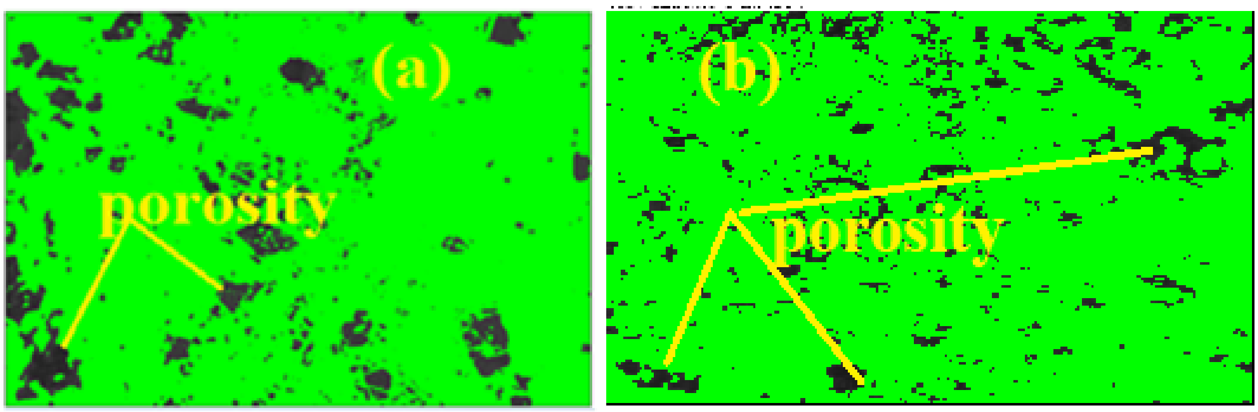

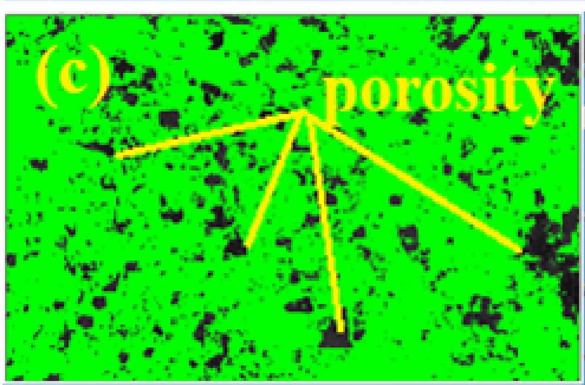

Sample code(No)	Sintered density(g/cm³)	Porosity from image analysis (%)
S4	4.357	10.75
S6	4.849	10.01
S9	4.573	15.45

Figure 4.4 Porosity analysis for specimen (S4,S6,S9) using imagej

As shown in Figure 4.4 with an increase in porosity fraction (>5%), the porosity tends to be interconnected in nature, as opposed to the situation where pores are relatively isolated (<5%) *N. Chawla, X. Deng (2005)*. Quantitative analysis of the microstructure was performed to determine the pore size distribution as a function of sintered density using Image j software. The greater porosity value is observed for the sample 9 which contain more reinforcement wt.% particle. The results aligned with the justification, Pores at the lowest density also appeared to be more clustered and segregated along the interstices between particles *N. Chawla, X. Deng (2005).*

4.3.3. Scanning electron macroscopy

As shown in Fig. 4.5. It can be observed that the reinforcements (SiC and ZrO_2) are homogeneously distributed in the Fe matrix without any significant agglomeration. It can be observed that the ZrO_2 phase (white color) is dispersed in the Fe matrix (grey color) and the SiC phase (dark grey color) shows the interfacial integrity and confirms the presence of reinforcement *P. Jha et al. (2021).* Figure 4.5(a) shows a few pore spaces in the morphology of the hybrid iron composite due to the homogeneous distribution of SiC and ZrO_2 reinforcement over the iron matrix.

The distribution of elements, such as Fe, Si, C, O, and Zr were analyzed using an energy-dispersive spectrometer (EDS, Haramaya University) mounted on the SEM. As shown in Fig. 4.5 (a) and (b) show the SEM micrograph and the EDS of the Fe-specimen respectively. In the EDS, each peak shows the presence of materials in the composite. Highest peak corresponds to iron, as it is the matrix material. Based on the microstructural and EDS analyses, it can be, concluded that Fe, ZrO_2, and SiC are present in the specimen with some minor new grain of Zr_6Fe_3O, which formed due to the reactive sintering between Fe and ZrO_2. Comparatively speaking, it could be speculated that SiC and ZrO_2 presented different behaviors in the sintering process. The SiC remained in the microstructure after sintering, while ZrO_2 could decompose according to the morphological features. An XRD test was carried out in order to verify the behavior of the SiC and ZrO_2 during the sintering, and it agreed with the morphological feature by showing the new phase (Zr_6Fe_3O). The phenomenon of partial reaction properties of ZrO_2 in an iron matrix is already described in *Jha et al. (2013).* There was no reaction between the iron matrix and SiC, and similar results were, reported from many research results which were done on iron-based metal matrix composite materials reinforced by SiC *Daud, S. N. A., et al. (2019), Mingtao Wang et al. (2021).* Which means SiC is a stable reinforcement material.

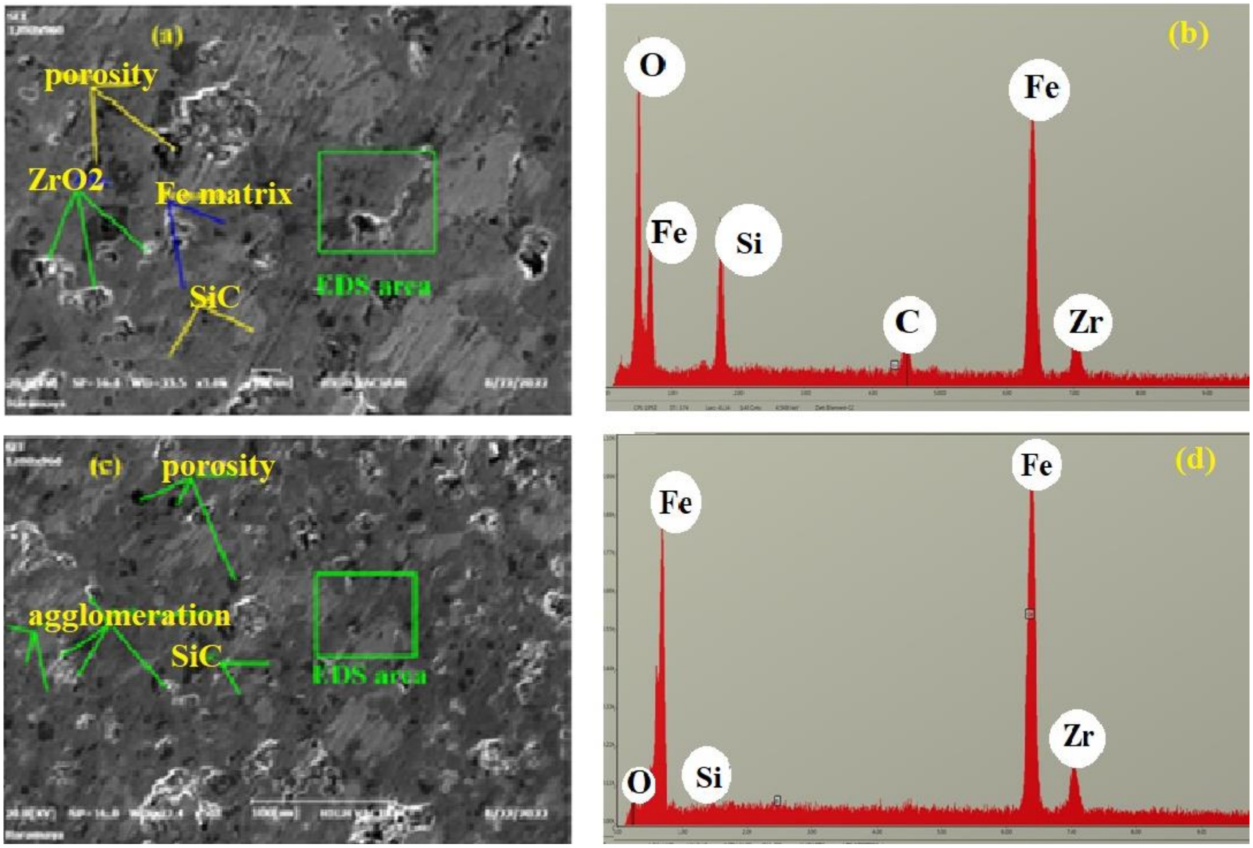

Figure 4.5 SEM morphology analysis of (a), Fe-10SiC-10ZrO$_2$ and (c) Fe-15SiC-15ZrO$_2$ composite with marked areas for (EDS) and (b), (d) show the compositional analysis of EDS.

4.4. Analysis of material behavior and optimization of material properties as per L9 orthogonal array.

4.4.1. Analysis of density measurement

From Table 4.3. the average sintered densities for 15%, 20% and 30% (SiC-ZrO$_2$) specimens, prepared by cold pressing at different load, were, found to be 4.553, 4.533, and 4.033 g/cm^3, respectively. The lowest measured density of the 30% reinforcement with 50MPa compaction pressure and 60min sintering time are (3.734 g/cm^3 of sample eight, S$_8$). The lowest density value for the Fe-15% SiC-15% ZrO$_2$ sample (S8) was, obtained due to the addition of high amount of reinforcement particles. The densities of iron, SiC and ZrO$_2$ are 7.87 3.21 and 5.68 g/cm^3, respectively. Since the density of both SiC and ZrO$_2$ are less than Fe, the density of the specimens' decreases with the increase in SiC and ZrO$_2$ concentration. The compaction pressure also has its own influence. When the compaction pressure is increase the density of the sample, also increase. The experimentally achieved value for density versus sintering time show little the variation. There is no direct correlation of sintered density with sintering time. These may be due to the different factors, which cause during the sintering process. The Densification in the specimen and the reaction is dependent on time of sintering and can be, affected with the other factor like the amount of the reinforcement and compaction pressure.

Table 4 3. Sintered density values of tested specimens

Trial No.	Powder metallurgy Parameters			Average Response Values for density	S/N ratio
	Composition	Compaction pressure (MPa)	Sintering time	Sintered Density (g/cm^3)	Predicted S/N ratio result (S/N ratio for various responses)
1	15	40	60	4.386	-12.8414
2	15	50	90	4.375	-12.8196
3	15	60	120	4.897	-13.7986
4	20	40	90	4.357	-12.7838
5	20	50	120	4.394	-12.8572
6	20	60	60	4.849	-13.7130
7	30	40	120	3.792	-11.5774
8	30	50	60	3.734	**-11.4435**
9	30	60	90	4.573	-13.2040

As it can be seen in Table 4.3 show the trend of average density of samples were aligned with the trend of, the applied pressure on cold applying more pressure caused better intimate contacting areas between powders particles. On the other hand, more pressure caused the particles to be deformed, crushed and fill the existing pores in the microstructure. As the amount of applied load on mixed powders increase, particles can touch each other more effectively and consequently the possibility of more bond formation increase in the entire structure. Similar concept are, reported from, *Jha et al. (2013).*

4.4.1.1. Optimization of the PM process parameters for density

The variables influence on the sintered density are optimized using Minitab software. The signal-to-noise (S/N) ratio helps for knowing the variables that have an effect on the acquired result. The S/N ratio designed rank for each factor, accordance with their significances, as shown in Table 4.4.

Table 4 4 The signal-to-noise ratios responses for sintered density (g/cm3) versus process parameters, with S/Ns "smaller is better" for product qualification.

Level	Reinforcement (wt %)	Compaction pressure(MPa)	Sinteringtime (min)
1	-13.15	-12.40	**-12.67**
2	-13.12	**-12.37**	-12.94
3	**-12.07**	-13.57	-12.74
Delta	1.08	1.20	0.27
Rank	2	1	3

From Table 4.4, the S/N ratio rank of the actual density response result shows that the compaction pressure has the greatest significant factor on the sintered density of hybrid composite. The left process parameter such like weight percentage of the reinforcements (SiC and ZrO_2) and sintering time have their own effect on the density increment of the composites. The effect of reinforcement material is almost the next factor and its effect on the density is high next to compaction pressure.

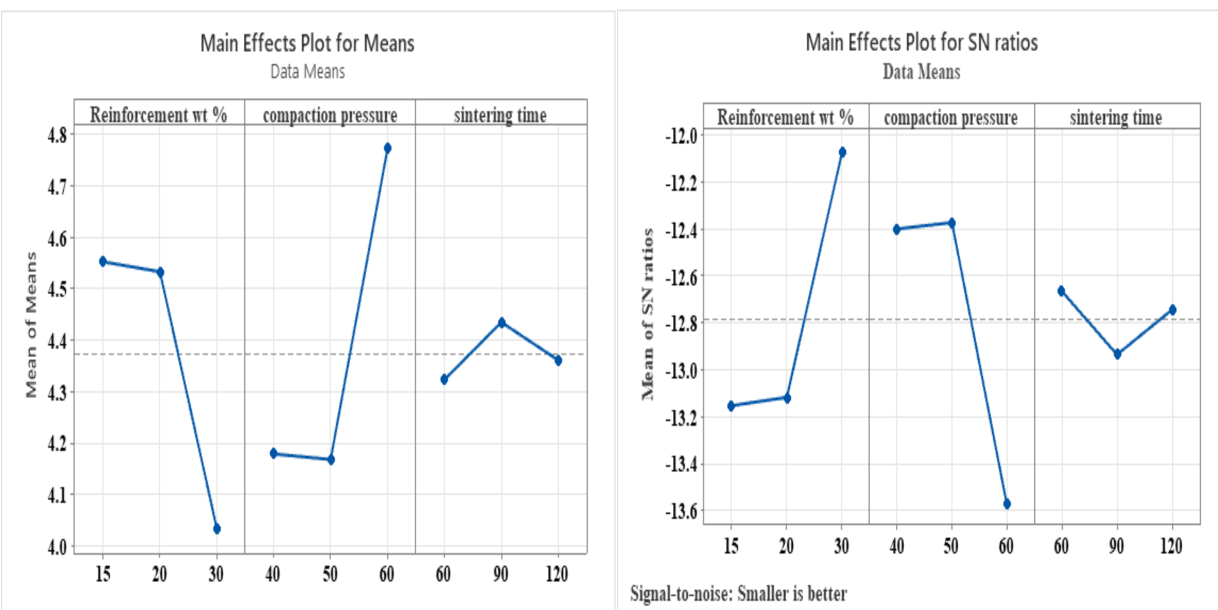

Figure 4.6 Main factor Vs density plot for S/N ratio.

The optimum prediction condition for the S/N ratio in which, the less actual-density of the hybrid composite (3.734g/cm^3) obtain with the terms setting show in Table 4.3 is **-11.4435** the significant effect on sintered-density of the Fe-SiC-ZrO_2 matrix sample was occurred at level one **(A3B2C1)** (i.e., as code shown in Table 3.5) of setting parameters.

From Figure 4.6 above, when the compaction pressure increased, the mean of signal-to-noise ratios for sintered-density is decreased, with the smaller is better product-qualification. As the compaction pressure is increase the density of the hybrid composite also increase. This results clearly shown after 50MPa with regard to reinforcement composition. The reason for sintered-density decrease in the Fe/SiC-ZrO_2 hybrid composite is, density of silicon carbide as well as ZrO_2 is lower than that of pure iron.

Table 4.5. The optimum conditions for hardness result prediction.

	Reinforcement wt (%)	Compaction pressure		Sintering time
1	30	50		60
Rank	2	1		3
		S/Ns ratio	Mean	
		-11.4435	116.733	

4.4.1.2. The sintered density model summary

The sintered density model of summary discloses that the statistics-data is excellently agreed with an investigate inquiry. The coefficient and correlation coefficient model expected of the S/N ratio for sintered density is, shown in Table 4.6. The R-square value for sintered density is **97.07%.** Since the is greater than 95% it the obtain results correlated.

Table 4.6 The actual-density correlation-coefficient.

S	R-Sq	R-Sq (adj)	R-sq(pred)
0.02793	97.07%	98.30%	98.76%

4.4.1.3. ANOVA for sintered density

The ANOVA result for actual density on Table 4.7 is used to demonstrate the variable that have significant statistics at the confidence level of 95-percentage with the approval of P-values. When the P value is ≤ 0.05, it is showing the higher significance level. ANOVA Table 4.7 for sintered density is showing the compaction pressure has the highest percentage contribution (i. e **52.67%).** Since, the P-value of compaction pressure (**0.043)** is ≤ 0.05), compaction pressure has the highest significance level. Following to it, the reinforcement wt.% **(42.23%).** Since the p-value of reinforcement wt% is less than 0.05 it has also significant effect on the sintered density. Sintering time, which has percentage contribution of **(2.168%),** has less significance because of its p value is greater than 0.05. ANOVA results for density are, depicted in Table 4.7.

Table 4.7 Analysis of variance (ANOVA) for sintered density.

Source	DF	Seq SS	Adj SS	Adj MS	F-value	P-value	PC (%)
Reinforcement wt%	2	2.2517	2.2517	1.12586	14.43	**0.049**	42.23%
Compaction pressure	2	2.8085	2.8085	1.40424	18.00	**0.043**	52.67%
Sintering time	2	0.1156	0.1156	0.05779	0.74	0.574	2.168%
Error	2	0.1560	0.1560	0.07800			
Total	8	5.3318					

4.4.2. Analysis of hardness measurement

The increase in hardness is quite, obvious and expected since both silicon carbide and zirconium dioxide are hard material, which helps effectively to improve the hardness of the composites. However, the other process parameter such like compaction pressure and sintering time also, has may be significant effect on the hardness of the material.

4.4.3. Signal-to-noise ratio (S/N) analysis of the responses

Hardness of the matrix and composite material was, investigated based on the L9 Taguchi experimental design, that is, shown in chapter three (Table 3.5). Upon the three signal-to-noise ratios “the bigger-the-better”, characteristics was chosen to reach the maximum value of products hardness. Since high hardness, value is required (example in wear resistance application areas). For each sample, three readings were, taken at different locations (shown at Appendix table A-I). The response characteristics of the process parameters, as well as the signal-to-noise ratio (S/N ratios), are displayed in Table 4.8

The experimental runs gave different responses per run. Further analyses of the results are, explained in details in subsequent sub-sections.

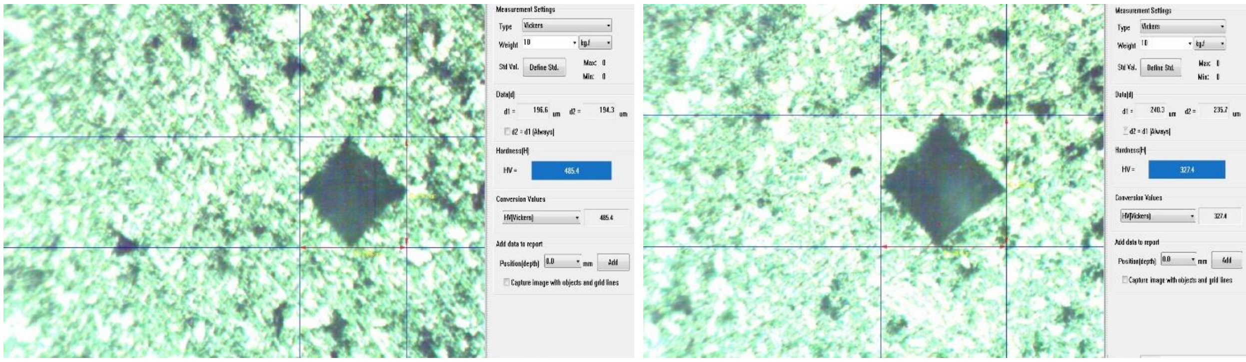

a) b)

Figure 4.7 Vickers hardness value of a) for S7 and b) for S9, Fe-SiC-ZrO_2 composite respectively

The hardness value of the specimen increase with increasing the compaction pressure. The direct relation of the reinforcement and hardness also seen, but it depend on the compaction pressure. The more the reinforcement is added, the more pressure is needed to compact the powder. The hardness value show big change upto specimen number six. The hardness value is show small variation.

Table 4.8The Vickers hardness experimental responses and their S/N ratios.

Experiments Samples No	Experimental result of hardness value	Predicted S/NL ratio result (S/N ratio for various responses)
S1	191.7	45.6524
S2	283.4	49.0480
S3	300.8	49.5424
S4	274.7	47.8785
S5	394.8	51.9275
S6	435.4	52.7778
S7	327.4	50.3016
S8	460.7	53.2684
S9	485.4	53.7220

4.4.3.1. Analysis of a response for hardness

The mean S/N ratios and the process parameters ranking order on the hardness value were, obtained. The major influence of each parameter on the hardness of the synthesized Fe Metal Composites is, displayed in Figure 4.8 below. The process parameters having the highest S/N ratio will contribute to the optimal process parameter variants *P.P. Ikubanni, M. Oki, A.A. Adeleke et al. (2021)*. The process parameters required for the optimal condition for the hardness were, obtained. This was when the reinforcement percentage was 30 wt. % at a compaction pressure of 60MPa and a sintering time of 90 min. By implication, when 15 wt. % of SiC and 15 wt. % of ZrO_2 were incorporated into Fe as hybrid reinforcements at a compaction pressure 60MPa of with a sintering time of 90min (**A3B3C3**), the optimum hardness can be attained. Hence, indicative of the optimum condition for the hardness. Based on the ranking, the reinforcement percentage influenced the optimum value the most followed by the compaction pressure, while sintering time had the lowest effect on the hardness. It was, observed that there has been significant change in hardness properties with addition of reinforcement (SiC-ZrO_2). Similarly *Jha et al. (2013)* reported a significant increase in the hardness of iron composite on the addition of zirconium dioxide. *Anjani Kumar and Anil Kumar Das (2020)* reported similar value for Fe-SiC composite.

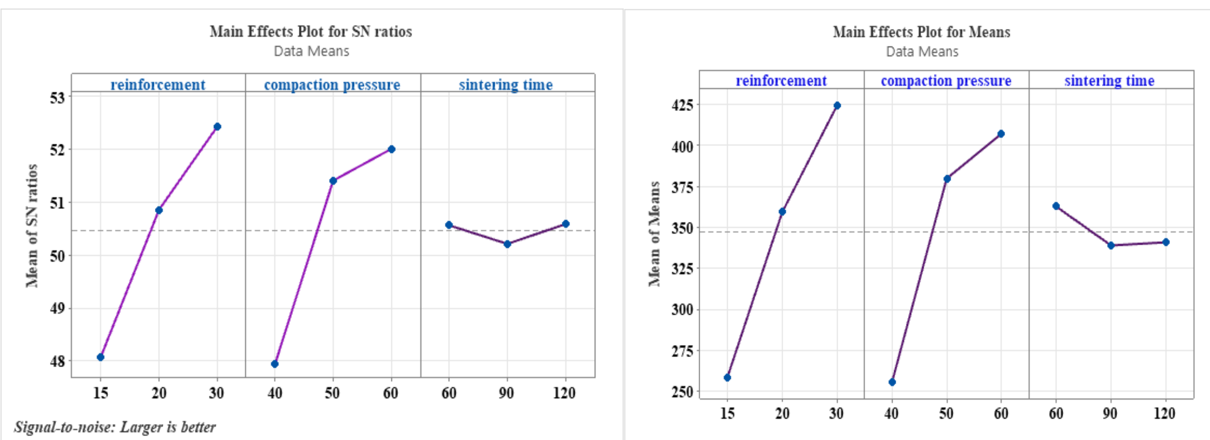

a) b)

Figure 4.8 Main effect plot of each parameter on (a) S/N ratio (b) Main effects

Initially, the hardness number was 191.7 HV for the specimen 15% (SiC-ZrO_2) (S_1). For the sample 30 %, (SiC-ZrO_2) (S_9) hardness (485.4HV) slightly increased as compared to the 15% (SiC-ZrO_2) reinforced hybrid iron metal matrix composite specimen. Hardness number for S_9 was, found out to be the highest. However, the change in hardness value is less after 50MPa at 30% of reinforcement percentage. Another reason for increased hardness is the strengthening mechanism of ceramic materials. The addition of ceramic material to metal matrix impedes dislocation motion, and this increases hardness. As it is shown in Figure 4.8 (a) and (b) increasing pressure from 40 to 50 MPa resulted in a big increase in the hardness value from 327.4 HV to 460.7 HV, however, application of pressures higher than 50 MPa showed no significant increase in hardness (from 460.7 to 485.4MPa).

The ranking of signal-to-noise (S/N) ratio helps for knowing the variables that have a significant effect on the acquired result. The S/N ratio designed rank for each factor accordance with their significances, as shown in Table 4.9.

Table 4.9 Ranking table from signal-to-noise ratios responses for hardness (HV) with "higher is, better" for product qualification.

Level	**Reinforcement**	**Compaction pressure**	**Sintering time**
1	48.08	47.94	50.57
2	50.86	51.41	50.22
3	**52.43**	**52.01**	**50.59**
Delta	4.35	4.07	0.37
Rank	1	2	3

From Table 4.9, the S/N ratio rank of the hardness response result shows that the reinforcement composition is the greatest significant factor on the composite hardness. The compaction pressure is the next significant effect on the hardness of the hybrid composite. Sintering time has less significant on the hardness of the sample as seen on the table since delta for sintering time is less and far from the delta of reinforcement and compaction pressure.

4.4.3.2. The optimal prediction conditions for hardness test

The optimum prediction condition for the S/N ratio in which, the higher hardness result of the composite obtain with the terms setting in Table 4.10 was 53.7220. As shown in Figure 4.4, the significant effect on hardness of the Fe-SiC-ZrO_2 hybrid composite sample was, achieved at level-**A3B3C3**, at the parameter settings in chapter three (Table 3.5). The hardness of the hybrid composite material increases with the increase in the content of the reinforcement and reaches the maximum when the content is 30%, which is **485.4 HV**. The addition of ceramic reinforcement such as SiC and ZrO_2 to iron matrix increases hardness, this is because SiC and ZrO_2 is naturally harder than iron. Another reason for increased hardness is the strengthening mechanism of ceramic materials. The addition of ceramic material to metal matrix impedes dislocation motion, and this increases hardness. Therefore, although increasing reinforcement wt. % above 20% should not slight improvement in mechanical properties as seen in sample No.S9, it was not considered as optimum parameters due to considerably lack of higher energy consumption to get more compacted specimens. Considering two factors of improved mechanical properties and cost effectiveness of the process, it was concluded that sample No.6 that, was compacted at 60MPa and sintered at 1000 °C for 60 minutes met the optimization requirements. The findings in this research were in good alignment with previously reported values for sintering parameters during fabrication Iron-based composites by P/M technique *Babak Jahani (2016).*

Table 4.10 The optimum conditions for hardness result prediction

	Reinforcement wt (%)	Compaction pressure	Sintering time
1	30	60	120
Rank	1	2	3

The hardness model of summary discloses that the statistics-data is excellently agreed with an investigate inquiry. The coefficient and correlation coefficient model expected of the S/N ratio for hardness is, shown in Table 4.11. The R-square value for sintered density is **99.79%.** Since the is greater than 95% it the obtain results correlated.

Table 4.11 The hardness test correlation coefficient.

S	**R-Sq**	**R-Sq(adj)**
0.24166	99.79%	97.63%

4.4.3.3. ANOVA for hardness responses

According to *.P. Ikubanni, M. Oki, A.A. Adeleke et al. (2021) and Sarıkaya & Güllü (2010)*, Taguchi analysis results should be validated using analysis of variance (ANOVA) for the statistical reliability of the results. Hence, the percentage contribution of each parameter of the Fe metal matrix composite samples on the hardness was determined.

The ANOVA results on the hardness of the Fe based metal matrix composite samples, in Table 4.12 display the amount of influence of each process parameter on the response in terms of percentage contributions. Based on the ANOVA analysis carried out, the higher percentage contribution was, derived to be **55.34%,** which was, attributed to the reinforcement percentage. The percentage contribution of compaction pressure was **45.04%,** while the least percentage contribution of **0.43%** was, observed for the sintering time. The value of percentage concentration of reinforcement and compaction pressure are almost the same.

Table 4.12 ANOVA results on the hardness value

Source	DF	Seq SS	Adj SS	Adj MS	F-value	P-value	Percentage contribution (%)
Reinforcement wt %	2	29.9034	29.9034	14.9517	257.97	0.004	**55.34**
Compaction pressure	2	24.6969	24.6969	12.3484	213.05	0.005	**45.04**
Sintering time	2	0.0104	0.0104	0.0052	0.09	0.918	0.43
Residual Error	2	0.1159	0.1159	0.0580			
Total	8	54.7266					

This implies that both the reinforcement percentage and compaction pressure have the greatest impact on the hardness, while sintering time has the least influence. This study is in agreement with the work of *Velickovi (2018).* In the study, the sintering time was, observed to have less significance compared to the reinforcement and compaction pressure of the composites considered. Therefore, increasing reinforcement and compaction pressure have high effects on the hardness of the iron based metal matrix composite. As reported by *Kumar & Birru (2003)* the increase Analysis of Compression measurement in compaction pressure could lead to an increase in the mechanical properties such as hardness, compression and so on. In addition, the p-value of each of the process parameters revealed those that have significant influences on the hardness. The p-value of reinforcement, compaction pressure, and sintering time is **0.004, 0.005,** and **0.918**, respectively. The p-value of the sintering time process parameter is far above 0.05 confidence level; hence, making sintering time is not significant effect on the hardness value. The reinforcement and compaction pressure have a great influence on the hardness values of the hybrid composites considered in this work.

4.4.4. Analysis of corrosion rate measurement

Corrosion rate of the hybrid composite material was, investigated based on the L9 Taguchi experimental design, that is, shown in chapter three (Table 3.5). For each sample, three repetitive test were, taken at different time (shown at Appendix table A-II). Upon the three signal-to-noise ratios “the small-the-better”, characteristics was chosen to reach the minimum value of sample corrosion rate using Eq. (3.14), Since, lower corrosion rate value is required to insure the life spam of the material. Several approaches are commonly employed to provide quantitative measurements of metal corrosion rates *T. Lei et al (2012).* The methods of recording weight-loss and thickness-loss over time are regarded by corrosion engineers to be the ‘‘real’’ corrosion testing. However, this method is a long-term process not suitable for rapid corrosion screening. Tafel plots provide an alternative electrochemical approach that has the advantage of speed and relative simplicity. The rate of corrosion can theoretically be calculated from the corrosion current which obtained from the intersection of two slopes of cathodic and anodic Tafel plots.

The corrosion potential of the samples with 20% SiC- ZrO_2 moved to a less negative potential (from 693.196V to 646.815V). Evaluating corrosion potential is one way to know the effect of parameters on the corrosion behavior of material. Consequently, the corrosion rate of the composites decreased with increasing amount of SiC-ZrO_2 particle. Furthermore, it is widely accepted that Tafel curves of materials that exhibit more positive corrosion potential (E_{corr}) and lower corrosion current density (I_{corr}) show enhanced corrosion resistance compared with materials that exhibit opposite behaviors many research agree with the result *T. Lei et al (2012).* Hence, the results indicated that the addition of calculated amount of SiC-ZrO_2 into the iron matrix can result in good corrosion resistance of the composite compared to the pure as seen from the Table 4.11 by changing the corrosion potential to positive value. The results agree with *Oladayo et al. (2017)* the addition of calculated amount of ZrO_2 into the ductile iron can result in good corrosion resistance of the composite compared to their wrought counterpart, as this is also evident by shifting the corrosion potentials to the positive value. When a metal corrodes, the rate at which it corrodes is generally, controlled by the cathodic reaction and their susceptibility to chloride ions.

The response characteristics of the process parameters, as well as the signal-to-noise ratio (S/N ratios), are displayed in Table 4.13. The experimental runs give different responses per run. Further analyses of the results are, explained in details in subsequent sub-sections.

Table 4.13 Electrochemical corrosion parameters and protective efficiency (μp) values for the various specimens in 3% NaCl solution.

Sample name (code)	Sample composition	E_{corr} (V)	I_{corr} (A/cm2)	Corrosion rate (mm/ yr)	Protective efficiency (μp) %
S1	Fe-7.5SiC-7.5ZrO$_2$(40)	-6.93.196	607.819	135.425	92.45
S2	Fe-7.5SiC-7.5ZrO$_2$(50)	-8.95.4	1067.45	335.252	87.92
S3	Fe-7.5SiC-7.5ZrO$_2$(60)	-6.59	168.436	158.060	97.91
S4	Fe-10SiC-10ZrO$_2$(40)	-7.82.562	403.275	109.530	94.99
S5	Fe-10SiC-10ZrO$_2$(50)	-7.21.617	34.944	88.567	99.37
S6	Fe-10SiC-10ZrO$_2$(60)	-6.67.815	12.45	24.470	99.85
S7	Fe-15SiC-15ZrO$_2$(60	-7.55.515	206.827	101.380	97.43
S8	Fe-15SiC-15ZrO$_2$(60	-7.34.352	34.88	50.020	99.57
S9	Fe-15SiC-15ZrO$_2$(60	-6.46.393	50.544	36.457	99.37
Sample	Pure iron	-8.96.667	8050	82080	-

Figure 4.9 and 4.10 shows the potentiodynamic polarization (Tafel plot) curves obtained for samples Fe-7.5SiC-7.5ZrO2(S1), Fe-7.5SiC-7.5ZrO2(S2), Fe-7.5SiC-7.5ZrO2(S3), compacted with 40,50 and 60MPa respectively are tested in 3% NaCl solution. Experiments were, done to observe the effect of reinforcement content, compaction pressure and sintering time, on the corrosion behavior of synthesized composite. Table 4.13 shows the E_{corr}, I_{corr}, corrosion rate and corrosion protection efficiency of specimens. The values of E_{corr}, and I_{corr}, were, obtained by extrapolating the linear segments of cathodic and anodic curves and corrosion protection efficiency (μp), also calculated by using the current density of pure iron, which perform on current work and near agree as referred from the number of research *Gupta et al. (2015), R. Bhattacharyya et al (2020)*.

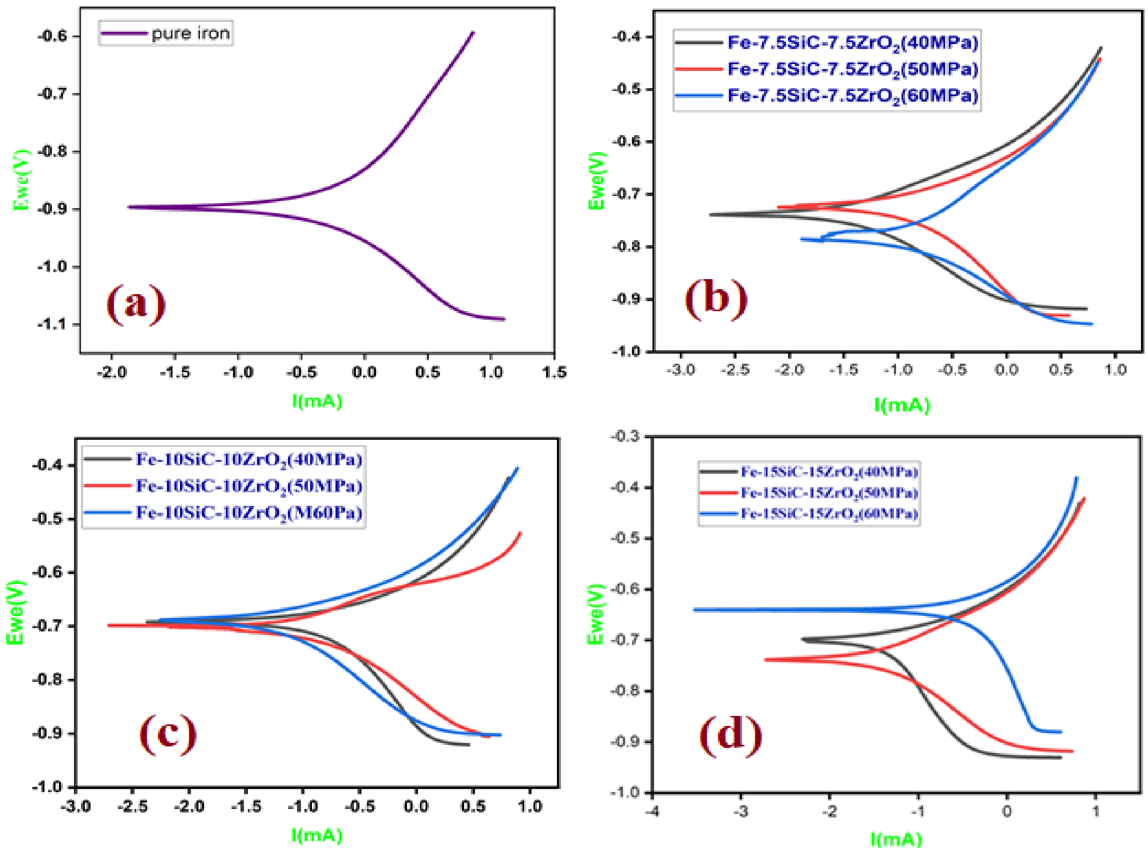

Figure 4.9 The Tafel plots of specimens, pure iron (a), Fe-7.5SiC-7.5ZrO_2 (b), Fe-10SiC-10ZrO_2 (c) and Fe-15SiC-15ZrO_2 (d) with different compaction pressure and sintered time

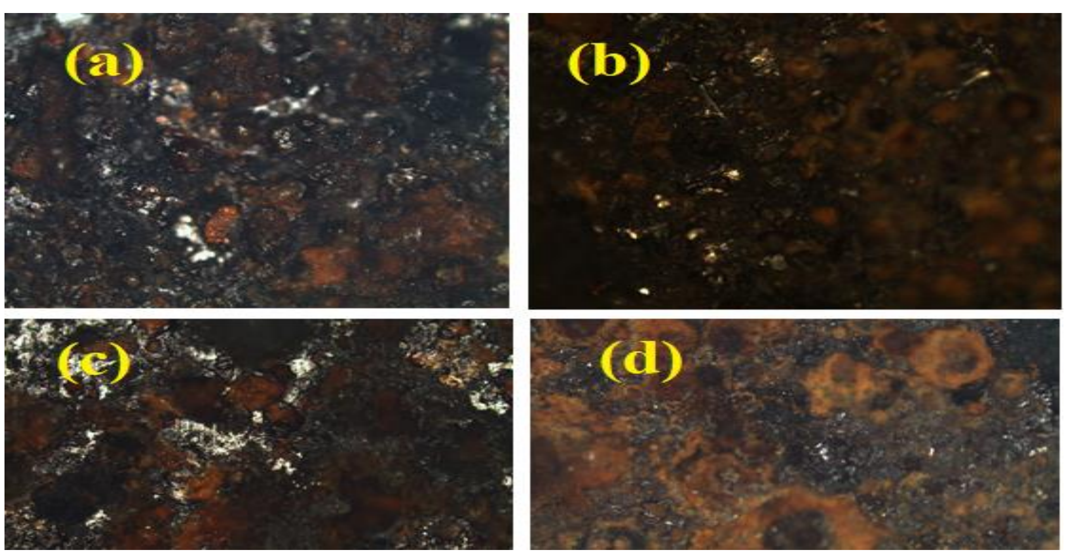

Figure 4.10 Optical image of corroded specimen in 3% NaCl solution

4.4.4.1. Analysis of signal to noise ratios for corrosion test

The response characteristics of the process parameters, as well as the signal-to-noise ratio (S/N ratios), are displayed in Table 4.14 the experimental runs gave different responses per run. Further analyses of the results are explained in details in subsequent sub-sections.

Table 4.14 The corrosion rate experimental results and their corresponding (S/NL) ratio based on L9 Taguchi design.

Experiments Samples No	Experimental result of corrosion rate	Predicted S/NL ratio result (S/N ratio for various responses)
S1	135.425	--42.6340
S2	335.252	-50.5074
S3	158.060	-43.9764
S4	109.530	-40.7907
S5	88.567	-38.9454
S6	24.470	**-27.7727**
S7	101.380	-40.1190
S8	50.020	-33.9829
S9	36.457	-31.2356

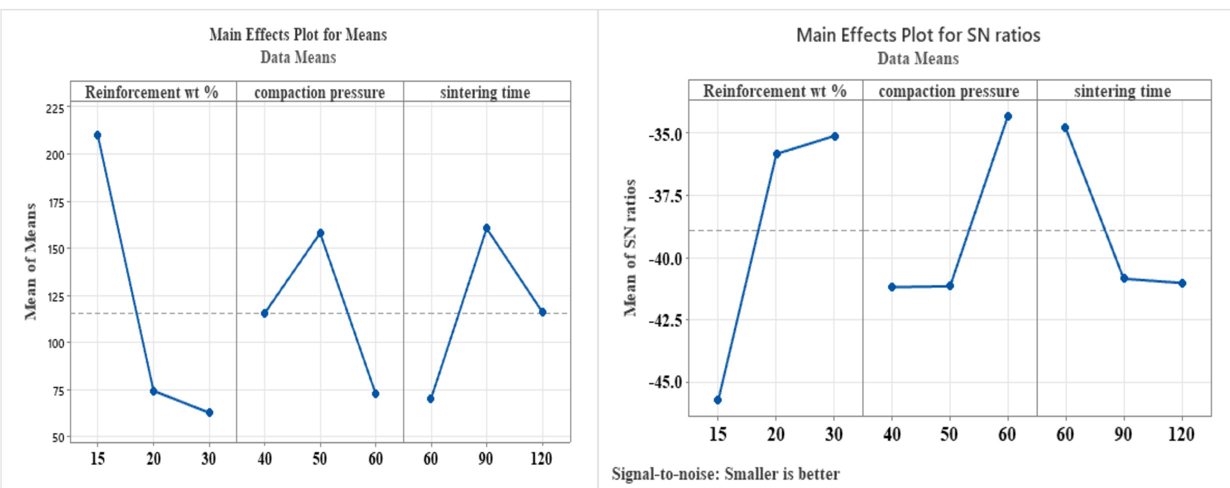

Figure 4.11 Main effect plots of each parameter on (a) S/N ratio (b) Means of corrosion rate.

From the plot shown on Figure 4.11 observed that the more positive the value of current potential, the better the corrosion resistance of the material. From the perspective of corrosion dynamics, corrosion current density represents the corrosion rate of materials. The smaller the corrosion current density, the better the corrosion resistance.

4.4.4.2. Optimization of the PM process parameters effect on corrosion rate.

The signal-to-noise (S/N) ratio helps for knowing the variables that have an effect on the acquired result. The S/N ratio designed rank for each factor leverage accordance with their significances, as shown in Table 4.15.

Table 4.15 The signal-to-noise ratios responses for corrosion test versus processing variables with S/N "small is better" product qualification.

Level	Reinforcement wt %	compaction pressure	sintering time
1	-45.71	-41.18	**-34.80**
2	-35.84	-41.15	-40.84
3	**-35.11**	**-34.33**	-41.01
Delta	10.59	6.85	6.22
Rank	1	2	3

From both Table 4.15 the S/N ratio rank of the corrosion rate, response result shows that the SiC and ZrO_2 weight percentage is the greatest significant factor on the composite corrosion rate decrement following to it, the sintering time and compaction pressure have contribution for decreasing the corrosion rate of the Fe-SiC-ZrO_2 composite materials.

4.4.4.3. The optimal prediction conditions for corrosion test

Table 4.16 The optimum conditions for compression strength result prediction-settings

Reinforcement composition	Compaction pressure	Sintering time
20	60	60

The optimum prediction condition of the predicted-values for the S/N ratio in which, the lower corrosion rate result of the composite, obtain with the terms setting in Table 4.16 is -27.7727. The significant effect on corrosion rate of the Fe-SiC-ZrO_2 composite sample was, achieved at level **(A3B3C1**), at the parameter settings code in table 4.16.

4.4.4.4. The corrosion test model summary

Another important statistic in the ANOVA results is the coefficient of determination or R^2 (reads as R-sq). This statistic reflects the amount of variability in the data explained by the linear statistical model. The corrosion test model of summary discloses that the statistics-data is excellently agreed with an investigate inquiry. The coefficient and correlation coefficient model expected of the S/N ratio for corrosion test is shown in Table 4.17 show that, the R-square value for corrosion test is **98.09%.**

Table 4.17 Corrosion test correlation-coefficient.

S	R-Sq	R-Sq(adj)
1.922	98.09%	92.34%

As shown on Table 4.17 the higher percentage contribution (**54.41%)** is calculated for reinforcement weight percentage and it seems that reinforcement has highly affect the corrosion behavior of material. Assuming a significance level of 95% (α = 0.05), this indicates that reinforcement concentration and compaction pressure a significant effect on corrosion behavior (p-value = **0.034**). On the other hand, sintering time evidently has a little effect on corrosion rate (p-value = 0.089).

Table 4.18 Analysis of variance (ANOVA) of factorial regression for corrosion test.

Source	DF	Seq SS	Adj SS	Adj MS	F	P-Value	Percentage contribution (%)
Reinforcement wt %	2	210.155	210.155	105.078	28.43	0.034	54.41
Compaction pressure	2	93.436	93.436	46.718	12.64	0.043	24.19
Sintering time	2	75.260	75.260	37.630	10.18	0.089	19.49
Error	2	7.392	7.392	3.696			
Total	8	386.244					

The next significant effect on corrosion behavior is compaction pressure, followed reinforcement. The value of percentage contribution and P-value show good agreement on the significant effect of reinforcement and compaction pressure.

4.4.5. Analysis of compression test

The universal testing machine conducted for compression test of three specimen. As it can be seen in the Figures 4.12 stress versus strain curve is plotted using collected data during test. The average ultimate stress of the three samples is 217, 253, and 116 MPa for Fe-7.5SiC-7.5ZrO_2, Fe-10SiC-10ZrO_2, and Fe-15SiC-15ZrO_2 respectively. The results indicate that the addition of reinforcement wt.% (SiC-ZrO_2) up to 20% on the iron matrix specimens are exhibiting marginally higher order yield strength compared to Fe-7.5SiC-7.5ZrO_2 specimen of the same material. Addition of (15SiC and 15ZrO_2) wt. % have not significantly improve mechanical properties compared to other two samples. The effect of these microstructural deteriorations was seen in mechanical behavior of sample with 30 wt. % of SiC-ZrO_2 in compression test which the sample failed in low stresses and exhibited a very brittle fracture. The reason for such a result could be refered to this fact that the number of porosities in the microstructure and their effects on mechanical properties were increase with the addition of more reinforcement. Addition of more than optimum volume percentage of hard ceramics to the metal matrix could not be resulted in improvement in the mechanical properties of composite. The addition of hard ceramic reinforcements with iron matrix can improves compression strength significantly *Sepideh Kamrani et al. (2019).*

Theoretical Young's modulus were also calculated through rule of mixtures as 240, 270 and 300 GPa respectively for MMCs reinforced by 10, 20 and 30 wt.% of SiC-ZrO_2. Adding 20wt.% of (SiC-ZrO_2) increased the Young's modulus comparatively. Addition of (15SiC and 15ZrO_2) wt.% have not significantly improve mechanical properties compared to other two samples. The reason for such a result could be referred to this fact that the amount of porosities in the microstructure and their effects on mechanical properties were increase with the addition of more reinforcement. Young's modulus, therefore, adding these particles up to a certain level, in this work 20 wt.% of reinforcement could favorably increase the compressive strength of composites if they were uniformly and sufficiently been added to the matrix. The same concept reported from *Wang et al. (2014).*

The result of the stress-strain curves of each composite indicate the increasing in compressive strength with the addition of SiC-ZrO_2 as presented in Figure 4.12. From the graph young modulus for Fe-7.5SiC-7.5ZrO_2, Fe-10SiC-10ZrO_2 and Fe-15SiC-15ZrO_2 hybrid composite were calculated. The young modulus of Fe-7.5SiC-7.5ZrO_2, Fe-10SiC-10ZrO_2 and Fe-15SiC-15ZrO_2 wt. % composite was calculated from experimental investigated value are 107.5, 185.1, and 119.6 GPa, respectively.

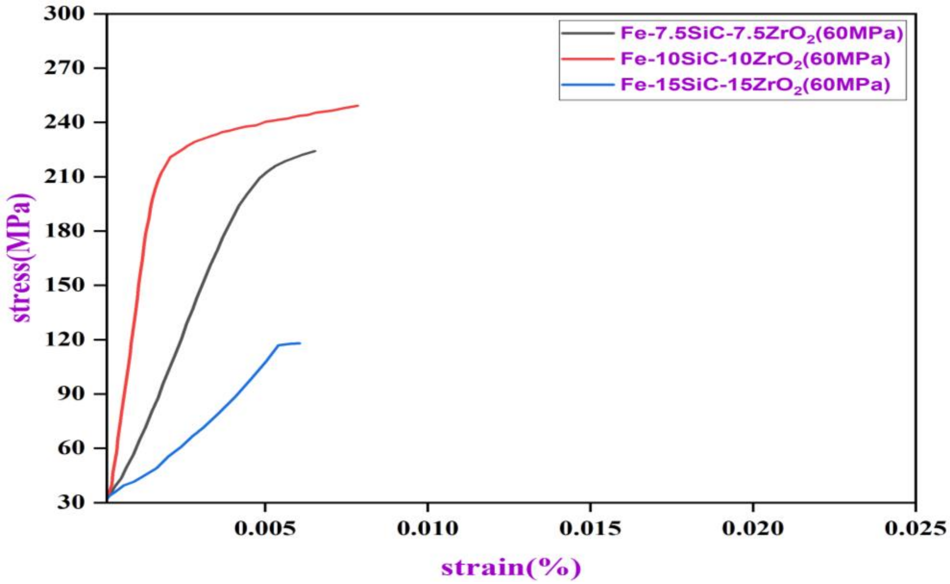

Figure 4.12 Stress-Strain curves of Fe-SiC-ZrO_2 composites at different reinforcement wt.% based on compression test.

It is seen that the Young's modulus increased steadily with the increase the optimum value of reinforcement particle content. Experimental analysis showed that it must be an optimum balance between the amount of reinforcement phase and matrix phase in the microstructure to improve mechanical properties of composites. At this optimum content, there is enough matrix phase to transfer the applied load and enough reinforcement phase to carry the load.

4.5. Multi objective Optimization of P/M Process parameters

For current research work, the GRA method used to optimize the process parameters. In this method, reinforcement wt.%, compaction pressure and sintering time are taken as main input process parameters and the experiment is performed as per L9 orthogonal array as shown in Table 3.4. The levels of various input process parameters according to the L9 orthogonal array for the experiments are shown in Table 3.5. Due to the porous structure of fabricated samples, density and the hardness test results had some variances. In this regard to get more reliable results, at least 3 tests were done on each sample and the average is taken. Table 4.19 shows the effect of reinforcement composition, compaction pressure and sintering time on the density, hardness and corrosion rate of the fabricated samples. For analyzing effects of input powder metallurgy parameters on response outcomes for P/M, Taguchi L9 orthogonal array was designed.

Table 4.19 Experimental results at different SiC-ZrO2 concentrations, compaction pressure and sintering times.

Trial No.	Powder metallurgy Parameters			Average Response Values		
	composition	Compaction pressure(MPa)	Sintering time	Density (g/cm^3)	Hardness (HV)	Corrosion rate (mm/y)
1	15	40	60	4.386	191.7	135.425
2	15	50	90	4.375	283.4	335.252
3	15	60	120	4.897	300.8	158.060
4	20	40	90	**4.357**	274.7	109.530
5	20	50	120	4.394	394.8	88.567
6	20	60	60	**4.849**	435.4	**24.470**
7	30	40	120	3.792	327.4	101.380
8	30	50	60	3.734	460.7	50.020
9	30	60	90	4.573	**485.4**	36.457

4.5.1. Performance evaluation using Taguchi's S/N ratio

Taguchi method uses a statistical tool to measure performance characteristics known as signal-to-noise (S/N) ratio to find out the optimum settings for the design parameters and it (s/n ratio) consists of both the mean and the variability of performance characteristics, *Dharmendra* *kumar singh (2014)*. Now relative closeness has been optimized using GRA. S/N ratio has been calculated considering smaller is-Better (SB) for density, higher is better (HB) for hardness and small is better (SB) for corrosion rate. The value of S/N ratio against each run of relative closeness has been shown in Table 4.20, for density, corrosion rate and hardness respectively.

Table 4.20 S/N ratio for density, hardness and corrosion rate

Run No	S/N ratio for Density	S/N ratio for hardness	S/N ratio for Corrosion rate
1	-12.8414	45.6524	-42.6340
2	-12.8196	49.0480	-50.5074
3	-13.7986	49.5656	-43.9764
4	-12.7838	48.7772	-40.7907
5	-12.8572	51.9275	-38.9454
6	-14.5655	52.7778	-27.7727
7	-11.5774	50.3016	-40.1190
8	-11.4435	53.2684	-33.9829
9	-13.2040	53.7220	-31.2356

Table 4.21 Normalized S/N ratios for the experimental results

S.N	Normalized S/N ratio for sintered density	Normalized S/N ratio for Hardness value	Normalized S/N ratio for corrosion rate
S1	0.4478	0.0000	0.6537
S2	0.4408	0.4208	1.0000
S3	0.7544	0.4849	0.7127
S4	0.4293	0.3872	0.5726
S5	0.4528	0.7776	0.4914
S6	1.0000	0.8830	0.0000
S7	0.0429	0.5761	0.5431
S8	0.0000	0.9438	0.2732
S9	0.5639	1.0000	0.1523

Table 4.22 Deviation Sequences.

Deviation Sequences	Density	Hardness	Corrosion rate
1	0.5522	1.0000	0.3463
2	0.5592	0.5792	0.0000
3	0.2456	0.5151	0.2873
4	0.5707	0.6128	0.4274
5	0.5472	0.2224	0.5086
6	0.0000	0.1170	1.0000
7	0.9571	0.4239	0.4569
8	1.0000	0.0562	0.7268
9	0.4361	0.0000	0.8477

Table 4.23 shows the grey relational coefficients and grade for each experiment. Based on Grey grade, the highest value of GRG is ranked 1 for experiment 6 and lowest rank for experimental trial run 7. The experiment number 6, highlighted in grey, is the align optimum controllable parameters combination: reinforcement wt.% of 20 (level 2), compaction pressure of 60MPa (level 3), and sintering time (level 1).

Table 4.23 Grey relational co-efficient and grey grade values

Trial run no	Grey relational coefficient			Grey relational Grade	Order(rank)
1	0.4752	0.3333	0.5908	0.4664	9
2	0.4720	0.4633	1.0000	0.6451	2
3	0.6706	0.4926	0.6351	0.5994	4
4	0.4670	0.4493	0.5391	0.4852	7
5	0.4775	0.6922	0.4958	0.5551	5
6	**1.0000**	**0.8104**	**0.3333**	**0.7146**	**1**
7	0.3431	0.5412	0.5225	0.4689	8
8	0.3333	0.8989	0.4076	0.5466	6
9	0.5341	1.0000	0.3710	0.6350	3
Mean GRC	0.5303	0.6312	0.5439		

The mean GRG of powder processing parameters was calculated and tabulated in the Table 4.23 The highest value of mean GRG response of parameters and levels is the optimal parameter. In the experimental conditions, initial optimum parameter level is **A2B3C1**. It has been found from main effects Table 4.23 for GRG, that the optimum factors level on sintered density, hardness and corrosion rate is, follows: factor A at level 2 i.e. reinforcement at 10wt.% ; factor B at level 3 i.e. compaction pressure at 60MPa, and factor C at level 1 i.e. sintering time at 60min. Therefore, optimum powder metallurgy processing parameter level combination is **A2B3C1**. It has been found from main effect Table 4.23 for GRG response that the compaction pressure rank first in the contribution of sintered density, hardness and corrosion rate followed by sintering time. The mean GRC of reference sequence for response hardness is **0.6544**, which is higher than the mean GRC of response sintered. Therefore, hardness has the strongest reference sequence as compared to sintered density. Therefore, hardness is easily influenced by factors considered. The compaction pressure is the strongest comparability sequence among controlled parameters as the difference of mean GRG between high and low level is highest as **0.6569** followed by sintering time and reinforcement weight percentage as shown in Table 4.23. It means that the compaction pressure has the strongest correlation to the responses: sintered density, hardness and corrosion rate of Fe-SiC-ZrO_2 composite followed by sintering time.

Table 4.24 Response table for Grey Relational Grade

Level	Reinforcement wt.%(A)	Compaction pressure(B)	Sintering time(C)
1	0.570	0.474	**0.586**
2	**0.585**	0.582	0.568
3	0.550	**0.650**	0.541
Delta	0.0353	0.2138	0.0672
Rank	3	1	2

The above Table 4.24 Clearly indicates that from the prediction the maximum grey relation grade occurs for the experiment number six. This indicates that the optimum results come for the experimental run 6**, (A2B3C1).** This optimized level is only for 9 experiments in which at this level we got maximum hardness, minimum density and corrosion rate. According to this level of parameters, we got **435.4 HV, 4.849g/cm^3** of density and **24.47mpy** of corrosion rate. From this optimum level, we cannot say that this is the optimum level for our responses because we have not conduct full factorial design of experiment.

4.5.2. Predicting optimal value and confirmation test

The optimal grey relational grade is predicted at the selected optimal setting of controllable variables. The most significant parameter with optimal level was already selected as A2 (reinforcement) followed by B3 (compaction pressure) and C1 (sintering time). The estimated grey relational grade can be calculated using equation (3.8). The **A2B3C1** is an optimal parameter combination of the powder metallurgy process obtained by means of GRA and was considered as a confirmation test. Based on Eqn (3.8) the estimated GRG can be obtained. In this article, confirmation tests are not necessary since the optimal parameter level combination i.e. **A2B3C1** already compare to experimental trial run 6 which available in the current work.

At optimal parameter level combination, experimental sintered density, hardness and corrosion rate value are **4.849 g/cm^3, 435HV** and **24.47mpy** respectively. Hence, the properties sintered density, hardness and corrosion rate value of Fe-SiC-ZrO_2 hybrid composite is improved by using integration of Taguchi method with GRA.

4.6. Analysis of results after extrusion process

The improvement of the properties of the composite samples after hot extrusion were, investigated by density, hardness and corrosion tests.

4.6.1. Density and hardness test after extrusion

Table 4.25 shows the density and Vickers hardness values of extruded Fe-10SiC-10ZrO_2 (60MPa) hybrid composites specimen after the extrusion process was investigated. The results of relative densities and hardness of the samples six after sintering and hot extrusion as shown in Table 4.25 It increased from **4.849 to 5.021 g/cm^3** and **435** to **544.6HV** respectively. Hot extrusion process has led to significant to reduce porosity due to its equal load distribution inter the specimen part. During powder metallurgy process as the component is, produced by one, way compaction process, the density of the component is not, distributed uniformly. The density near the punch is maximum and at the center is minimum. There exists a density difference between boundary zone and the center zone, which is, removed by the secondary operations. The bond strength between matrix and reinforcement material improves after extrusion, which improves porosity. The homogeneous density distribution in the PM component can be, achieved after secondary operations *Sambit Kumar Mohapatra (2016).*

Table 4.25 Density and hardness value of extruded specimen

Specimen (name) code	Sintered density(g/cm^3)	Extrudate density (g/cm^3)	Sintered hardness (HV)	Extrudate hardness(HV)
Fe-10SiC-10ZrO_2	4.849	5.021	435	544.6

The result, indicate that there is also an increase in hardness, about 25% comparatively with the hardness of the sample before hot extrusion, which may be due to healing of porosity; re-crystallization and it may be due to straining of composite with silicon carbide and zirconium dioxide particles. Both silicon carbide and zirconium dioxide are being hard and brittle which lead to dispersion hardening of matrix. These the hard ceramics particles are act as second phase and resist the movement of dislocation more due to the uniform load distribution during extrusion process. Similar results that higher hardness is associated with lower porosity of MMCs reported from *Ramesh et al. (2012*).

4.6.2. Corrosion test

Figure 4.13 show the result of corrosion rate of extruded specimen to analysis the effect of extrusion process on corrosion behavior Fe-SiC-ZrO_2 specimen. After hot extrusion of the hybrid composite, there is a significant amount of decrease in porosity and increase in hardness. Several researchers have reported the direct proportionality relation of hardness with corrosion resistance. The bond strength between matrix and reinforcement material improves after extrusion, which improves corrosion resistance, *K.C. Mohanakumara et al. (2014)*. The results also indicate that the extruded hybrid composite specimens are exhibiting marginally lower order corrosion rate compared to sintered specimen of the similar specimen from **24.4 to 12.43 (mpy).**

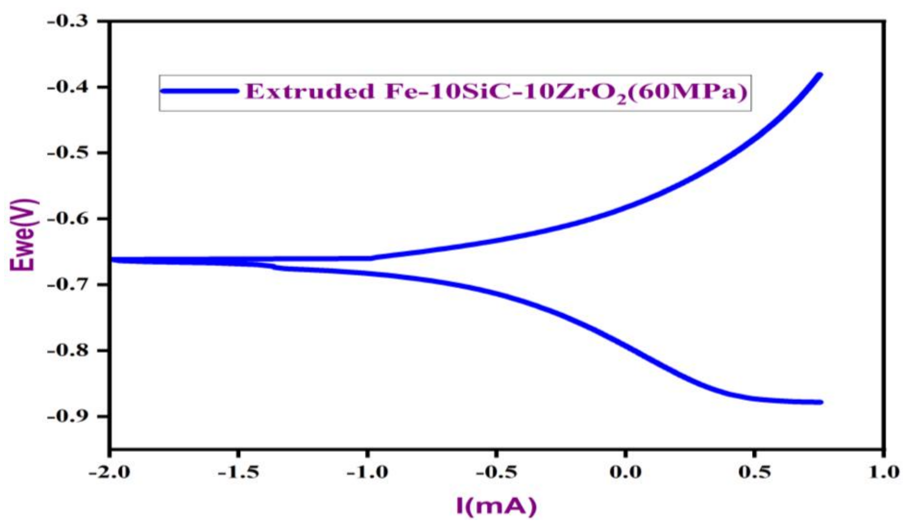

Figure 4.13 Corrosion test current density and potential graph

4.6.3. Microstructure of extruded specimen

As the optical microscopy, observation shows on the Figure 4.14 the extruded composites specimen showed better and uniform distribution of reinforcement particles. The study could provide information like dispersion trend of the reinforcements in the matrix, presence of defects, geometrical irregularities, grain orientation and other micro level changes in the composite. The size of agglomeration of ZrO_2 found, in case of the sintered composite specimen also decrease for extruded specimen. The porosity measured by image analysis yielded values for extruded sample measured using Image j and measured 3.27%. The extrusion process can improve the mechanical, physical and electrochemical properties of the material by minimizing the porosity. Uniform distribution of porosity also seen when compared with unextruded specimen and it's due to the uniform load applied during the extrusion process. Comparatively speaking before and after extrusion value of the porosity, decrease by more than 200% after extrusion.

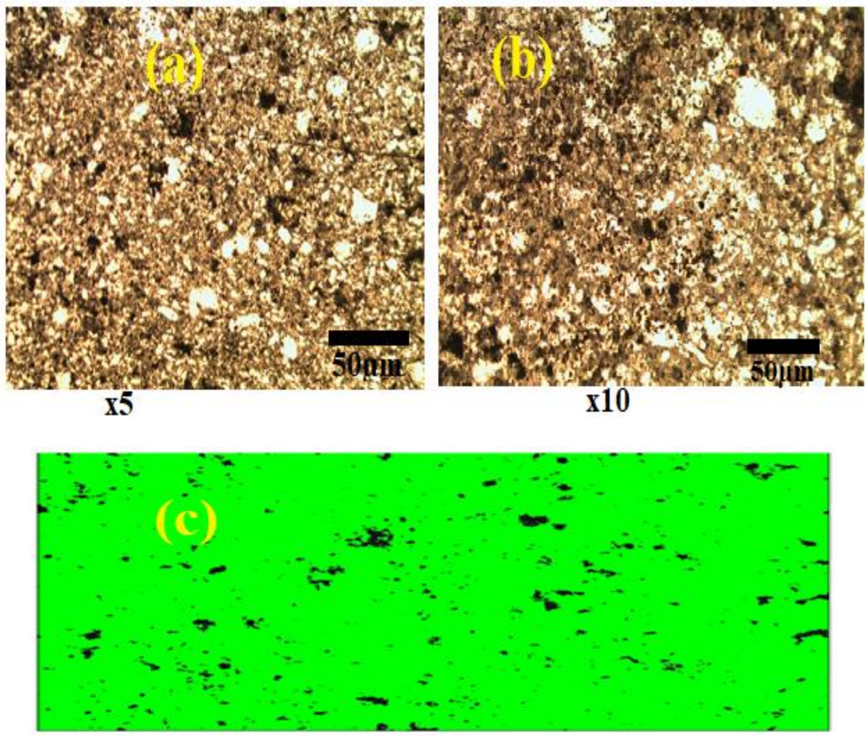

Sample code	Sintered density(g/cm³)	Extruded density(g/cm³)	Hardness(HV)	Porosity(%)
S6	4.849	5.021	544.6	3.27

Figure 4.14 Optical microscopy of specimen Fe-10SiC-10ZrO_2 (60MPa) at (a) 5X (b) 10X magnifications and porosity analysis after hot extrusion.

Scanning Electron Microscopic images are used to make morphological analysis of the extruded composites. The analysis of these micrographs provide answers for the change in properties of the composites. The SEM morphological analysis of the hot extruded samples are given in Figure 4.15. (a) and (b). It is observed that the homogeneity of particle distribution improved after extrusion. As *M. Y. Abdellah et al. (2014)* reported, the number of small particle increase as result of particle fracture during the hot extrusion. Although a minuscule amount of porosity remains in the material after extrusion, which is evident from the Figure 4.15 the porosity is much smaller than that of unextruded samples. The distribution of reinforced particles in the extruded product is uniform. It also shows good dispersion of reinforcements in matrix elements. The extent of distribution of reinforcement particle in extruded composites is more homogeneous, suggesting that rearrangement and recrystallization had taken place during hot extrusion *Ramesh et al. (2012).*

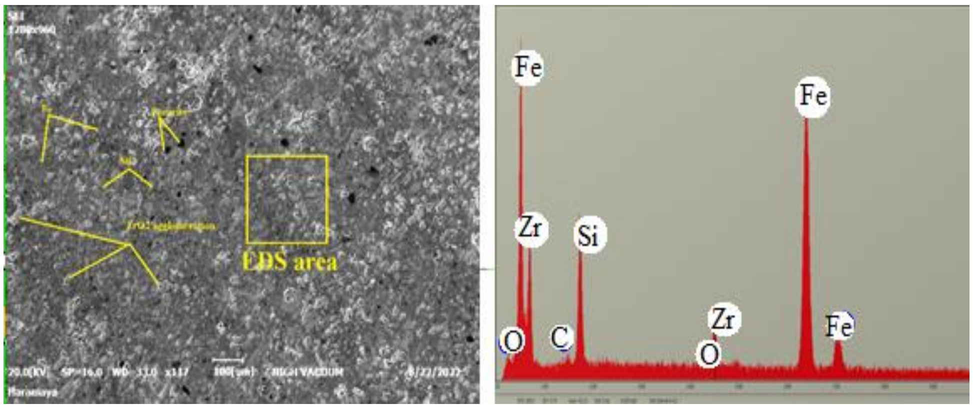

Figure 4.15 Morphology of Fe-10SiC-10ZrO_2 (60MPa) specimen after extrusion.

A macroscopic view on the samples prepared in extrusion direction and in perpendicular direction shows the interface between the capsule and the Fe based MMC with no macroscopic pores visible, *Karlsohn et al (2013).* This can be attributed to partial crushing of the agglomerated SiC and more reaction ZrO_2 with Fe during the extrusion process and realignment of the fragments. These changes in structure from hot working result in an increase in ductility, toughness and strength. Effect of extrusion on the improvement of the density, hardness, corrosion resistance and microstructural properties of the iron-based metal matrix was investigated. The results of this investigation are summarized as follows:

Significant improvement of mechanical properties of Fe based composite is observed which can be attributed to improved bond strength and grain refinement after extrusion through conical profiled die. Hardness of the extruded composite specimen also increase due to the homogenously dispersion of reinforcement particle. The minimal product defects (few cracks at the corner zone and fine pores) in the extruded samples are observed, which support the improvement of compression strength and corrosion resistance properties. The corrosion rate of the extruded specimen is lesser compared to the sintered specimen.

5. Conclusions and Recommendations

In this research work, metal matrix composites reinforced by particulate were fabricated by a P/M route, which was experimentally explored. In order to study the effect of weight percentage of reinforcement on microstructure, corrosion behavior and mechanical properties of MMCs, different samples with different weight percentage of reinforcement were fabricated and studied. After the characterization, the developed material was deformed through hot extrusion process in order to study the deformational behavior of iron-based metal matrix composite.

To summarize the current work, the results recorded from several experimental work are organized. Those results are fairly align with the scientific theory of metal matrix composite. Observation of the microstructure is the basic investigation during material characterization process. Different experiments support each other and it seems good experimental study was done in current work. The optimization process also show the alignment with theory and science of metal matrix composite. Significant improvement of mechanical properties of Fe based composite is observed which can be attributed to improved bond strength and grain refinement after extrusion through conical profiled die. Hardness of the extruded composite specimen also increase due to the homogenously dispersion of reinforcement particle. The minimal product defects (few cracks at the corner zone and fine pores) in the extruded samples were observed, which support the improvement of compression strength and corrosion resistance properties. The corrosion rate of the extruded specimen is lesser compared to the sintered specimen. The grain refinement after extrusion process show good alignment with theoretic science of the effect of extrusion process on the materials. The conclusions are as follows:

5.1. Conclusions

- The Fe-SiC-ZrO_2 composites were fabricated successfully through powder metallurgy techniques.
- Density measurement, hardness, corrosion test and compression tests indicated that, addition of SiC and ZrO_2 to Fe matrix improved the mechanical properties of Fe material.
- The P/M process for fabrication of Fe- SiC-ZrO_2 composite was optimized and the process factors were suggested. The following route obtained the best results: pressing at 60MPa, and sintering at 1000 ℃ for 60 minutes.

- Increasing the volume percent of reinforcement, improved the mechanical properties of Fe-SiC and ZrO_2 composites up to 20wt. % and above this level adding more reinforcement adversely affected the mechanical properties.
- It was observed that adding more SiC and ZrO_2 particles increased the chance of agglomeration of reinforcement particles in the microstructure. The SiC and ZrO_2 rich areas lead to crack initiation zones.
- Increasing the weight percentage of SiC and ZrO_2 increased the volume percent of porosity in composite due to the low density of SiC and ZrO_2, which consequently increased the chance of formation of interconnected porosities visualized from the microstructure. These interconnected porosities negatively affected the mechanical properties of Fe-SiC-ZrO_2 composites.
- The in-situ formation of the Fe_2O_3, Zr_6Fe_3O and SiO_2 from the reaction of ZrO_2 and Fe during sintering was confirmed based on the XRD and EDS analysis results.
- After extrusion, the microstructure of the specimens was observed. The volume of the reinforcement added and its distribution after extrusion is well observed from these microstructures.
- The hot extrusion process for reinforced Fe-SiC-ZrO_2 increases the bonding between the matrix material (Fe) and the reinforcements (SiC and ZrO_2). This process leads in turn to enhancement of ductility, hardness, corrosion resistance.
- The highest hardness (485.4HV) and compression strength (310MPa) for the composite was obtained with Fe -10% SiC-10% ZrO_2 specimen. The higher corrosion resistance of the composites was obtained for Fe-10%SiC-10% ZrO_2 due to the addition of corrosion resistance reinforcement and well compacted of the sample. The density and hardness of the sample after deformation was found to be 5.021 g/cm^3 and 544.6HV respectively which have shown remarkable improvement in material properties.
- The results also indicate that the extruded hybrid composite specimens are exhibiting marginally lower order corrosion rate compared to sintered specimen of the similar specimen from 24.47 to 12.23(mpy).

5.2. Recommendations

For better property and application of the metal matrix composite, the following recommendation are mentioned:-

- The secondary operation (extrusion) can be replaced using hot compaction of powder rather than extruded after powder metallurgy process.
- Addition of other natural reinforcement which is compatible with exist material can be used to improve performance of hybrid metal matrix composite for several applications.
- Machining of developed hybrid composite material can be done.
- Optimization for extrusion process can be done to investigate the effect of various process parameters on the deformation behavior.
- In this research, analysis and characterization for few mechanical properties was performed. For the similar investigations, other test such like Tensile, impact test can be focused.
- The die profile design for the conical extrusion process was successful performed. The design methodology can be extended for the cosine die design for hot extrusion.

REFERENCES

Abdul Nazeer and Mir Safiulla, (2018) A Review on Secondary Process of Hot Extrusion on Aluminum Metal Matrix Composite.

Abdul Nazeer, Mir Safiulla (2020), Mechanical and Wear Properties of Cold Extruded Al6063 Metal Matrix Alloy Reinforced with Silicon Carbide, Alumina and Cerium Oxide, (IJEAT)

Abdellah, M. Y., Moustafa, M. M., Mohamed, A. T., & Abdel-Jaber, G. T. (2014). Wear Properties of Hot Extruded Aluminum Powder Compacts. Open Access Library Journal, 1(4).

Agbalyan, S. G., Petrosyan, A. S., Amalyan, E. S., Galstyan, L. G., & Vasilyan, G. A. (2004). A metallographic study of extruded reinforced composites based on iron and copper. Powder Metallurgy and Metal Ceramics, 43(9), 469-472.

A. Loganathan, (2013).The effect of powder metallurgy process parameters on mechanical properties of micro and nano-iron powder. pages: 20-28

Adnan Khan, Motasem W. Abdelrazeq, Manohar Reddy Mattli , Moinuddin M. Yusuf, Abdullah Alashraf , Penchal Reddy Matli and R. A. Shakoor, (2020),Structural and Mechanical Properties of Al-SiC-ZrO2 Nanocomposites Fabricated by Microwave Sintering Technique.

Avadesh K Sharma1*, Rajeev Singh, Arun K Tiwari , Ajay K Sharma, (2022), Design, fabrication and analysis of compaction die for powder processing.

Bayraktar,E, Katundi, D.,Ayari,F.,Chevaier,JP,Bonnet,F. (2011). Damage Analysis of the ceramic reinforced steel Matrix Composites Sheets: Experimental and Numerical Study. In:proulx,T. (eds) Experimental and Applied Mechanics, Volume 6.

Bai, H., Zhong, L., Kang, L., Wei, J., Lv, Z., & Xu, Y. (2021). A novel iron matrix composite fabricated by two-step in situ reaction: Microstructure, formation mechanism and mechanical properties. Journal of Alloys and Compounds, 855, 157442.

Bai, H., Zhong, L., Cui, P., Lv, Z., & Xu, Y. (2020). Preparation of V_8C_7-Fe/iron dual-scale composite via two-step in situ reaction. Journal of Materials Research and Technology, 9(3), 4114-4122.

Baghel, A. S., Tiwari, A., Rana, R. S., & Warudkar, V. (2015). A Short Review on Effect of Heat Treatment on Microstructure and Mechanical Properties of ADC12/SiC Metal Matrix

Composite. In applied Mechanics and Materials (Vol. 813, pp. 3-8). Trans Tech Publications Ltd.

Bhattacharyya, R., Iqbal, A., Gaur, T., & Gupta, P. (2021). Effect of ceramic reinforcement on the properties of iron based metal matrix nanocomposites. Materials Today: Proceedings, 38, 305-312.

Cyriac, A. J. (2011). Metal matrix composites: History, status, factors and future. Oklahoma State University

Chawla, N., & Deng, X. (2005). Microstructure and mechanical behavior of porous sintered steels. Materials Science and Engineering: A, 390(1-2), 98-112.

Ch. Kishore Reddy, M. Gopi Krishna, V.S.N. Venkata Ramana (2020). Corrosion Characterization of Al-4mg Based Metal-Metal Composite with High Strength Alloy Particulate as Reinforcement (IJRTE).

Chawla, N., Williams, J. J., Deng, X., McClimon, C., Hunter, L., & Lau, S. H. (2009). Three-dimensional characterization ahd modeling of porosity in PM steels. International Journal of Powder Metallurgy (Princeton, New Jersey), 45(2), 19-27

Chandrasekaran, D. (2003). Grain size and solid solution strengthening in metals (Doctoral dissertation, Materialvetenskap).

Chen, W. C. (1995). Extrusion of alumina particulate reinforced metal matrix composites (Doctoral dissertation, University of British Columbia).

Dammak, M., Gaspérini, M., & Barbier, D. (2014). Microstructural evolution of iron based metal–matrix composites submitted to simple shear. Materials Science and Engineering: A, 616, 123-131.

Danninger, H., Calderon, R. D. O., & Gierl-Mayer, C. (2017). Powder metallurgy and sintered materials. Additive Manufacturing, 19(4).

Daud, S. A., Tahir, S. M., Anuar, M. S., Jaafar, C. A., & Yusoff, M. M. (2019). Physical and strength properties of Fe/SiC composites under microwave hybrid sintering method. Journal of Metals, Materials and Minerals, 29(2).

Delavari, M., Salarvand, A., Rahi, A., & Shahri, F. (2011). The effect of powder metallurgy process parameters on mechanical properties of micro and nano-iron powder. International Journal of Engineering, Science and Technology, 3(9), 86-94.

Debasis Chaira, (2021), Powder Metallurgy Routes for Composite Materials Production.

Edosa, O. O., Tekweme, F. K., & Gupta, K. (2022). A review on the influence of process parameters on powder metallurgy parts. Engineering and Applied Science Research, 49(3), 433-443.

Emamian, A. (2011). In-situ TiC-Fe deposition on mild steel using a laser cladding process.

Flachmann, M. L., Seitz, M., Liebig, W. V., & Weidenmann, K. A. (2022). Characterization of the Corrosion Resistance of Composite Peened Aluminum. Journal of Materials Engineering and Performance, 31(4), 3185-3191.

Feijoo, I., Merino, P., Pena, G., Rey, P., & Cabeza, M. (2020). Microstructure and mechanical properties of an extruded 6005A al alloy composite reinforced with TiC nanosized particles and strengthened by precipitation hardening. Metals, 10(8), 1050.

Gupta, P., Kumar, D., Parkash, O., & Jha, A. K. (2014). Effect of sintering on wear characteristics of Fe-Al_2O_3 metal matrix composites. Proceedings of the Institution of Mechanical Engineers, Part J: Journal of Engineering Tribology, 228(3), 362-368.

Gupta, P., Kumar, D., Parkash, O., & Jha, A. K. (2014). Sintering and hardness behavior of Fe-Al_2O_3 metal matrix nanocomposites prepared by powder metallurgy. Journal of Composites, 2014.

Gupta, P., Kumar, D., Quraishi, M. A., & Parkash, O. (2015). Effect of sintering parameters on the corrosion characteristics of iron-alumina metal matrix nanocomposites. Journal of Materials and Environmental Science, 6(1), 155-167.

Gupta, pallav & Kumar, D. & Parkash, Om & Jha, A. (2013). Structural and mechanical behavior of 5% Al_2O_3 reinforced Fe metal matrix composites (MMC) produced by powder metallurgy (P/M) route. Bulletin of Materials Science. 36. 10.1007/s12034-013-0545-1.

Gomes, Daniel de Souza, & Giovedi, Claudia (2019). Comparative analysis of silicon carbide with zirconium-based alloys. Brazil: ABEN.

G. S. Upadhyaya, (2002) powder metallurgy technology, isbn 1 898326 40 1

Ghazi SS and Mashloosh KM (2015) Influence of heat treatment on resistance of wear and mechanical properties of die steel kind D3, American Journal of Scientific and Industrial Research 5(II) 33–40.

He, K., Chen, N., Wang, C., Wei, L., & Chen, J. (2018). Method for determining crystal grain size by x-ray diffraction. Crystal Research and Technology, 53(2), 1700157.

Hassanein Ibraheem Khalaf (2016). Metal forming extrusion, manufacturing processes, University of Basrah

Hadjem-Hamouche, Z., Derrien, K., Héripré, E., & Chevalier, J. P. (2018). In-situ experimental and numerical studies of the damage evolution and fracture in a Fe-TiB_2 composite. Materials Science and Engineering: A, 724, 594-605.

H Hill, S Weber, S Siebert & W Theisen (2011) Investigation of corrosion and wear properties of Fe based metal matrix composites consolidated by sintering and hot isostatic pressing, Powder Metallurgy, 54:3, 455-462

Jahani, B. (2016). Development of an Advanced Composite Material Consisting of Iron Matrix Reinforced with Ultra High Temperature Ceramic Particulate (TiB_2) with Optimum Properties.

Jha, P., Kumar, D., & Mishra, V. K. (2021). Development of mathematical models to predict the density and hardness of Fe-ZrO_2 composites. Advances in Materials and Processing Technologies, 1-15.

Jha, P., Gupta, P., Kumar, D., & Parkash, O. (2014). Synthesis and characterization of Fe–ZrO_2 metal matrix composites. Journal of Composite Materials, 48(17), 2107-2115.

Janerka, K., Kostrzewski, Ł., Stawarz, M., & Jezierski, J. (2020). The Importance of SiC in the Process of Melting Ductile Iron with a Variable Content of Charge Materials. Materials, 13(5), 1231.

J.J. Williams, Z. Flom, A.A. Amell, N. Chawla, X. Xiao, F. De Carlo. (2010) Damage evolution in SiC particle reinforced Al alloy matrix composites by X-ray synchrotron tomography,Acta Materialia,Volume 58, Issue 18, ,Pages 6194-6205,ISSN 1359-6454,

Jayaprakash, H.V, Chandrasekhar N, M.K.Veeraiah, P.V.Krupakara, (2017) Corrosion Characterization of ZA-27 / Red Mud Metal Matrix Composites in Sodium Chloride Solutions.

John, C. F., Paul, R. C., Singh, S. C. E., Jacobjose, J., Ramkumar, T., Hikku, G. S. Sengottuvel, P. (2018). Corrosion behavior of ZrC particles reinforcement with Al-12Si composites by weight loss method using acidic media. Bulletin of the Polish Academy of Sciences. Technical Sciences, 66(1), 9–16.

Khosla, P., Singh, H. K., Katoch, V., Dubey, A., Singh, N., Kumar, D., & Gupta, P. (2018). Synthesis, mechanical and corrosion behaviour of iron–silicon carbide metal matrix nanocomposites. Journal of Composite Materials, 52(1), 91-107.

Kamrani S, Hübler D, Ghasemi A, Fleck C.(2019) Enhanced Strength and Ductility in Magnesium Matrix Composites Reinforced by a High Volume Fraction of Nano- and Submicron-Sized SiC Particles Produced by Mechanical Milling and Hot Extrusion. Materials (Basel). Oct 21;12:3445.

Karl Ulrich Kainer (2006), Basics of Metal Matrix Composites, Custom-made Materials for Automotive and Aerospace Engineering, ISBN: 3-527-31360-5.

Karlsohn, M., Weber, S., Zaree, A. S., Müller, S., Theisen, W., Reimers, W., & Pyzalla, A. R. (2008). Manufacturing, microstructure and wear resistance of novel hot extruded Fe based metal matrix composites. Powder metallurgy, 51(1), 31-37.

Kalra, C., Tiwari, S., Sapra, A., Mahajan, S., & Gupta, P. (2018). Processing and characterization of hybrid metal matrix composites. Journal of Materials and Environmental Science, 9(7), 1979-1986.

Królczyk G, Feldshtein E, Dyachkova L, Michalski M, Baranowski T, Chudy R. On the Microstructure, Strength, Fracture, and Tribological Properties of Iron-Based MMCs with Addition of Mixed Carbide Nanoparticulates. Materials (Basel). 2020 Jun 27;13 (13):2892

K. Sekar, Gudla Jayachandra, S. Aravindan,(2018), Mechanical and Welding Properties of A6082-SiC-ZrO_2 Hybrid Composite Fabricated by Stir and Squeeze Casting,Materials Today: Proceedings,Volume 5.

Konopka, K., and Oziębło, A. (2001). Microstructure and the fracture toughness of the Al2O3–Fe composites. Materials characterization, 46(2-3), 125-129.

Khuntia, S. K., and Samal, B. P. (2019). Fabrication of Ferrous based Composites via Different Processes and their Characterization. International Journal of Applied Engineering Research, 14(12), 2817-2820.

Kuroyanagi, Y., Nishida, M., Ogura, T., Häggblad, H. Å, Jonsén, P., & Gustafsson, G. (2015). Effects of aspect ratio and specimen size on uniaxial failure stress of iron green bodies at high strain rates. In EPJ Web of Conferences (Vol. 94, p. 01060). EDP Sciences.

Kumar, N., Bharti, A., Dixit, M. et al. (2020) Effect of Powder Metallurgy Process and its Parameters on the Mechanical and Electrical Properties of Copper-Based Materials: Literature Review. Powder Metall Met Ceram 59, 401–410.

Kumar, A., & Das, A. K. (2020). Mechanical properties of Fe+SiC metal matrix composite fabricated on stainless steel 304 by TIG coating process. International Journal of Materials Engineering Innovation, 11(3), 181-197.

Liu, Z. S., Shao, G., Chen, D. L., & Zhang, R. (2010). Preparation and characterization of Fe/SiC ceramic-metal composites. In Key Engineering Materials (Vol. 434, pp. 66-68). Trans Tech Publications Ltd.

Laghari, R. A., Li, J., Laghari, A. A., & Wang, S. Q. (2020). A review on application of soft computing techniques in machining of particle reinforcement metal matrix composites. Archives of Computational Methods in Engineering, 27(5), 1363-1377.

Lu, H. (2016). The Synthesis of High Strength Titanium Alloy and Titanium Alloy Matrix Composite by Powder Compact Extrusion from Blended Elemental Powders (Doctoral dissertation, University of Waikato).

Liu, J. Y., Tao, Q., Lai, W., Tang, W. W., Wang, J., & Liu, W. (2016). Influence of Ti on the Microstructure and Performance of Fe-Cr Alloy Cladding Layer. In Materials Science Forum (Vol. 849, pp. 709-715). Trans Tech Publications Ltd.

Lei, T., Tang, W., Cai, S. H., Feng, F. F., & Li, N. F. (2012). On the corrosion behaviour of newly developed biodegradable Mg-based metal matrix composites produced by in situ reaction. Corrosion Science, *54*, 270-277.

Meignanamoorthy, M., & Ravichandran, M. (2018). Synthesis of metal matrix composites via powder metallurgy route: a review. Mechanics and Mechanical Engineering, 22(1), 65-76.

M.Mamatha, P.V.Krupakara, K Sreenivasa, (2015) Corrosion Characterization of Aluminium 7075 / Red Mud Metal Matrix Composites

Md Zakir Hussain , Sabah Khan, Pranjal Sarmah (2019) Optimization of powder metallurgy processing parameters of Al_2O_3/Cu composite through Taguchi method with Grey relational analysis.

Mohapatra, S. K. (2016). Aluminium Based Material Extrusion through Mathematical Contoured Die: Numerical & Experimental Investigation (Doctoral dissertation).

Magid, H. M., Kadhim, K. J., & Hawas, M. N. (2017). Exploration the extrudability of aluminum matrix composite (LM6/TIC) through modeling, simulation and experimental process. Journal of Fundamental and Applied Sciences, 9(7S), 1493-1507.

N. Poornaprakash , N. Selvakumar , K. Jeyasubramanian & K. Karthikeyan (2011) Evaluating the effect of SiC content on iron-based nanocomposite, Journal of Experimental Nanoscience, 6:5, 557-566.

Nair, F., & Hamamcı, M. (2020). Effect of In-Situ Synthesized Boride Phases on the Impact Behavior of Iron-Based Composites Reinforced by B_4C Particles. Metals, 10(5), 554.

Oladayo O, Folorunso DO, Oke SR, et al. (2017) Effect of zirconia dispersion on mechanical and corrosion properties of ductile iron. Material Sci & Eng Int J.;1 (3):95–98.

Pelleg, J. (2009). Reactions in the matrix and interface of the Fe–SiC metal matrix composite system. Materials Science and Engineering: A, 269(1-2), 225-241.

Parswajinan, C., Vijaya Ramnath, B., Vetrivel, M., Ramanarayanan, P., Bharath, S., Ajay, T., & Raghav Chander, R. (2015). A Review on Composite Materials with Ferrous, CNT and Powder Metallurgy. In applied Mechanics and Materials (Vol. 813, pp. 9-13). Trans Tech Publications Ltd.

P.P. Ikubanni, M. Oki, A.A. Adeleke, O.O. Agboola, (2021) Optimization of the tribological properties of hybrid reinforced aluminium matrix composites using Taguchi and Grey's relational analysis,Scientific African,Volume 12, ,ISSN 2468-2276..

P.S., Syed. (2010). chapter-5 powder metallurgy 5.1 Introduction Powder Metallurgy.

Patil, O. M., Khedkar, N. N., Sachit, T. S., & Singh, T. P. (2018). A review on effect of powder metallurgy process on mechanical and tribological properties of Hybrid nano composites. Materials Today: Proceedings, 5(2), 5802-5808.

Rosso, M. (2006). Ceramic and metal matrix composites: Routes and properties. Journal of materials processing technology, 175(1-3), 364-375.

Roy, D., Ghosh, S., Basumallick, A., & Basu, B. (2006). Preparation of Fe-aluminide reinforced in situ metal matrix composites by reactive hot pressing. Materials Science and Engineering: A, 415(1-2), 202-206.

Ranjan Kumar Behera, Sudipta Sen and Subash Chandra Mishra, (2019), Microstructure and Property Co-relation of 4% Carbon Fe-C Alloy System.

R. E. Smallman, R. J. Bishop, (2000) Modern Physical Metallurgy and Materials Engineering

Ramesh, C. S., Hirianiah, A., Harishanad, K., and Noronha, N. P. (2012). A review on hot extrusion of Metal Matrix Composites (MMC's). International Journal of Engineering and Science, 1(10), 30-35.

Raichur, S. (2016). A Study on Mechanical Behaviour of Hot Extruded Aluminium based MMC Reinforced with Varying Alumina Particles (A356-Al_2O_3). International Journal of Engineering Research, 5(03).

Ramesh, C. S., Keshavamurthy, R., & Naveen, G. J. (2011). Effect of extrusion ratio on wear behaviour of hot extruded Al6061–SiCp (Ni–P coated) composites. Wear, 271(9-10), 1868-1877.

Rohit Chandel1 & Neeraj Sharma2 & Suneev Anil Bansal, (2021), A review on recent developments of aluminum-based hybrid composites for automotive applications

Szewczyk-Nykiel, A. (2017). Microstructure and properties of sintered metal matrix composites reinforced with SiC particles. Czasopismo Techniczne, 2017(Volume 6), 179-190.

Sachin, 2015, A Review on Powder Metallurgy of Iron Oxide and Iron, international journal of engineering research & technology (ijert) ncetems ,(Volume 3 – Issue 10).

Singh, A., Singh, J., Sinha, M. K., Kumar, R., & Verma, V. (2021). Compaction and Densification Characteristics of Iron Powder/Coal Fly Ash Mixtures Processed by Powder Metallurgy Technique. Journal of Materials Engineering and Performance, 30(2), 1207-1220.

Shen, T. D., Wang, K. Y., Wang, J. T., Quan, M. X., & Wei, W. D. (2002). Preparation and reactivities of composite nanocrystalline solids prepared by mechanical alloying. Journal of non-crystalline solids, 150(1-3), 468-471.

Saxena, A., Singh, N., Singh, B., Kumar, D., Sadasivuni, K. K., & Gupta, P. (2020). Phase, microstructure, and wear behavior of Al2O3-reinforced Fe–Si alloy-based metal matrix nanocomposites. Proceedings of the Institution of Mechanical Engineers, Part L: Journal of Materials: Design and Applications, 234(3), 467-480.

Subramani Nanjana , Janakiram Ganesh Murali, (2020) Analysing the Mechanical Properties and Corrosion Phenomenon of Reinforced Metal Matrix Composite.

Saravanan. R1, Mukesh. Y. B, T. P. Bharathesh, R. Keshavamurthy, (2018), Influence of Hot Extrusion on Mechanical Characteristics of Al6063-TiC Metal Matrix Composites

Santhosh Kumar H N , Dr. Srinivas H K , Shashank B , (2020), Corrosion Characterization of Boron Carbide and Tungsten carbide Aluminium 7075 T6 Hybrid Composites, international journal of engineering research & technology (ijert) Volume 09

Springer, H., Fernandez, R. A., Duarte, M. J., Kostka, A., & Raabe, D. (2015). Microstructure refinement for high modulus in-situ metal matrix composite steels via controlled solidification of the system Fe–TiB_2. Acta Materialia, 96, 47-56.

Srinivasa, K., Parashivamurthy, K. I., Prajwal, A. S., & Rakshith, N. sliding wear behaviour of Fe-Cr-TiC composites.

Singh RB, Seema and Kumar D (2019) Heat treatment of tool steel D3 and effects on mechanical properties, International Journal of Recent Scientific Research 10(V) 32540–32545.

Tang, W. M., Zheng, Z. X., Ding, H. F., & Jin, Z. H. (2003). Control of the interface reaction between silicon carbide and iron. Materials chemistry and physics, 80(1), 360-365.

T. Guna and M. Simsirb, (2017), Investigation of Mechanical Properties of Fe-Based Metal Matrix Composites by Warm Compaction for Gear Production, 58140.

Tiernan, P., Hillery, M. T., Draganescu, B., & Gheorghe, M. (2005). Modelling of cold extrusion with experimental verification. Journal of Materials Processing Technology, 168(2), 360-366.

Vani, V. V., & Chak, S. K. (2018). The effect of process parameters in aluminum metal matrix composites with powder metallurgy. Manufacturing Review, 5, 7.

Vasanthapriyan, S., Abdullah, K. S., MohammedYahiya, S., & Yakoob, s. Hybrid metal matrix composites–review. Journal homepage: www. ijrpr. Com ISSN, 2582, 7421.

Venkatesh, C., & Venkatesan, R. (2014). Design and analysis of streamlined extrusion die for round to hexagon using area mapping technique, upper bound technique and finite element method. Journal of Mechanical Science and Technology, 28(5), 1867-1874.

Wang, M., Wang, Z., Yang, Z., Jin, J., Ling, G., and Zong, Y. (2021). Sintering and Mechanical Properties of (SiC+ TiCx) p/Fe Composites Synthesized from Ti3AlC2, SiC, and Fe Powders. Materials, 14(9), 2453.

Wang, M., Chen, D., Chen, Z., Wu, Y., Wang, F., Ma, N., & Wang, H. (2014). Mechanical properties of in-situ TiB_2/A356 composites. Materials Science and Engineering: A, 590, 246-254.

Wang, Z. T., Zhou, X. H., & Zhao, G. G. (2008). Microstructure and formation mechanism of in-situ TiC-TiB_2/Fe composite coating. Transactions of Nonferrous Metals Society of China, 18(4), 831-835.

Yang, Y. F., & Li, K. J. (2012). Study on Effect of Particle Size of Matrix and Reinforcement on Properties of Iron Matrix Composites. In applied Mechanics and Materials (Vol. 182, pp. 328-331). Trans Tech Publications Ltd.

. Yi, X. S., Du, S., & Zhang, L. (2018). Composite Materials Engineering, Volume 2. Berlin/Heidelberg, Germany: Springer.

Yodkaew, T., Morakotjinda, M., Tosangthum, N., Coovattachai, O., Krataitong, R., Siriphol, P and Tongsri, R. (2009). Effect of non-reactive hard particles on sintered Fe material. Sonklanakarin Journal of Science and Technology, 31(5), 555

Yang, X., Guo, H., Liang, H., Yao, Z., & Yuan, S. (2016). Flow behavior and constitutive equation of Ti-6.5 Al-2Sn-4Zr-4Mo-1W-0.2 Si titanium alloy. Journal of Materials Engineering and Performance, 25(4), 1347-1359.

Zakaria, H. M. (2014). Microstructural and corrosion behavior of Al/SiC metal matrix composites. Ain Shams Engineering Journal, 5(3), 831-838.

Zou Lin∗, Xia Juchen, Wang Xinyun, Hu Guoan, (2003), Optimization of die profile for improving die life in the hot extrusion process.

APPENDIX-AI

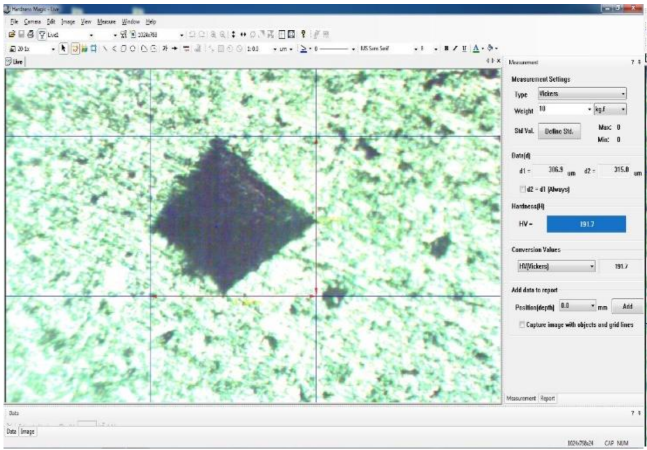

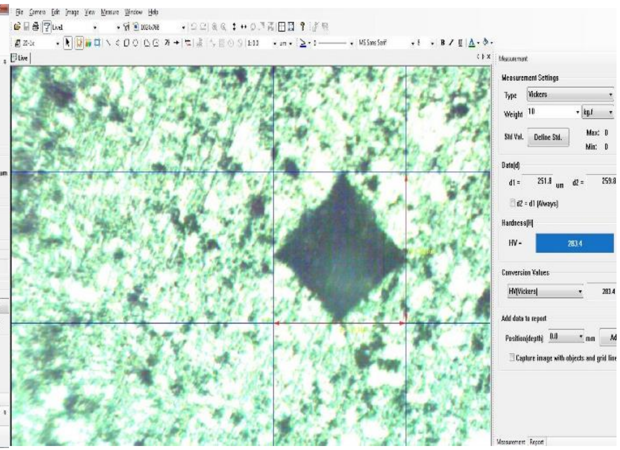

a) b)

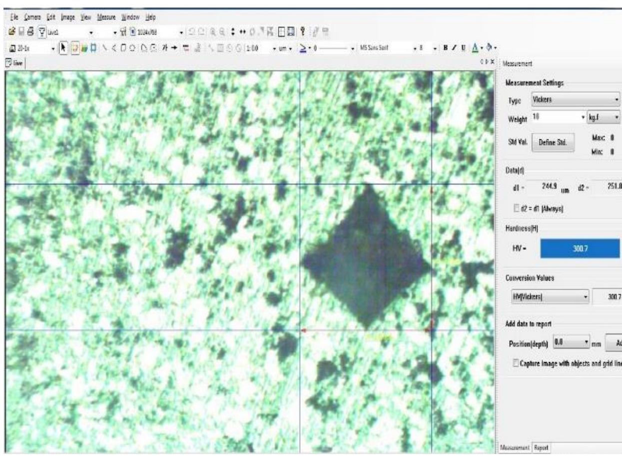

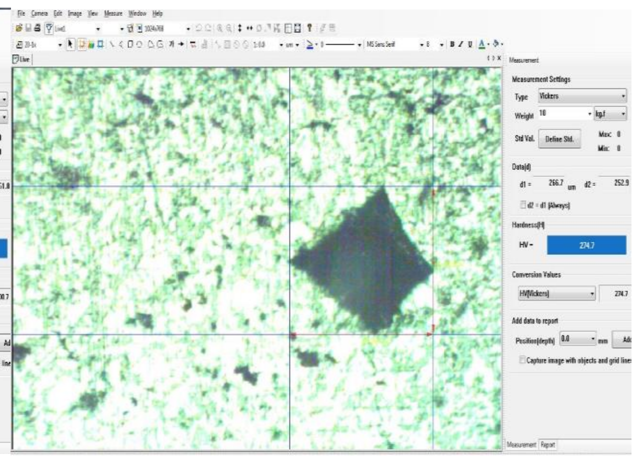

c)

Figure A-1. Vickers hardness value for Fe-SiC-ZrO_2 composite samples (S1, S2 and S3) in a),b),c) respectively.

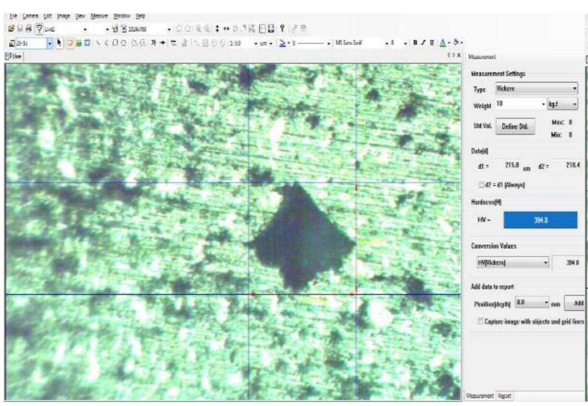

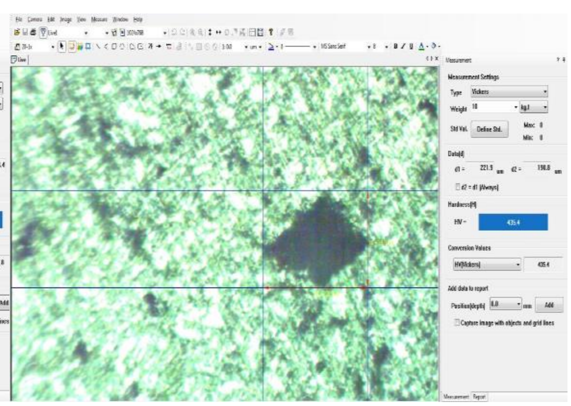

b) c)

Figure A-2. Vickers hardness value for Fe-SiC-ZrO_2 composite samples (S4, S5 and S6) in a),b),c) respectively.

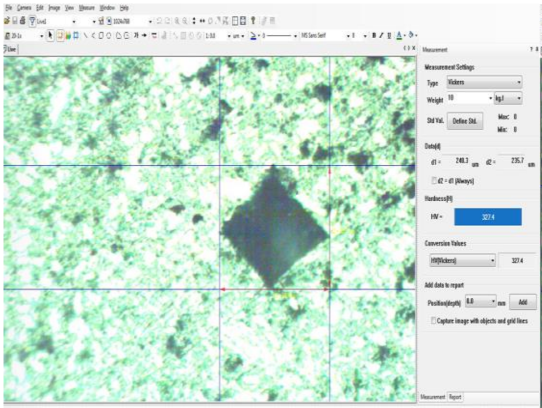

a)

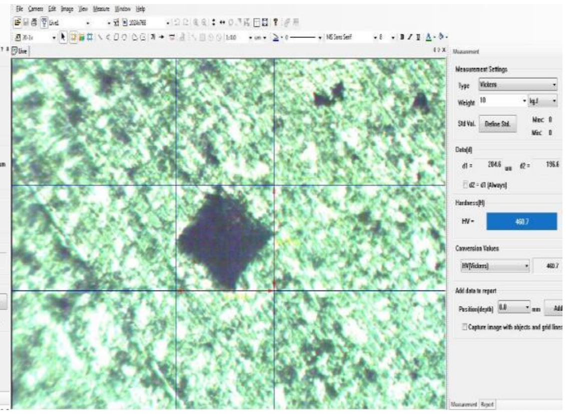

b)

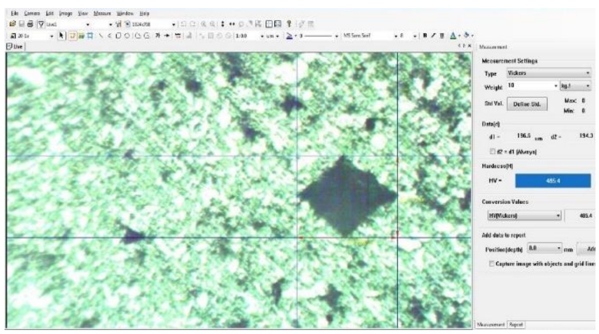

c)

Figure A-3. Vickers hardness value for Fe-SiC-ZrO_2 composite samples (S7, S8 and S9) in a),b),c) respectively.

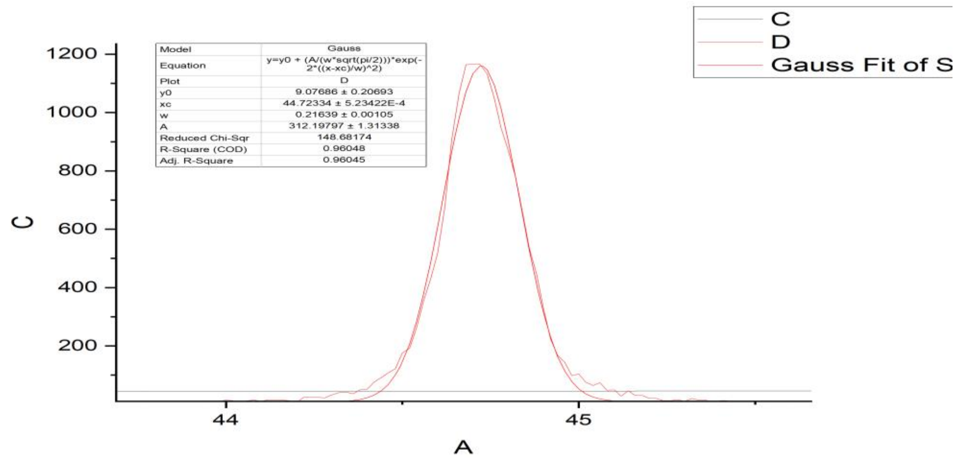

Crystallite size analysis from XRD data

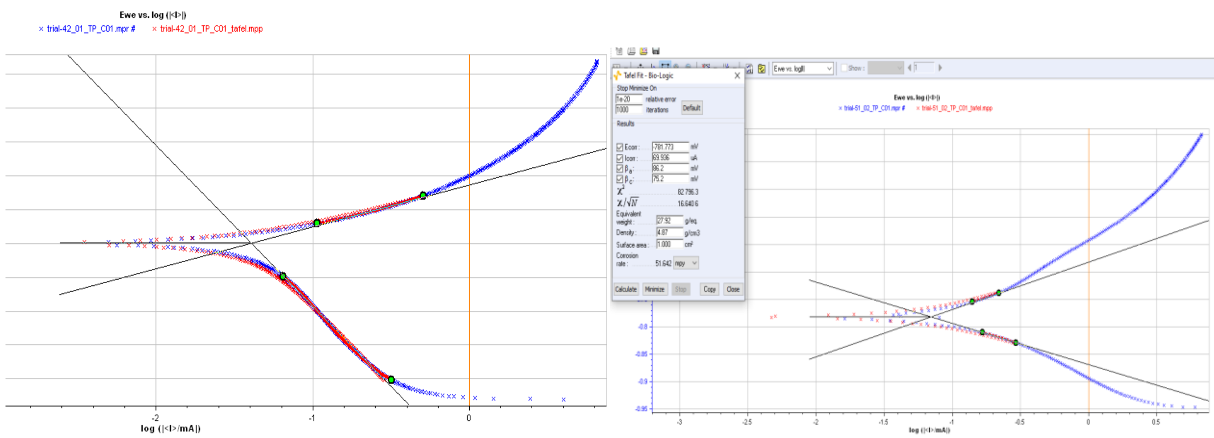

Corrosion rate calculation method from tafel plot